SMAI-JCM
SMAI Journal of Computational Mathematics

Construction, analysis and implementation of two nodal finite volume schemes for the P_N model for particle transport in 2D

Christophe Buet, Stéphane Del Pino & Victor Fournet

Volume 11 (2025), p. 39-84.
https://doi.org/10.5802/smai-jcm.119

The SMAI Journal of Computational Mathematics is a member of the Centre Mersenne for Open Scientific Publishing
http://www.centre-mersenne.org/
Submissions at https://smai-jcm.centre-mersenne.org/ojs/submission
e-ISSN: 2426-8399

SMAI Journal of Computational Mathematics
Vol. 11, 39-84 (2025)

Construction, analysis and implementation of two nodal finite volume schemes for the P_N model for particle transport in 2D

Christophe Buet [1]
Stéphane Del Pino [2]
Victor Fournet [3]

[1] CEA, DAM, DIF, F-91297, Arpajon, France and Université Paris-Saclay, CEA, Laboratoire en Informatique Haute Performance pour le Calcul et la simulation, 91297 Arpajon, France
E-mail address: christophe.buet@cea.fr
[2] CEA, DAM, DIF, F-91297, Arpajon, France and Université Paris-Saclay, CEA, Laboratoire en Informatique Haute Performance pour le Calcul et la simulation, 91297 Arpajon, France
E-mail address: stephane.delpino@cea.fr
[3] Laboratoire Jacques Louis Lions, Sorbonne Université, 4 place Jussieu, 75005 Paris, France, CEA, DAM, DIF, F-91297, Arpajon, France
E-mail address: fournet@ljll.math.upmc.fr.

Abstract. In this paper, we present two new nodal finite volume schemes for the P_N model on arbitrary polygonal meshes in 2D. We show that these schemes are well-defined, conservative and stable, finally we prove their convergence. We also present some numerical results.

2020 Mathematics Subject Classification. 65M08, 65M12.
Keywords. nodal solver, P_N approximation, transport equation, hyperbolic.

1. Introduction

In this work we consider the linear kinetic equation that governs the evolution of a particle distribution f

$$\partial_t f(\mathbf{x},\omega,t) + \nabla\cdot(\omega f(\mathbf{x},\omega,t)) + (\sigma_a+\sigma_s) f(\mathbf{x},\omega,t) = \frac{1}{4\pi}\sigma_s \int_{\mathbb{S}^2} f(\mathbf{x},\omega,t) d\omega.$$

Under appropriate scaling this equation can be viewed as a simplified model of radiative transfer (see for instance [19] or [23]). Because the function f lives on a high dimensional space (one dimension of time, three of space and two for the velocity), solving this linear kinetic equation by a discretization directly in the phase space is in general too expensive with regard to the computational time. Moreover, the evolution of f is non-local due to the collision operator, so it is necessary to use an approximate model. There are many such models (we can mention for instance P_N [8, 14, 28], S_N [4] and M_N [17]). In this document, we are interested in the P_N model. It consists in using a spectral Galerkin discretization of the velocity space using the spherical harmonics as basis. The dimension of the phase space is thus reduced by two at the cost of replacing an equation by a system of equations, which can be written, as initially proposed by Vladimirov [28] and Kuznetsov [15], in the form

$$\begin{cases} \partial_t \mathbf{g} + A\partial_x \mathbf{h} + B\partial_y \mathbf{h} + C\partial_z \mathbf{h} = -\left((\sigma_a+\sigma_s)\mathrm{I} - \sigma_s \mathbf{e}_1\otimes\mathbf{e}_1\right)\mathbf{g}, \\ \partial_t \mathbf{h} + A^T\partial_x \mathbf{g} + B^T\partial_y \mathbf{g} + C^T\partial_z \mathbf{g} = -(\sigma_a+\sigma_s)\mathbf{h}, \end{cases}$$

where $\mathbf{e}_1 = (1,0,\dots,0)^T$ and where $\mathbf{g}$ and $\mathbf{h}$ denote respectively the compound vectors of even and odd moments of f. This even-odd splittings for P_N expansions have been used previously by

https://doi.org/10.5802/smai-jcm.119

Hermeline [14] or by Egger and Schlottbom [8] to define numerical methods for the P_N model. In has also be used to approximate stationary solutions of P_N by Van Criekingen et al. [26, 27] or by Egger and Schlottbom [7].

On rectangular grids, finite volume and staggered discretizations have been proposed in [21] and [24]. In [14], a DDFV[1] scheme [13] was proposed to approximate the P_N model on general grids. Mixed-hybrid finite element methods have been proposed and analyzed in [7, 8, 26, 27] to solve P_N in both stationary and instationary cases. A Trefftz Discontinous Galerkin method was studied in [20].

In view of multiphysics simulations, the use of centered finite volume methods provides natural coupling (with compressible hydrodynamics for instance) that ensures total energy conservation, which is important when dealing with shocks. Thus, this work differs from mixed finite element methods such as [8], since it is based on approximate Riemann solvers that are efficient for approximating non-regular solutions. Similarly, the DDFV method, proposed in [14], is a staggered scheme, using primal and dual meshes cell values. It makes it difficult to couple with finite volume schemes for gas dynamics, especially in the case of Lagrangian solvers.

The strategy chosen here, is to discretize this new model using a nodal finite volume scheme: the fluxes are not computed at the edges, but at the vertices of the mesh. Such schemes have been first developed for Lagrangian hydrodynamics [6, 16, 18]. The construction and analysis of such a scheme has already been done for the P_1 model in 2D on polygonal meshes, in order to write a scheme called *asymptotic preserving* [1]. Indeed, using a face-based finite volume scheme leads in the diffusive regime to a two-point scheme which is not consistent with the limit diffusion operator on arbitrary meshes. The aim of this work, in order to generalize these results to the P_N model for $N > 1$, is, in a first step, to construct a nodal solver for this model. As it is typically done is the literature, we assume that N is an odd integer.

In the work of Buet, Després, Franck [1], the authors have considered the P_1 model

$$\begin{cases} \partial_t g + \nabla \cdot \mathbf{h} = 0, \\ \partial_t \mathbf{h} + \nabla g = -\sigma_s \mathbf{h}, \end{cases}$$

and they studied a nodal finite volume scheme. Here, we consider only the free streaming case ($\sigma_a = \sigma_s = 0$), since it is the first step in order to write an asymptotic preserving nodal scheme[2] for P_N. Following the work of Després, Mazeran [18] for Lagrangian hydrodynamics, the scheme proposed in [1] (the Glace scheme) reads, when $\sigma_a = \sigma_s = 0$: for all cell j of the mesh,

$$\begin{cases} \dfrac{d}{dt} g_j + \dfrac{1}{V_j} \displaystyle\sum_{r \in \mathcal{R}_j} l_{jr}(\mathbf{h}_r, \mathbf{n}_{jr}) = 0, \\ \dfrac{d}{dt} \mathbf{h}_j + \dfrac{1}{V_j} \displaystyle\sum_{r \in \mathcal{R}_j} l_{jr} g_{jr} \mathbf{n}_{jr} = \mathbf{0}, \end{cases}$$

where V_j is the volume of the cell j, $l_{jr} := \|\nabla_{\mathbf{x}_r} V_j\|$ and $\mathbf{n}_{jr} = \frac{1}{l_{jr}} \nabla_{\mathbf{x}_r} V_j$. Actually, $\nabla_{\mathbf{x}_r} V_j$ denotes the gradient of volume variation due to the displacement of the node r of coordinate $\mathbf{x}_r$.[3]

The fluxes are then given by

$$\begin{cases} g_{jr} = g_j + (\mathbf{h}_j - \mathbf{h}_r, \mathbf{n}_{jr}), \\ \left(\displaystyle\sum_{j \in \mathcal{J}_r} l_{jr} \mathbf{n}_{jr} \otimes \mathbf{n}_{jr} \right) \mathbf{h}_r = \displaystyle\sum_{j \in \mathcal{J}_r} l_{jr} (g_j \mathbf{n}_{jr} + \mathbf{n}_{jr} \otimes \mathbf{n}_{jr} \mathbf{h}_j), \end{cases}$$

[1] Discrete Duality Finite Volume

[2] As it is shown in [1], it is important to consider nodal solvers to build a consistent scheme in the diffusion limit.

[3] In order to fix ideas, let us remark that in the case of triangles, $\nabla_{\mathbf{x}_r} V_j$ is nothing else but the gradient of the finite element $\mathbb{P}_1$ shape function λ_{jr} in cell j that satisfies $\forall s,\ w_{jr}(\mathbf{x}_s) = \delta_{rs}$.

where we denoted by $\mathcal{R}_j$ the set of nodes of the cell j and by $\mathcal{J}_r$ the set of cells connected to the node r. They show in particular, in a very simple way, that the matrix

$$\sum_{j\in\mathcal{J}_r} l_{jr}\mathbf{n}_{jr}\otimes\mathbf{n}_{jr}$$

is invertible as soon as the mesh is non-degenerate. In this paper, we write the analog of the Glace scheme for the P_N model

$$\begin{cases} \dfrac{d}{dt}\mathbf{g}_j + \dfrac{1}{V_j}\displaystyle\sum_{r\in\mathcal{R}_j} l_{jr}\mathcal{U}^{\mathbf{g}}_{\theta_{jr}} A\mathcal{U}^{\mathbf{h}}_{-\theta_{jr}}\mathbf{h}_r = \mathbf{0}, \\ \dfrac{d}{dt}\mathbf{h}_j + \dfrac{1}{V_j}\displaystyle\sum_{r\in\mathcal{R}_j} l_{jr}\mathcal{U}^{\mathbf{h}}_{\theta_{jr}} A^T\mathcal{U}^{\mathbf{g}}_{-\theta_{jr}}\mathbf{g}_{jr} = \mathbf{0}, \end{cases}$$

with

$$\begin{cases} \mathbf{g}_{jr} = \mathbf{g}_j + \mathcal{U}^{\mathbf{g}}_{\theta_{jr}} P_{\mathbf{g}} P^T_{\mathbf{h}} \mathcal{U}^{\mathbf{h}}_{-\theta_{jr}}(\mathbf{h}_j - \mathbf{h}_r), \\ \left(\displaystyle\sum_{j\in\mathcal{J}_r} M_{jr}\right)\mathbf{h}_r = \displaystyle\sum_{j\in\mathcal{J}_r} M_{jr}\mathbf{h}_j + \sum_{j\in\mathcal{J}_r} l_{jr}\mathcal{U}^{\mathbf{h}}_{\theta_{jr}} A^T\mathcal{U}^{\mathbf{g}}_{-\theta_{jr}}\mathbf{g}_j. \end{cases}$$

Here, $\mathcal{U}^{\mathbf{g}}_{\theta_{jr}}$ and $\mathcal{U}^{\mathbf{h}}_{\theta_{jr}}$ are the rotation matrices that express the rotational invariance of the spherical harmonics (known as Wigner D-matrices). The matrices $P_{\mathbf{g}}$ and $P_{\mathbf{h}}$, whose columns are orthonormal vectors, are defined in Proposition 2.7. Finally, the matrices M_{jr} are defined by (3.21) or (3.29), according to the scheme.

The problem of the invertibility of the matrix $\sum_{j\in\mathcal{J}_r} M_{jr}$ is much more difficult than in the case P_1. This is due in particular to the fact that the space generated by the odd spherical harmonics is of higher dimension than the physical space, contrary to the case $N = 1$ where the dimensions are equal. Our first main result establishes that under the same mesh conditions as for the finite nodal volume scheme for the P_1 model, this matrix is invertible. We also propose another nodal solver, based on the Eucclhyd Scheme [16] for hydrodynamics. The difference between the two schemes is that, if the Glace scheme solve an approximate Riemann problem in the direction of a "normal" at the nodes. The Eucclhyd decomposes this nodal Riemann problem using the two normal directions to the edges adjacent to the node. Our second main result is the proof of convergence of theses two nodal schemes for the P_N model.

In the first part, we recall how to obtain the P_N model from the linear kinetic equation considered and we recall several properties of the P_N model in 3D and 2D. In the second part, we recall some results related to the P_N model. In the third part, whose results are new, we propose two nodal finite volume schemes and demonstrate their properties: these schemes are well defined, conservative, L^2-stable and finally they converge. Finally in the fourth part, we show several numerical results.

2. The P_N model

In this Section, we recall how to derive the P_N model from the linear kinetic equation. We then recall some important properties of the P_N model which will allow us to write the nodal finite volume scheme. We use the presentation of the P_N model made in [14].

2.1. From linear kinetic equation to the P_N model

Let $f : \mathbb{R}^3 \times \mathbb{S}^2 \times [0, +\infty[\longrightarrow \mathbb{R}$ solution of the following linear kinetic equation

$$\partial_t f + \nabla\cdot(\omega f) + (\sigma_a + \sigma_s)f = \frac{1}{4\pi}\sigma_s \int_{\mathbb{S}^2} f d\omega, \tag{2.1}$$

where σ_a and σ_s are the absorption and scattering coefficients respectively. We use a parametrization of the sphere

$$\omega = (\omega_1, \omega_2, \omega_3) = (\cos\psi \sin\beta, \sin\psi \sin\beta, \cos\beta),$$

with $0 \leq \psi < 2\pi$ and $0 \leq \beta \leq \pi$. In the following, we assume $\sigma_a = \sigma_s = 0$.

Let k and m be two integers with $0 \leq |m| \leq k$. Suppose that for all $(\mathbf{x}, t) \in \mathbb{R}^3 \times [0, +\infty[$, the function $(\psi, \beta) \mapsto f(\mathbf{x}, \psi, \beta, t)$ is in $L^2(\mathbb{S}^2)$. Consider the expansion of f in the real spherical harmonics basis X_k^m (see [14] for the definition of the X_k^m)

$$\forall (\mathbf{x}, \psi, \beta, t) \in \mathbb{R}^3 \times \mathbb{S}^2 \times [0, +\infty[\,, \qquad f(\mathbf{x}, \psi, \beta, t) = \sum_{k=0}^{+\infty} \sum_{m=-k}^{k} f_k^m(\mathbf{x}, t) X_k^m(\psi, \beta),$$

where f_k^m are called the moments of f,

$$f_k^m(\mathbf{x}, t) = \frac{1}{4\pi} \int_{\mathbb{S}^2} f(\mathbf{x}, \psi, \beta, t) X_k^m(\psi, \beta) d\psi d\beta.$$

We note $\mathbf{X} = (X_k^m)_{k \in \mathbb{N}, |m| \leq k}$ and $\mathbf{u} = (f_k^m)_{k \in \mathbb{N}, |m| \leq k}$. Let us inject the development of f in (2.1). Noting that $f = \mathbf{X} \cdot \mathbf{u}$, we can write

$$\mathbf{X} \cdot \partial_t \mathbf{u} + \sum_{i=1}^{3} \omega_i \mathbf{X} \cdot \partial_i \mathbf{u} = \mathbf{0}.$$

Multiplying by $\mathbf{X}$, one gets

$$\mathbf{X}(\mathbf{X} \cdot \partial_t \mathbf{u}) + \sum_{i=1}^{3} \omega_i \mathbf{X}(\mathbf{X} \cdot \partial_i \mathbf{u}) = \mathbf{0},$$

which is also written

$$(\mathbf{X} \otimes \mathbf{X}) \partial_t \mathbf{u} + \sum_{i=1}^{3} \omega_i (\mathbf{X} \otimes \mathbf{X}) \partial_i \mathbf{u} = \mathbf{0}.$$

Finally, by integrating over $\mathbb{S}^2$ and dividing by 4π, we find

$$\frac{1}{4\pi} \int_{\mathbb{S}^2} \mathbf{X} \otimes \mathbf{X} d\omega \partial_t \mathbf{u} + \frac{1}{4\pi} \sum_{i=1}^{3} \int_{\mathbb{S}^2} \omega_i \mathbf{X} \otimes \mathbf{X} d\omega \partial_i \mathbf{u} = \mathbf{0}.$$

Moreover, since the spherical harmonics form an Hilbertian basis of $L^2(\mathbb{S}^2)$, one gets

$$\frac{1}{4\pi} \int_{\mathbb{S}^2} \mathbf{X} \otimes \mathbf{X} d\omega = I.$$

We pose

$$\mathcal{A}_i = \frac{1}{4\pi} \int_{\mathbb{S}^2} \omega_i \mathbf{X} \otimes \mathbf{X} d\omega, \quad 1 \leq i \leq 3. \tag{2.2}$$

Note that the matrices $\mathcal{A}_i$ are symmetric. We then obtain the P_N model

$$\partial_t \mathbf{u} + \mathcal{A}_1 \partial_x \mathbf{u} + \mathcal{A}_2 \partial_y \mathbf{u} + \mathcal{A}_3 \partial_z \mathbf{u} = \mathbf{0}. \tag{2.3}$$

Moreover, for $1 \leq i \leq 3$

$$\begin{aligned} \int_{\mathbb{S}^2} \omega_i \mathbf{X} \otimes \mathbf{X} d\omega \partial_i \mathbf{u} &= \partial_i \int_{\mathbb{S}^2} \omega_i \underbrace{\mathbf{X} \otimes \mathbf{X}\mathbf{u}}_{=(\mathbf{X}\cdot\mathbf{u})\mathbf{X}} d\omega, \\ &= \partial_i \int_{\mathbb{S}^2} \omega_i f \mathbf{X} d\omega, \\ &= \partial_i \left(\int_{\mathbb{S}^2} \omega_i f X_k^m d\omega \right)_{\substack{k \in \mathbb{N} \\ |m| \leq k}}. \end{aligned}$$

After a calculation [14], we obtain[4]

$$\frac{1}{4\pi}\int_{\mathbb{S}^2}\omega f X_k^m d\omega = \begin{pmatrix} \varepsilon^m(A_k^m f_{k+1}^{m+1} - B_k^m f_{k-1}^{m+1}) - \zeta^m(C_k^m f_{k+1}^{m-1} - D_k^m f_{k-1}^{m-1}) \\ \eta^m(A_k^m f_{k+1}^{-m-1} - B_k^m f_{k-1}^{-m-1}) + \theta^m(C_k^m f_{k+1}^{-m+1} - D_k^m f_{k-1}^{-m+1}) \\ E_k^m f_{k+1}^m + F_k^m f_{k-1}^m \end{pmatrix}, \tag{2.4}$$

with the notations

$$A_k^m = \sqrt{\frac{(k+m+1)(k+m+2)}{(2K+1)(2k+3)}}, \qquad B_k^m = \sqrt{\frac{(k-m-1)(k-m)}{(2k-1)(2k+1)}},$$
$$C_k^m = \sqrt{\frac{(k-m+1)(k-m+2)}{(2k+1)(2k+3)}}, \qquad D_k^m = \sqrt{\frac{(k+m-1)(k+m)}{(2k-1)(2k+1)}},$$
$$E_k^m = \sqrt{\frac{(k-m+1)(k+m+1)}{(2k+1)(2k+3)}}, \qquad F_k^m = \sqrt{\frac{(k-m)(k+m)}{(2k-1)(2k+1)}},$$

and

$$\varepsilon^m = \begin{cases} -\frac{1}{2} & \text{if } m < -1, \\ 0 & \text{if } m = -1, \\ \frac{\sqrt{2}}{2} & \text{if } m = 0, \\ \frac{1}{2} & \text{if } m = 1, \\ \frac{1}{2} & \text{if } m > 1, \end{cases} \qquad \zeta^m = \begin{cases} -\frac{1}{2} & \text{if } m < -1, \\ -\frac{1}{2} & \text{if } m = -1, \\ 0 & \text{if } m = 0, \\ \frac{\sqrt{2}}{2} & \text{if } m = 1, \\ \frac{1}{2} & \text{if } m > 1, \end{cases}$$

$$\eta^m = \begin{cases} -\frac{1}{2} & \text{if } m < -1, \\ -\frac{\sqrt{2}}{2} & \text{if } m = -1, \\ \frac{\sqrt{2}}{2} & \text{if } m = 0, \\ \frac{1}{2} & \text{if } m = 1, \\ \frac{1}{2} & \text{if } m > 1, \end{cases} \qquad \theta^m = \begin{cases} -\frac{1}{2} & \text{if } m < -1, \\ -\frac{1}{2} & \text{if } m = -1, \\ 0 & \text{if } m = 0, \\ 0 & \text{if } m = 1, \\ \frac{1}{2} & \text{if } m > 1. \end{cases}$$

For the moment, the matrices $\mathcal{A}_i$ and the vector $\mathbf{u}$ are infinite. The P_N model consists in truncating the development of f to the order N.

$$f_N(\mathbf{x}, \psi, \beta, t) := \sum_{k=0}^{N}\sum_{m=-k}^{k} f_k^m(\mathbf{x}, t) X_k^m(\psi, \beta),$$

which amounts to truncate the terms corresponding to $k > N$ in $\mathbf{u}$ and the $\mathcal{A}_i$ and thus to obtain a finite vector and matrices. For the following, based on [14], we note

$$\mathbf{g} = \left(f_{2p}^m\right)_{\substack{2p \le N \\ |m| \le 2p}},$$

the compound vector of even moments, and

$$\mathbf{h} = \left(f_{2p+1}^m\right)_{\substack{2p+1 \le N \\ |m| \le 2p+1}},$$

the compound vector of odd moments. We will then reorder the basis of the spherical harmonics in order to put first the even moments and then the odd moments, that is to say multiplying $\mathbf{u}$ and the $\mathcal{A}_i$ by a permutation matrix, that we still denote $\mathbf{u}$ and $\mathcal{A}_i$. We obtain

$$\mathbf{u} = \begin{pmatrix} \mathbf{g} \\ \mathbf{h} \end{pmatrix}.$$

[4] with the convention that $f_k^m = 0$ if $|m| > k$.

Moreover we notice that in this basis, from (2.4), the matrices $\mathcal{A}_i$ have the following block structure [14]

$$\mathcal{A}_1 = \begin{pmatrix} 0 & A \\ A^T & 0 \end{pmatrix}, \qquad \mathcal{A}_2 = \begin{pmatrix} 0 & B \\ B^T & 0 \end{pmatrix}, \qquad \mathcal{A}_3 = \begin{pmatrix} 0 & C \\ C^T & 0 \end{pmatrix}.$$

Thus (2.3) writes

$$\begin{cases} \partial_t \mathbf{g} + A\partial_x \mathbf{h} + B\partial_y \mathbf{h} + C\partial_z \mathbf{h} = \mathbf{0}, \\ \partial_t \mathbf{h} + A^T\partial_x \mathbf{g} + B^T\partial_y \mathbf{g} + C^T\partial_z \mathbf{g} = \mathbf{0}. \end{cases}$$

We note m^{3D} the size of $\mathbf{u}$, i.e. the number of unknowns in the system, m_e^{3D} the number of even moments and m_o^{3D} the number of odd moments. Following [14, 20], one has

$$m^{3D} = m_e^{3D} + m_o^{3D} = (N+1)^2, \quad m_e^{3D} = \frac{1}{2}N(N+1) \quad \text{and} \quad m_o^{3D} = \frac{1}{2}(N+1)(N+2).$$

2.2. **3D configuration**

In this Section, we recall some important properties of the P_N model in dimension 3. The first one is the eigenvalue structure of matrices $\mathcal{A}_i$. The second one is the rotational invariance of the 3D model.

2.2.1. *Eigenvalue structure*

We recall a result on the structure of the spectrum of matrices $\mathcal{A}_i$, established by Garrett and Hauck.

Proposition 2.1 ([11])**.** *For any $\mathbf{v}$, $\mathbf{v}_* \in \mathbb{S}^2$, the matrices defined by*

$$M := \frac{1}{4\pi}\int_{\mathbb{S}^2} (\mathbf{v}\cdot\omega)\,\mathbf{X}\otimes\mathbf{X}d\omega, \quad \textit{and} \quad M_* := \frac{1}{4\pi}\int_{\mathbb{S}^2} (\mathbf{v}_*\cdot\omega)\,\mathbf{X}\otimes\mathbf{X}d\omega,$$

have the same eigenvalues, and their eigenvectors differ only by one unitary transformation. That is, if $M = \lambda\mathbf{v}$, then $M_*(U\mathbf{v}) = \lambda(U\mathbf{v})$ with U a unitary matrix.

From this, they deduced the following Corollary which is important from both the theoretical and the practical point of view.

Corollary 2.2 ([11])**.** *The eigenvalues of $\mathcal{A}_1$, $\mathcal{A}_2$ and $\mathcal{A}_3$ are equal and their eigenvectors differ only by one unitary transformation. Moreover, if λ is a nonzero eigenvalue of $\mathcal{A}_i$, then $-\lambda$ is also an eigenvalue.*

We finally recall a last important result about the eigenvalues of AA^T that has been established in Morel's PhD Thesis.

Proposition 2.3 ([20])**.** *The matrix AA^T is invertible and all its eigenvalues are strictly positive.*

2.2.2. *Rotational invariance in 3D*

We use the rotation matrices in the spherical harmonic basis (see [22])

$$\mathcal{U}(\alpha,\beta,\gamma) \in \mathbb{R}^{m^{3D}\times m^{3D}},$$

where α, β, γ are the rotation angles around the axes Ox, Oy, Oz respectively. In the configuration stated above, $\mathcal{U}(\alpha,\beta,\gamma)$ is a block matrix of the form (see [20, 22])

$$\mathcal{U}(\alpha,\beta,\gamma) = \operatorname{diag}\left(\Delta_0(\alpha,\beta,\gamma), \Delta_2(\alpha,\beta,\gamma), \ldots, \Delta_{m_e^{3D}}(\alpha,\beta,\gamma), \ldots, \Delta_{m_o^{3D}}(\alpha,\beta,\gamma)\right),$$

with

$$\Delta_k(\alpha,\beta,\gamma) = \mathcal{W}_k(\alpha)\mathcal{D}_k(\beta)\mathcal{W}_k(\gamma) \in \mathbb{R}^{(2k+1)\times(2k+1)}.$$

The matrix $\mathcal{D}_k \in \mathbb{R}^{(2k+1)\times(2k+1)}$ is a Wigner D-matrix [29] and the matrix $\mathcal{W}_k$ has nonzero elements only on its diagonal and its anti diagonal

$$\mathcal{W}_k(\alpha) = \begin{pmatrix} \cos k\alpha & & & & & & \sin k\alpha \\ & \ddots & & & & \iddots & \\ & & \cos 2\alpha & & \sin 2\alpha & & \\ & & & \cos\alpha & \sin\alpha & & \\ & 0 & & 1 & & 0 & \\ & & & -\sin\alpha & \cos\alpha & & \\ & & -\sin 2\alpha & & \cos 2\alpha & & \\ & \iddots & & & & \ddots & \\ -\sin k\alpha & & & & & & \cos k\alpha \end{pmatrix}.$$

Let us consider a rotation of angle θ in the xy plane

$$\mathcal{U}_\theta := \mathcal{U}(0,0,\theta) \in \mathbb{R}^{m^{3D}\times m^{3D}}.$$

It reads

$$\mathcal{U}_\theta = \operatorname{diag}\left(\mathcal{W}_0(\theta), \mathcal{W}_2(\theta), \ldots, \mathcal{W}_{m_e^{3D}}(\theta), \mathcal{W}_1(\theta), \ldots, \mathcal{W}_{m_o^{3D}}(\theta)\right).$$

The matrix $\mathcal{U}$ represents the action of an orthogonal transformation on $\mathbf{X}(\omega)$, that is, if $Q \in \mathbb{R}^{3\times 3}$ is an orthogonal matrix, then

$$\mathbf{X}(Q\omega) = \mathcal{U}(\alpha,\beta,\gamma)\mathbf{X}(\omega). \tag{2.5}$$

2.3. **2D configuration**

In the following, we limit ourselves to the 2D case. We assume that the solution has a symmetry with respect to the xy plane. This is equivalent to the fact that f is an even function of $\cos\beta$.

Proposition 2.4 ([14, 20])**.** *If f is even with respect to $\cos\beta$, moments f_k^m where $k+m$ is odd are zero.*

This choice simplifies the $\mathcal{A}_i$ matrices by removing rows and columns where $k+m$ is odd. We now describe the P_N model in 2D. We have for N an odd integer

$$m^{2D} = \frac{1}{2}(N+1)(N+2), \qquad m_e = \frac{1}{4}(N+1)^2, \qquad m_o = \frac{1}{4}(N+1)(N+3),$$

where m^{2D} is the number of unknowns, m_e the number of even moments and m_o the number of odd moments. Note that we always have $m_o > m_e$. The P_N model in dimension 2 writes

$$\partial_t \begin{pmatrix} \mathbf{g} \\ \mathbf{h} \end{pmatrix} + \mathcal{A}_1 \partial_x \begin{pmatrix} \mathbf{g} \\ \mathbf{h} \end{pmatrix} + \mathcal{A}_2 \partial_y \begin{pmatrix} \mathbf{g} \\ \mathbf{h} \end{pmatrix} = \mathbf{0}, \tag{2.6}$$

with

$$\mathcal{A}_1 = \begin{pmatrix} 0 & A \\ A^T & 0 \end{pmatrix}, \qquad \mathcal{A}_2 = \begin{pmatrix} 0 & B \\ B^T & 0 \end{pmatrix}. \tag{2.7}$$

After deleting the rows and columns that correspond to moments where $k+m$ is odd, the rotation matrix $\mathcal{U}_\theta$ reduces to [20]

$$\mathcal{U}_\theta = \begin{pmatrix} \mathcal{U}_\theta^{\mathbf{g}} & 0 \\ 0 & \mathcal{U}_\theta^{\mathbf{h}} \end{pmatrix}, \tag{2.8}$$

with

$$\mathcal{U}_\theta^{\mathbf{g}} = \begin{pmatrix} W_0 & & & 0 \\ & W_2 & & \\ & & \ddots & \\ 0 & & & W_{N-1} \end{pmatrix}, \qquad \mathcal{U}_\theta^{\mathbf{h}} = \begin{pmatrix} W_1 & & & 0 \\ & W_3 & & \\ & & \ddots & \\ 0 & & & W_N \end{pmatrix},$$

and where the W_k are defined by

$$W_{2k+1}(\theta) = \begin{pmatrix} \cos(2k+1)\theta & & & & & & & \sin(2k+1)\theta \\ & \ddots & & & 0 & & \iddots & \\ & & \cos 3\theta & & & \sin 3\theta & & \\ & 0 & & \cos\theta & \sin\theta & & 0 & \\ & & & -\sin\theta & \cos\theta & & & \\ & & -\sin 3\theta & & & \cos 3\theta & & \\ & \iddots & & & 0 & & \ddots & \\ -\sin(2k+1)\theta & & & & & & & \cos(2k+1)\theta \end{pmatrix},$$

and

$$W_{2k}(\theta) = \begin{pmatrix} \cos 2k\theta & & & & & & \sin 2k\theta \\ & \ddots & & 0 & & \iddots & \\ & & \cos 2\theta & & \sin 2\theta & & \\ & 0 & & 1 & & 0 & \\ & & -\sin 2\theta & & \cos 2\theta & & \\ & \iddots & & 0 & & \ddots & \\ -\sin 2k\theta & & & & & & \cos 2k\theta \end{pmatrix}. \tag{2.9}$$

In order to fix ideas, we provide examples of matrices A, $\mathcal{U}_\theta^{\mathbf{g}}$ and $\mathcal{U}_\theta^{\mathbf{h}}$ in Appendix C.

Finally we have as in 3D, the relations

Proposition 2.5 (Invariance by 2D rotation [20])**.** *The matrices $\mathcal{A}_1$ and $\mathcal{A}_2$ satisfy the relations*

$$\mathcal{A}_1\cos\theta + \mathcal{A}_2\sin\theta = \mathcal{U}_\theta\mathcal{A}_1\mathcal{U}_{-\theta}, \qquad -\mathcal{A}_1\sin\theta + \mathcal{A}_2\cos\theta = \mathcal{U}_\theta\mathcal{A}_2\mathcal{U}_{-\theta}.$$

Remark 2.6. An interesting particular case is $\theta = \frac{\pi}{2}$

$$\mathcal{A}_2 = \mathcal{U}_{\frac{\pi}{2}}\mathcal{A}_1\mathcal{U}_{-\frac{\pi}{2}}.$$

Let us give a last result that plays a significant role in the construction and in the analysis of the numerical scheme that will be proposed in the next Section. Actually, we will use a particular diagonalization of $\mathcal{A}_1$.

Proposition 2.7 ([3])**.** *The matrix $\mathcal{A}_1$ admits the diagonalization $\mathcal{A}_1 = PDP^T$ with*

$$P = \frac{1}{\sqrt{2}}\begin{pmatrix} P_{\mathbf{g}} & P_{\mathbf{g}} & 0 \\ P_{\mathbf{h}} & -P_{\mathbf{h}} & \sqrt{2}P_{0,\mathbf{h}} \end{pmatrix}, \qquad D = \begin{pmatrix} D_+ & 0 & 0 \\ 0 & -D_+ & 0 \\ 0 & 0 & 0 \end{pmatrix},$$

such that

- *$D_+ \in \mathbb{R}^{m_e\times m_e}$ is positive definite diagonal,*
- *$P_{\mathbf{g}} \in \mathbb{R}^{m_e\times m_e}$ is orthogonal,*

- *the columns of* $P_{\mathbf{h}} \in \mathbb{R}^{m_o \times m_e}$ *are orthonormal vectors,*
- *the columns of* $P_{0,\mathbf{h}} \in \mathbb{R}^{m_o \times (m_o - m_e)}$ *form an orthonormal basis of* $\operatorname{Ker} A$ *and are orthogonal to the columns of* $P_{\mathbf{h}}$.

Moreover one has $A = P_{\mathbf{g}} D_+ P_{\mathbf{h}}^T$.

Lemma 2.8 ([2])**.** *If* N *is odd, one has* $\dim \operatorname{Ker} A = m_o - m_e = \frac{N+1}{2}$.

3. Finite volume scheme

In this Section, we define the Glace [5, 6, 18] and Eucclhyd [16] schemes for the P_N model. We first study the 1D case, using a formalism close to the 2D. Then we study the 2D case and we show that these schemes are well defined if the mesh is not degenerated, i.e. under the same conditions as the nodal finite volume scheme for P_1. We then give several properties of the Glace and Eucclhyd schemes for P_N, in particular we show their convergences for a sufficiently regular initial data.

3.1. Definition of the scheme

In order to ease the introduction of the nodal finite volume scheme in 2D, we first consider the 1D case.

3.1.1. *Dimension 1*

In dimension 1, the P_N model recasts as

$$\partial_t \begin{pmatrix} \mathbf{g} \\ \mathbf{h} \end{pmatrix} + \mathcal{A}_1 \partial_x \begin{pmatrix} \mathbf{g} \\ \mathbf{h} \end{pmatrix} = \mathbf{0}.$$

We use the Proposition 2.7 to write $\mathcal{A}_1 = PDP^T$, with

$$P = \begin{pmatrix} P_+ & P_- & P_0 \end{pmatrix},$$

where P_+ (respectively P_-) is the matrix composed of the eigenvectors corresponding to the positive (respectively negative) eigenvalues, and P_0 the matrix composed of the eigenvectors corresponding to the null eigenvalues. We then rewrite the system as

$$\partial_t \mathbf{w} + D \partial_x \mathbf{w} = \mathbf{0},$$

with $\mathbf{w} = P^T \begin{pmatrix} \mathbf{g} \\ \mathbf{h} \end{pmatrix}$ the Riemann invariants.

Standard finite volume scheme. The derivation of such a scheme is quite straightforward following [12] or [25]. It is detailed here to fix ideas and to enlighten the difficulties that arise in the case of a nodal finite volume discretization.

Let $\mathcal{M}$ be an admissible mesh, and $j \in \mathcal{J} = \{1, \dots, N_c\}$ be a cell of the mesh. Here, $N_c = \#\mathcal{J}$ denotes the number of cells of the mesh. We note $\Delta x_j > 0$ the length of the cell j ($\Delta x_j = x_{j+\frac{1}{2}} - x_{j-\frac{1}{2}}$). We write the finite volume scheme

$$\frac{d}{dt}\mathbf{w}_j + \frac{1}{\Delta x_j} \begin{pmatrix} D_+ & 0 & 0 \\ 0 & D_- & 0 \\ 0 & 0 & 0 \end{pmatrix} (\mathbf{w}_{j+\frac{1}{2}} - \mathbf{w}_{j-\frac{1}{2}}) = \mathbf{0}. \tag{3.1}$$

Recall that, due to the eigenvalue structure of $\mathcal{A}_1$, we have $D_- = -D_+$.

We compute the value of the first order fluxes by using the upwind value

$$\begin{cases} \mathbf{w}^+_{j+\frac{1}{2}} = \mathbf{w}^+_j, \\ \mathbf{w}^-_{j+\frac{1}{2}} = \mathbf{w}^-_{j+1}. \end{cases}$$

With $\mathbf{w}^\pm_j$ the vector of Riemann invariants corresponding to positive (respectively negative) eigenvalues. We also note $\mathbf{w}^0_j$ the vector of Riemann invariants corresponding to zero eigenvalues.

Injecting these fluxes in (3.1), we get

$$\frac{d}{dt}\begin{pmatrix} \mathbf{w}^+_j \\ \mathbf{w}^-_j \\ \mathbf{w}^0_j \end{pmatrix} + \frac{1}{\Delta x_j}\begin{pmatrix} D_+ & 0 & 0 \\ 0 & -D_+ & 0 \\ 0 & 0 & 0 \end{pmatrix}\begin{pmatrix} \mathbf{w}^+_j - \mathbf{w}^+_{j-1} \\ \mathbf{w}^-_{j+1} - \mathbf{w}^-_j \\ 0 \end{pmatrix} = \mathbf{0}.$$

Multiplying by P on the left, we finally find

$$\frac{d}{dt}\begin{pmatrix} \mathbf{g}_j \\ \mathbf{h}_j \end{pmatrix} + \frac{1}{\Delta x_j} P \begin{pmatrix} D_+ & 0 & 0 \\ 0 & -D_+ & 0 \\ 0 & 0 & 0 \end{pmatrix}\left[\begin{pmatrix} P^T_+ \\ 0 \\ 0 \end{pmatrix}\begin{pmatrix} \mathbf{g}_j - \mathbf{g}_{j-1} \\ \mathbf{h}_j - \mathbf{h}_{j-1} \end{pmatrix} + \begin{pmatrix} 0 \\ P^T_- \\ 0 \end{pmatrix}\begin{pmatrix} \mathbf{g}_{j+1} - \mathbf{g}_j \\ \mathbf{h}_{j+1} - \mathbf{h}_j \end{pmatrix}\right] = \mathbf{0}. \tag{3.2}$$

Proposition 3.1. *The scheme* (3.2) *is conservative.*

Proof. Without any loss of generality the proof is performed in the case of periodic boundary conditions. The system (3.1) being entirely decoupled and composed of m^{2D} scalar equations, we can write directly that

$$\begin{aligned} \sum_{j\in\mathcal{J}} \Delta x_j \frac{d}{dt}\mathbf{w}_j &= -\sum_{j\in\mathcal{J}}\begin{pmatrix} D_+ & 0 & 0 \\ 0 & -D_+ & 0 \\ 0 & 0 & 0 \end{pmatrix}(\mathbf{w}_{j+\frac{1}{2}} - \mathbf{w}_{j-\frac{1}{2}}), \\ &= -\begin{pmatrix} D_+ & 0 & 0 \\ 0 & -D_+ & 0 \\ 0 & 0 & 0 \end{pmatrix}\sum_{j\in\mathcal{J}}(\mathbf{w}_{j+\frac{1}{2}} - \mathbf{w}_{j-\frac{1}{2}}) = \mathbf{0}, \end{aligned}$$

where we used the fact that the sum of the second line is telescopic. Finally, since $\mathbf{w} = P^T\begin{pmatrix} \mathbf{g} \\ \mathbf{h} \end{pmatrix}$, we have

$$\sum_{j\in\mathcal{J}} \Delta x_j \frac{d}{dt}\begin{pmatrix} \mathbf{g}_j \\ \mathbf{h}_j \end{pmatrix} = \mathbf{0}. \qquad \blacksquare$$

Nodal finite volume scheme. Following the work of [1, 5], we now write the solver at nodes

$$\frac{d}{dt}\begin{pmatrix} \mathbf{g}_j \\ \mathbf{h}_j \end{pmatrix} + \frac{1}{\Delta x_j}\mathcal{A}_1\begin{pmatrix} \mathbf{g}_{j,j+\frac{1}{2}} - \mathbf{g}_{j,j-\frac{1}{2}} \\ \mathbf{h}_{j+\frac{1}{2}} - \mathbf{h}_{j-\frac{1}{2}} \end{pmatrix} = \mathbf{0}. \tag{3.3}$$

One should note that in view of writing a nodal solver in 2D, the fluxes $\mathbf{g}_{j,j+\frac{1}{2}}$ may differ from $\mathbf{g}_{j+1,j+\frac{1}{2}}$. The continuity of the fluxes and thus the local conservativity are no more encoded directly in the scheme structure.

Also, in view of 2D case, we will write the scheme using new notations and substitute $\mathcal{A}_1$ according to (2.7). It gives

$$\begin{cases} \dfrac{d}{dt}\mathbf{g}_j + \dfrac{1}{\Delta x_j}\displaystyle\sum_{r\in\mathcal{R}_j} AC_{jr}\mathbf{h}_r = \mathbf{0} \\ \dfrac{d}{dt}\mathbf{h}_j + \dfrac{1}{\Delta x_j}\displaystyle\sum_{r\in\mathcal{R}_j} A^T C_{jr}\mathbf{g}_{jr} = \mathbf{0}, \end{cases} \tag{3.4}$$

with $\mathcal{R}_j = \{j - \frac{1}{2}, j + \frac{1}{2}\}$, and

$$C_{jr} = \begin{cases} +1 & \text{if } r = j + \frac{1}{2}, \\ -1 & \text{if } r = j - \frac{1}{2}. \end{cases}$$

At this stage, there are more unknowns than equations. However, following [18], we first restore the conservation of the scheme by adding the condition

$$\sum_{j \in \mathcal{J}_r} A^T C_{jr} \mathbf{g}_{jr} = \mathbf{0}, \tag{3.5}$$

where $\mathcal{J}_r$ is the set of cells connected to the vertex r (for example if $r = j + \frac{1}{2}$, $\mathcal{J}_r = \{j, j+1\}$).

Proposition 3.2. *The scheme* (3.4)–(3.5) *is conservative.*

Proof. Without any loss of generality, the proof is written in the case of periodic boundary conditions. Let us treat each equation of (3.4) separately. On the one hand, for the first equation

$$\sum_{j \in \mathcal{J}} \Delta x_j \frac{d}{dt} \mathbf{g}_j = - \sum_{j \in \mathcal{J}} \sum_{r \in \mathcal{R}_j} A C_{jr} \mathbf{h}_r, \tag{3.6}$$

$$= - \sum_{r \in \mathcal{R}} \underbrace{\left(\sum_{j \in \mathcal{J}_r} C_{jr} \right)}_{=0} A \mathbf{h}_r = \mathbf{0}. \tag{3.7}$$

On the other hand, for the second equation

$$\sum_{j \in \mathcal{J}} \Delta x_j \frac{d}{dt} \mathbf{h}_j = - \sum_{j \in \mathcal{J}} \sum_{r \in \mathcal{R}_j} A^T C_{jr} \mathbf{g}_{jr}, \tag{3.8}$$

$$= - \sum_{r \in \mathcal{R}} \underbrace{\left(\sum_{j \in \mathcal{J}_r} A^T C_{jr} \mathbf{g}_{jr} \right)}_{= \mathbf{0} \text{ by } (3.5)} = \mathbf{0}. \tag{3.9}$$

The scheme (3.4)–(3.5) is therefore conservative. ∎

As for standard finite volume schemes, the fluxes are computed thanks to the Riemann invariants

$$\begin{cases} P_+^T \begin{pmatrix} \mathbf{g}_{j,j+\frac{1}{2}} \\ \mathbf{h}_{j+\frac{1}{2}} \end{pmatrix} = P_+^T \begin{pmatrix} \mathbf{g}_j \\ \mathbf{h}_j \end{pmatrix}, \quad \text{and} & (3.10) \\ P_-^T \begin{pmatrix} \mathbf{g}_{j+1,j+\frac{1}{2}} \\ \mathbf{h}_{j+\frac{1}{2}} \end{pmatrix} = P_-^T \begin{pmatrix} \mathbf{g}_{j+1} \\ \mathbf{h}_{j+1} \end{pmatrix}, & (3.11) \end{cases}$$

with the notations of (3.3). We can write this system of equations in a unified way with the use of the rotation matrices $\mathcal{U}_\theta$ (2.8)

$$P_+^T \mathcal{U}_{-\theta_{jr}} \begin{pmatrix} \mathbf{g}_{jr} \\ \mathbf{h}_r \end{pmatrix} = P_+^T \mathcal{U}_{-\theta_{jr}} \begin{pmatrix} \mathbf{g}_j \\ \mathbf{h}_j \end{pmatrix}. \tag{3.12}$$

As we are in 1D, the only possible values of θ_{jr} are

$$\theta_{jr} = \begin{cases} 0 & \text{if } r = j + \frac{1}{2}, \\ \pi & \text{if } r = j - \frac{1}{2}, \end{cases}$$

moreover we have

$$P_+^T \mathcal{U}_\pi = P_-^T.$$

To calculate the $\mathbf{g}_{jr}$ fluxes, we write the decomposition of the Proposition 2.7

$$P_{\pm}^T = \begin{pmatrix} P_{\mathbf{g}}^T & \pm P_{\mathbf{h}}^T \end{pmatrix}, \qquad \mathcal{U}_{\theta_{jr}} = \begin{pmatrix} \mathcal{U}_{\theta_{jr}}^{\mathbf{g}} & 0 \\ 0 & \mathcal{U}_{\theta_{jr}}^{\mathbf{h}} \end{pmatrix}. \tag{3.13}$$

We then develop the matrix products of (3.12)

$$P_{\mathbf{g}}^T \mathcal{U}_{-\theta_{jr}}^{\mathbf{g}} \mathbf{g}_{jr} + P_{\mathbf{h}}^T \mathcal{U}_{-\theta_{jr}}^{\mathbf{h}} \mathbf{h}_r = P_{\mathbf{g}}^T \mathcal{U}_{\theta_{jr}}^{\mathbf{g}} \mathbf{g}_j + P_{\mathbf{h}}^T \mathcal{U}_{\theta_{jr}}^{\mathbf{h}} \mathbf{h}_j,$$

so we can compute

$$\mathbf{g}_{jr} = \mathbf{g}_j + \mathcal{U}_{\theta_{jr}}^{\mathbf{g}} P_{\mathbf{g}} P_{\mathbf{h}}^T \mathcal{U}_{-\theta_{jr}}^{\mathbf{h}} (\mathbf{h}_j - \mathbf{h}_r). \tag{3.14}$$

We then inject (3.14) into (3.5) which gives

$$\sum_{j \in \mathcal{J}_r} A^T \mathcal{U}_{\theta_{jr}}^{\mathbf{g}} P_{\mathbf{g}} P_{\mathbf{h}}^T \mathcal{U}_{-\theta_{jr}}^{\mathbf{h}} C_{jr} \mathbf{h}_r = \sum_{j \in \mathcal{J}_r} A^T C_{jr} \mathbf{g}_j + \sum_{j \in \mathcal{J}_r} A^T \mathcal{U}_{\theta_{jr}}^{\mathbf{g}} P_{\mathbf{g}} P_{\mathbf{h}}^T \mathcal{U}_{-\theta_{jr}}^{\mathbf{h}} C_{jr} \mathbf{h}_j.$$

By writing the sum explicitly (with $\mathcal{J}_r = \{j, j+1\}$), we finally find that

$$\begin{aligned} A^T \mathcal{U}_0^{\mathbf{g}} P_{\mathbf{g}} P_{\mathbf{h}}^T \mathcal{U}_0^{\mathbf{h}} \mathbf{h}_r + A^T \mathcal{U}_{\pi}^{\mathbf{g}} P_{\mathbf{g}} P_{\mathbf{h}}^T \mathcal{U}_{-\pi}^{\mathbf{h}} (-\mathbf{h}_r) \\ = A^T (\mathbf{g}_j - \mathbf{g}_{j+1}) + A^T \mathcal{U}_0^{\mathbf{g}} P_{\mathbf{g}} P_{\mathbf{h}}^T \mathcal{U}_0^{\mathbf{h}} \mathbf{h}_j + A^T \mathcal{U}_{\pi}^{\mathbf{g}} P_{\mathbf{g}} P_{\mathbf{h}}^T \mathcal{U}_{-\pi}^{\mathbf{h}} (-\mathbf{h}_{j+1}). \end{aligned}$$

Denoting by I the identity matrix, one observes that

$$\begin{aligned} \mathcal{U}_0^{\mathbf{g}} &= -\mathcal{U}_{\pi}^{\mathbf{g}} = -I, \\ \text{and} \quad \mathcal{U}_0^{\mathbf{h}} &= -\mathcal{U}_{\pi}^{\mathbf{h}} = -I. \end{aligned}$$

Therefore we get

$$2 A^T P_{\mathbf{g}} P_{\mathbf{h}}^T \mathbf{h}_r = A^T (\mathbf{g}_j - \mathbf{g}_{j+1}) + A^T P_{\mathbf{g}} P_{\mathbf{h}}^T (\mathbf{h}_j - \mathbf{h}_{j+1}). \tag{3.15}$$

Actually, the matrix $A^T P_{\mathbf{g}} P_{\mathbf{h}}^T$ is not invertible. Indeed, we have $A^T \in \mathbb{R}^{m_o \times m_e}$ and $P_{\mathbf{g}} P_{\mathbf{h}}^T \in \mathbb{R}^{m_e \times m_o}$. By the Rank Theorem we have

$$\dim \operatorname{Ker} P_{\mathbf{g}} P_{\mathbf{h}}^T + \operatorname{rank} P_{\mathbf{g}} P_{\mathbf{h}}^T = m_o.$$

As $\operatorname{rank} P_{\mathbf{g}} P_{\mathbf{h}}^T \leq m_e$, then $\dim \operatorname{Ker} P_{\mathbf{g}} P_{\mathbf{h}}^T \geq m_o - m_e > 0$, thus $\operatorname{Ker} P_{\mathbf{g}} P_{\mathbf{h}}^T \neq \{\mathbf{0}\}$. Take $\mathbf{v} \in \operatorname{Ker} P_{\mathbf{g}} P_{\mathbf{h}}^T$ not null, then

$$A^T P_{\mathbf{g}} P_{\mathbf{h}}^T \mathbf{v} = A^T \mathbf{0} = \mathbf{0} \quad \text{and} \quad \operatorname{Ker} A^T P_{\mathbf{g}} P_{\mathbf{h}}^T \neq \{\mathbf{0}\},$$

therefore the matrix is not invertible.

This is due to the fact that we started from the 2D equation to get to the 1D, assuming that $\partial_y = 0$. This has the expected effect that the matrix $\mathcal{A}_1$ always has zero eigenvalues.

We shall show in the following, that in 2D, the nodal finite volume scheme is well defined, the nodal matrix will be invertible under classical assumptions on the mesh.

3.1.2. *Dimension 2*

We will now write the nodal scheme in dimension 2, still inspired by the work of [1, 5].

Definition 3.3 (Admissible mesh)**.** Let $\mathcal{M}$ denote a conformal mesh of a polygonal connected open set $\Omega \subset \mathbb{R}^2$. Let $\mathcal{J}$ denote the set of all cells of the mesh $\mathcal{M}$. Let also denote by $\mathcal{R}$ the set of all vertices of the mesh.

The mesh is admissible if one has

(1) $\forall j \in \mathcal{J}$, j is a simple polygon: it does not intersect itself and has no holes. This implies that the area of j is positive.

(2) $\forall r \in \mathcal{R}$, their exists $j \in \mathcal{J}$ such that r is a vertex of the polygon j.

(3) $\forall j \in \mathcal{J}$, if s is a vertex of j, then $s \in \mathcal{R}$.

(4) $\forall j \neq k \in \mathcal{J}$, one has

$$\overline{j} \cap \overline{k} = \begin{cases} \text{the unique common edge of } j \text{ and } k, \text{ or,} \\ \text{the unique common vertex of } j \text{ and } k, \text{ or,} \\ \varnothing. \end{cases}$$

(5) $\forall r \neq s \in \mathcal{R}$, $\mathbf{x}_r \neq \mathbf{x}_s$.

Let us first precise the difficulty of the construction of a nodal scheme for P_N. In [1, 5] and in this work, the scheme is well-defined as soon as the odd fluxes $\mathbf{h}_r$, which are solutions of linear systems of the form $M_r \mathbf{h}_r = \mathbf{b}_r$, can be computed. In the case of the proposed P_N nodal solvers, $\mathbf{h}_r$ is given below by (3.20), with (3.21) for the Glace scheme and with (3.29) for the Eucclhyd scheme.

In [1, 5], $\mathbf{h}_r \in \mathbb{R}^d$ and the M_r matrices are invertible (omitting boundary conditions) as soon as $\forall r$, $\text{span}(\{\mathbf{C}_{jr}\}_{j \in \mathcal{J}_r}) = \mathbb{R}^d$. ($\mathbf{C}_{jr}$ vectors are represented on Figure 3.1). This geometrical constraint is naturally satisfied considering admissible meshes.

For the P_N nodal schemes that are studied in this paper, $\mathbf{h}_r \in \mathbb{R}^{m_o}$ and the invertibility of matrices M_r is more difficult to prove. We establish below that the scheme is well-defined under the exact same mesh condition.

Glace scheme. Recall that the P_N model in 2D reads

$$\partial_t \begin{pmatrix} \mathbf{g} \\ \mathbf{h} \end{pmatrix} + \mathcal{A}_1 \partial_x \begin{pmatrix} \mathbf{g} \\ \mathbf{h} \end{pmatrix} + \mathcal{A}_2 \partial_y \begin{pmatrix} \mathbf{g} \\ \mathbf{h} \end{pmatrix} = \mathbf{0}.$$

Let $\mathcal{M}$ be an admissible mesh, and $j \in \mathcal{J}$, $\mathcal{J}$ denoting the set of cells of $\mathcal{M}$. We write the finite volume scheme in semi-discrete form

$$\begin{cases} \dfrac{d}{dt}\mathbf{g}_j + \dfrac{1}{V_j} \displaystyle\sum_{r \in \mathcal{R}_j} l_{jr}(n_{jr}^x A + n_{jr}^y B)\mathbf{h}_r = \mathbf{0} \\ \dfrac{d}{dt}\mathbf{h}_j + \dfrac{1}{V_j} \displaystyle\sum_{r \in \mathcal{R}_j} l_{jr}(n_{jr}^x A^T + n_{jr}^y B^T)\mathbf{g}_{jr} = \mathbf{0}, \end{cases} \tag{3.16}$$

where $\mathbf{n}_{jr} = (n_{jr}^x, n_{jr}^y)$ is the outgoing normal to the vertex r of the cell j. More precisely, following [5] for instance, one sets

$$\mathbf{C}_{jr} := \nabla_{\mathbf{x}_r} V_j, \quad l_{jr} := \|\mathbf{C}_{jr}\| \quad \text{and} \quad \mathbf{n}_{jr} := \frac{1}{l_{jr}} \mathbf{C}_{jr}.$$

In the particular case of polygonal cells, one has

$$\mathbf{C}_{jr} = -\frac{1}{2}(\mathbf{x}_{r+1} - \mathbf{x}_{r-1})^{\perp}.$$

Here, we also denoted by $\mathcal{R}_j$ the set of vertices of the cell j and $\mathcal{J}_r$ is the set of cells that have r as a vertex, V_j denotes the area of the cell j. See Figure 3.1 for an illustration.

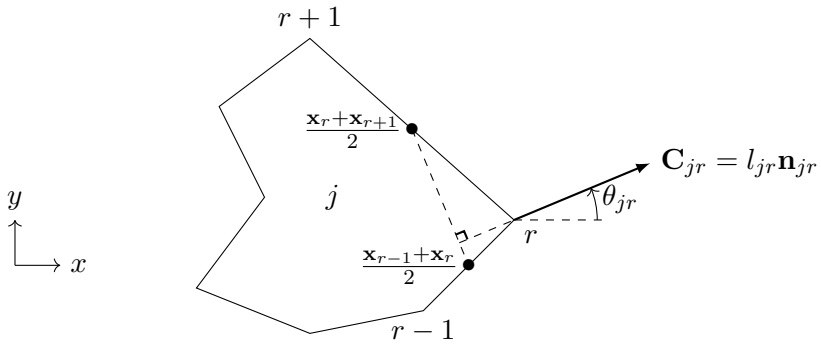

FIGURE 3.1. Illustration of the notations for the Glace scheme

In the following, we note $\mathbf{n}_{jr} = (\cos\theta_{jr}, \sin\theta_{jr})$, and $\mathcal{U}_{\theta_{jr}}$ the rotation matrix described above (2.8). Using that

$$\mathcal{U}_{\theta_{jr}} = \begin{pmatrix} \mathcal{U}^{\mathbf{g}}_{\theta_{jr}} & 0 \\ 0 & \mathcal{U}^{\mathbf{h}}_{\theta_{jr}} \end{pmatrix},$$

we write

$$\begin{aligned} \mathcal{U}_{\theta_{jr}}\mathcal{A}_1\mathcal{U}_{-\theta_{jr}} &= \begin{pmatrix} \mathcal{U}^{\mathbf{g}}_{\theta_{jr}} & 0 \\ 0 & \mathcal{U}^{\mathbf{h}}_{\theta_{jr}} \end{pmatrix} \begin{pmatrix} 0 & A \\ A^T & 0 \end{pmatrix} \begin{pmatrix} \mathcal{U}^{\mathbf{g}}_{-\theta_{jr}} & 0 \\ 0 & \mathcal{U}^{\mathbf{h}}_{-\theta_{jr}} \end{pmatrix}, \\ &= \begin{pmatrix} 0 & \mathcal{U}^{\mathbf{g}}_{\theta_{jr}} A \mathcal{U}^{\mathbf{h}}_{-\theta_{jr}} \\ \mathcal{U}^{\mathbf{h}}_{\theta_{jr}} A^T \mathcal{U}^{\mathbf{g}}_{-\theta_{jr}} & 0 \end{pmatrix}. \end{aligned}$$

Thus (3.16) rewrites, using the Proposition 2.5

$$\begin{cases} \dfrac{d}{dt}\mathbf{g}_j + \dfrac{1}{V_j}\displaystyle\sum_{r\in\mathcal{R}_j} l_{jr}\mathcal{U}^{\mathbf{g}}_{\theta_{jr}} A \mathcal{U}^{\mathbf{h}}_{-\theta_{jr}}\mathbf{h}_r = \mathbf{0}, \\ \dfrac{d}{dt}\mathbf{h}_j + \dfrac{1}{V_j}\displaystyle\sum_{r\in\mathcal{R}_j} l_{jr}\mathcal{U}^{\mathbf{h}}_{\theta_{jr}} A^T \mathcal{U}^{\mathbf{g}}_{-\theta_{jr}}\mathbf{g}_{jr} = \mathbf{0}. \end{cases} \tag{3.17}$$

By noting $P_{\theta_{jr}}$ the eigenvector matrix of $\mathcal{U}_{\theta_{jr}}\mathcal{A}_1\mathcal{U}_{-\theta_{jr}}$, we have

$$P^T_{\theta_{jr}} = P^T\mathcal{U}_{-\theta_{jr}}.$$

We then impose the Riemann invariants in the direction of the positive eigenvalues

$$P^T_+\mathcal{U}_{-\theta_{jr}}\begin{pmatrix}\mathbf{g}_{jr}\\ \mathbf{h}_r\end{pmatrix} = P^T_+\mathcal{U}_{-\theta_{jr}}\begin{pmatrix}\mathbf{g}_j\\ \mathbf{h}_j\end{pmatrix},$$

by doing the same decomposition as for the 1D case, we obtain the system

$$P^T_{\mathbf{g}}\mathcal{U}^{\mathbf{g}}_{-\theta_{jr}}\mathbf{g}_{jr} + P^T_{\mathbf{h}}\mathcal{U}^{\mathbf{h}}_{-\theta_{jr}}\mathbf{h}_r = P^T_{\mathbf{g}}\mathcal{U}^{\mathbf{g}}_{-\theta_{jr}}\mathbf{g}_j + P^T_{\mathbf{h}}\mathcal{U}^{\mathbf{h}}_{-\theta_{jr}}\mathbf{h}_j.$$

Then recalling that according to Proposition 2.7, $P_{\mathbf{g}}$ is an orthogonal matrix, one gets

$$\mathbf{g}_{jr} = \mathbf{g}_j + \mathcal{U}^{\mathbf{g}}_{\theta_{jr}} P_{\mathbf{g}} P^T_{\mathbf{h}} \mathcal{U}^{\mathbf{h}}_{-\theta_{jr}}(\mathbf{h}_j - \mathbf{h}_r). \tag{3.18}$$

At this stage, there are more unknowns than equations, so we add the following conservation constraint

$$\sum_{j\in\mathcal{J}_r} l_{jr}\mathcal{U}^{\mathbf{h}}_{\theta_{jr}} A^T \mathcal{U}^{\mathbf{g}}_{-\theta_{jr}}\mathbf{g}_{jr} = \mathbf{0}. \tag{3.19}$$

Injecting (3.18) into (3.19), we obtain the following linear system

$$\left(\sum_{j\in\mathcal{J}_r} M_{jr}\right)\mathbf{h}_r = \sum_{j\in\mathcal{J}_r} M_{jr}\mathbf{h}_j + \sum_{j\in\mathcal{J}_r} l_{jr}\mathcal{U}^{\mathbf{h}}_{\theta_{jr}} A^T \mathcal{U}^{\mathbf{g}}_{-\theta_{jr}}\mathbf{g}_j, \tag{3.20}$$

with

$$M_{jr} = l_{jr}\mathcal{U}^{\mathbf{h}}_{\theta_{jr}} A^T P_{\mathbf{g}} P^T_{\mathbf{h}} \mathcal{U}^{\mathbf{h}}_{-\theta_{jr}}. \tag{3.21}$$

Remark 3.4. The semi-discrete Glace scheme is thus defined by (3.17) with the fluxes given by (3.18) and (3.19).

For the scheme to be well defined it remains to show that $\mathbf{h}_r$ is uniquely defined. In other words, one has to show that

$$M_r := \sum_{j\in\mathcal{J}_r} M_{jr}$$

is invertible. This is the purpose of the remaining of this Section.

To do so, we shall first rewrite M_{jr} in a more convenient way. According to Proposition 2.7, $A = P_{\mathbf{g}} D_+ P^T_{\mathbf{h}}$, so

$$M_{jr} = l_{jr}\mathcal{U}^{\mathbf{h}}_{\theta_{jr}} A^T P_{\mathbf{g}} P^T_{\mathbf{h}} \mathcal{U}^{\mathbf{h}}_{-\theta_{jr}} = l_{jr}\mathcal{U}^{\mathbf{h}}_{\theta_{jr}} P_{\mathbf{h}} D_+ \underbrace{P^T_{\mathbf{g}} P_{\mathbf{g}}}_{=I} P^T_{\mathbf{h}} \mathcal{U}^{\mathbf{h}}_{-\theta_{jr}},$$

that is

$$M_{jr} = l_{jr}\mathcal{U}^{\mathbf{h}}_{\theta_{jr}} P_{\mathbf{h}} D_+ P^T_{\mathbf{h}} \mathcal{U}^{\mathbf{h}}_{-\theta_{jr}}. \tag{3.22}$$

Note that we have

$$A^T A = P_{\mathbf{h}} D_+ P^T_{\mathbf{g}} P_{\mathbf{g}} D_+ P^T_{\mathbf{h}} = P_{\mathbf{h}} D^2_+ P^T_{\mathbf{h}},$$

so we can write

$$P_{\mathbf{h}} D_+ P^T_{\mathbf{h}} = \left(A^T A\right)^{1/2}.$$

Finally

$$M_{jr} = l_{jr}\mathcal{U}^{\mathbf{h}}_{\theta_{jr}} \left(A^T A\right)^{1/2} \mathcal{U}^{\mathbf{h}}_{-\theta_{jr}}. \tag{3.23}$$

Proposition 3.5. *The matrix M_{jr} is a symmetric, positive semidefinite matrix.*

The proof is obvious by (3.22) since $\mathcal{U}^{\mathbf{h}}_{-\theta_{jr}} = {\mathcal{U}^{\mathbf{h}}_{\theta_{jr}}}^T$

In the following, we denote $M = P_{\mathbf{h}} D_+ P^T_{\mathbf{h}} = \left(A^T A\right)^{1/2}$. We now show that $M_r = \sum_{j\in\mathcal{J}_r} M_{jr}$ is invertible and under which conditions.

One has the equality

$$\operatorname{Ker} M = \operatorname{Ker} A, \tag{3.24}$$

thus we are brought back to study $\operatorname{Ker} A$.

Lemma 3.6. *Let $\mathbf{h} = (h^m_k)_{k,m \text{ odd}} \in \operatorname{Ker} A$, then $h^m_k = 0$ for all $k, m > 0$.*

Proof. Let us make a remark about the notations. Let us note (k_i, m_i) the index of a row, and (k_j, m_j) the index of a column, and $a_{(k_i,m_i),(k_j,m_j)}$ the coefficients of the matrix A. Note that we necessarily have that k_i and m_i are even, while k_j and m_j are odd. Indeed, since we are in dimension 2, according to Proposition 2.4, $h^m_k = 0$ if $m + k$ is odd. Thus since $\mathbf{h}$ corresponds to the odd moments of f, k is odd then so m must be odd too for h^m_k to be non zero. This sets that we are only interested in the case where k_j and m_j are odd. Now since we are looking for

$$\forall i, \qquad \sum_j a_{(k_i,m_i),(k_j,m_j)}\, h_{(k_j,m_j)} = 0,$$

one can check that the structure of A, first line of (2.4), that the only coefficients that are involved in the product are such that k_i and m_i are even.
We prove by induction.

Initialization. Let us study the result for $N = 3$. The matrix A is written as

$$A = \begin{pmatrix} 0 & \frac{1}{\sqrt{3}} & 0 & 0 & 0 & 0 \\ \frac{1}{\sqrt{5}} & 0 & \sqrt{\frac{3}{14}} & -\frac{1}{\sqrt{70}} & 0 & 0 \\ 0 & -\frac{1}{\sqrt{15}} & 0 & 0 & \sqrt{\frac{6}{35}} & 0 \\ 0 & -\frac{1}{\sqrt{5}} & 0 & 0 & -\frac{1}{\sqrt{70}} & \sqrt{\frac{3}{14}} \end{pmatrix}.$$

If $\mathbf{h} \in \operatorname{Ker} A$, the linear system $A\mathbf{h} = \mathbf{0}$ writes

$$\begin{cases} \frac{1}{\sqrt{3}} h_1^1 = 0, \\ \frac{1}{\sqrt{5}} h_1^{-1} + \sqrt{\frac{3}{14}} h_3^{-3} - \frac{1}{\sqrt{70}} h_3^{-1} = 0, \\ -\frac{1}{\sqrt{15}} h_1^1 + \sqrt{\frac{6}{35}} h_3^1 = 0, \\ -\frac{1}{\sqrt{5}} h_1^1 - \frac{1}{\sqrt{70}} h_3^1 + \sqrt{\frac{3}{14}} h_3^3 = 0. \end{cases}$$

So we get $h_1^1 = h_3^1 = h_3^3 = 0$. The result is true for $N = 3$.

Heredity. Let $\mathbf{h} = (h_{k_j}^{m_j})_{k_j, m_j \text{ odd}} \in \operatorname{Ker} A$. Recall that for (k, m) even then, according to (2.4)

$$(A\mathbf{h})_k^m = \varepsilon^m (A_k^m h_{k+1}^{m+1} - B_k^m h_{k-1}^{m+1}) - \zeta^m (C_k^m h_{k+1}^{m-1} - D_k^m h_{k-1}^{m-1}),$$

with the convention $h_k^m = 0$ if $k > N$ or $|m| > k$.
Suppose that for all $k_j < N - 1$, $0 < m_j \leq k_j$, odd, $h_{k_j}^{m_j}$=0. We distinguish three cases:

- Line of index $k_i = N - 1$ and $m_i < 0$.

  There is nothing to say because then $m_j = m_i - 1$ and $m_j = m_i + 1$ are always negative.

- Line of index $k_i = N - 1$ and $m_i = 0$.

  We have four *a priori* nonzero coefficients, which correspond to the index columns $(k_j = N - 2, m_j = -1)$, $(k_j = N - 2, m_j = 1)$, $(k_j = N, m_j = -1)$, $(k_j = N, m_j = 1)$. The coefficient $a_{(N-1,0),(N-2,-1)} = \zeta^0 D_{N-1}^0$ of A is null because $\zeta^0 = 0$. The coefficient h_{N-2}^1 is zero by hypothesis. The coefficient $a_{(N-1,0),(N,-1)} = -\zeta^0 C_{N-1}^0$ of A is null because $\zeta^0 = 0$. There remains then a coefficient, h_N^1 which is thus null.

- Line of index $k_i = N - 1$ and $m_i > 0$ even.

  We have four *a priori* nonzero coefficients, h_{N-2}^{m-1}, h_{N-2}^{m+1}, h_N^{m-1} and h_N^{m+1}. The coefficients h_{N-2}^{m-1}, h_{N-2}^{m+1} are zero by induction assumption. The fact that the last coefficients are zero follows from the structure of the matrix A. This can be seen by induction. The coefficient h_N^1 is zero according to the previous case, and so, on the next row, we will have the coefficients h_N^1 and h_N^3, so h_N^3 is also zero. Suppose that on the line $(N - 1, m_i - 2)$ with $m_i > 2$, the coefficients $h_N^{m_i-3}$ and $h_N^{m_i-1}$ are zero. If we now look at the line $(N - 1, m_i)$, the two a priori nonzero coefficients are $h_N^{m_i-1}$ and $h_N^{m_i+1}$, but $h_N^{m_i-1} = 0$ according to the work done in the previous line and so $h_N^{m_i+1}$ is also zero. It follows that we have $h_N^m = 0$ if $m > 0$.

In conclusion, for any odd k, if $m > 0$, odd, then $h_k^m = 0$. ∎

Theorem 3.7. *Take $\theta \in]0, \pi[$, thus the matrix*

$$M_\theta = M + \mathcal{U}_\theta^{\mathbf{h}} M \mathcal{U}_{-\theta}^{\mathbf{h}}$$

is invertible.

Proof. As M is symmetric positive semidefinite,

$$\operatorname{Ker} M_\theta = \operatorname{Ker} M \cap \operatorname{Ker} \mathcal{U}_\theta^{\mathbf{h}} M \mathcal{U}_{-\theta}^{\mathbf{h}}.$$

By using (3.24)

$$\operatorname{Ker} M_\theta = \operatorname{Ker} A \cap \operatorname{Ker} A \mathcal{U}_{-\theta}^{\mathbf{h}}.$$

We want to show that this intersection is null, as soon as $\theta \neq 0 \bmod \pi$. Let $\mathbf{h} = (h_k^m) \in \operatorname{Ker} A$, we want to show that if $\mathcal{U}_{-\theta}^{\mathbf{h}} \mathbf{h} \in \operatorname{Ker} A$, then $\mathbf{h} = \mathbf{0}$. By the Lemma 3.6, $\mathbf{h}$ is of the form

$$\mathbf{h} = \begin{pmatrix} h_1^{-1} \\ 0 \\ h_3^{-3} \\ h_3^{-1} \\ 0 \\ 0 \\ \vdots \end{pmatrix}$$

and therefore

$$\mathcal{U}_{-\theta}^{\mathbf{h}} \mathbf{h} = \begin{pmatrix} h_1^{-1} \cos\theta \\ h_1^{-1} \sin\theta \\ h_3^{-3} \cos 3\theta \\ h_3^{-1} \cos\theta \\ h_3^{-1} \sin\theta \\ h_3^{-3} \sin 3\theta \\ \vdots \end{pmatrix}.$$

If $\mathcal{U}_{-\theta}^{\mathbf{h}} \mathbf{h} \in \operatorname{Ker} A$ then, $h_k^m \sin(-m\theta) = 0$ for all k and $m < 0$. Three cases are possible:

- First case: If $\theta = 0 \bmod \pi$, this is forbidden by our assumptions.
- Second case: If $h_k^m = 0$ if $m < 0$, in this case we have $\mathbf{h} = \mathbf{0}$.
- Third case: If $h_k^m = 0$ for all $m < 0$ odd except for the m which are written $m = lp$ with $l \in \mathbb{N}^*$ and p a prime different from 2, in this case if we take $\theta = \frac{\pi}{p}$, we would have $\mathbf{h} \neq 0$ and $\mathcal{U}_{-\theta}^{\mathbf{h}} \mathbf{h} \in \operatorname{Ker} A$. However, this is impossible, because if we suppose that we are in this configuration and that $\mathbf{h} \neq \mathbf{0}$, we would then have at least $h_k^{-1} = 0$ for any $k \leq N$ odd, there are exactly $\frac{N+1}{2}$ coefficients of $\mathbf{h}$ of this form. However, the dimension of $\operatorname{Ker} A$ is $\frac{N+1}{2}$, so this necessarily imposes that all the other coefficients of $\mathbf{h}$ are zero, which gives rise to a contradiction.

In conclusion, we have shown that

$$\operatorname{Ker} M_\theta = \{\mathbf{0}\}.$$ ∎

Corollary 3.8. *If at least two $\mathbf{n}_{jr}$ with $j \in \mathcal{J}_r$ are non-collinear, then M_r is invertible.*

Proof. One writes

$$M_r = M_{j_1 r} + M_{j_2 r} + \sum_{j \in \mathcal{J}_r \setminus \{j_1, j_2\}} M_{jr},$$

and we suppose that $\mathbf{n}_{j_1 r}$ is not collinear to $\mathbf{n}_{j_2 r}$, we write

$$M_{j_1 r} + M_{j_2 r} = \mathcal{U}^{\mathbf{h}}_{\theta_{j_1 r}} M \mathcal{U}^{\mathbf{h}}_{-\theta_{j_1 r}} + \mathcal{U}^{\mathbf{h}}_{\theta_{j_2 r}} M \mathcal{U}^{\mathbf{h}}_{-\theta_{j_2 r}},$$

so

$$\mathcal{U}^{\mathbf{h}}_{-\theta_{j_1 r}} (M_{j_1 r} + M_{j_2 r}) \mathcal{U}^{\mathbf{h}}_{-\theta_{j_1 r}} = M + \mathcal{U}^{\mathbf{h}}_{-\theta_{j_2 r} + \theta_{j_1 r}} M \mathcal{U}^{\mathbf{h}}_{-(\theta_{j_2 r} - \theta_{j_1 r})}.$$

We are thus brought back to the case of the Theorem 3.7 by posing $\theta = \theta_{j_2 r} - \theta_{j_1 r} \neq 0 \bmod \pi$. Let $\mathbf{x} \in \operatorname{Ker} M_r$, then

$$\begin{aligned}(\mathbf{x}, M_r \mathbf{x}) &= \sum_{j \in \mathcal{J}_r} (\mathbf{x}, M_{jr} \mathbf{x}), \\ &= \sum_{j \in \mathcal{J}_r \setminus \{j_1, j_2\}} (\mathbf{x}, M_{jr} \mathbf{x}) + (\mathbf{x}, (M_{j_1 r} + M_{j_2 r}) \mathbf{x}).\end{aligned}$$

As $M_{j_1 r} + M_{j_2 r}$ is invertible and since it is positive semidefinite then it is positive definite. If $(\mathbf{x}, M_r \mathbf{x}) = 0$, then $(\mathbf{x}, (M_{j_1 r} + M_{j_2 r}) \mathbf{x}) = 0$ and so $\mathbf{x} = 0$, and M_r is invertible. ∎

Finally we rewrite the obtained Glace scheme on a more convenient form

$$\begin{cases} \dfrac{d}{dt} \mathbf{g}_j + \dfrac{1}{V_j} \displaystyle\sum_{r \in \mathcal{R}_j} l_{jr} \mathcal{U}^{\mathbf{g}}_{\theta_{jr}} A \mathcal{U}^{\mathbf{h}}_{-\theta_{jr}} \mathbf{h}_r = \mathbf{0}, \\ \dfrac{d}{dt} \mathbf{h}_j + \dfrac{1}{V_j} \displaystyle\sum_{r \in \mathcal{R}_j} \mathbf{F}_{jr} = \mathbf{0}, \end{cases} \tag{3.25}$$

with

$$\begin{cases} \mathbf{F}_{jr} = l_{jr} \mathcal{U}^{\mathbf{h}}_{\theta_{jr}} A^T \mathcal{U}^{\mathbf{g}}_{-\theta_{jr}} \mathbf{g}_j + M_{jr} (\mathbf{h}_j - \mathbf{h}_r), \\ \displaystyle\sum_{j \in \mathcal{J}_r} \mathbf{F}_{jr} = \mathbf{0}, \end{cases} \tag{3.26}$$

where $M_{jr} = l_{jr} \mathcal{U}^{\mathbf{h}}_{\theta_{jr}} M \mathcal{U}^{\mathbf{h}}_{-\theta_{jr}}$.

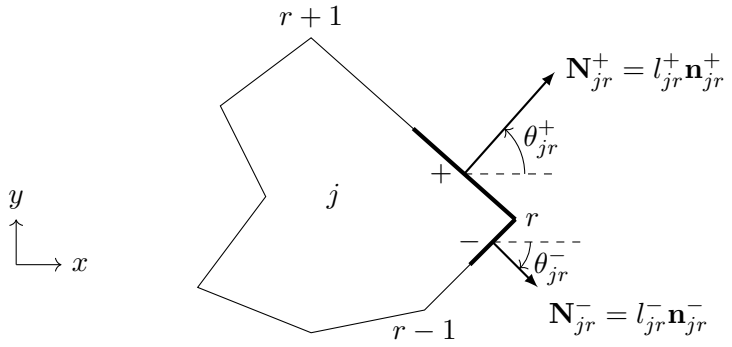

Figure 3.2. Illustration of the notations for the Eucclhyd scheme

Eucclhyd scheme. The Eucclhyd version of the nodal scheme consists in considering not one, but two Riemann invariants per cell and per vertex

$$\begin{cases} P_{\mathbf{g}}^T \mathcal{U}^{\mathbf{g}}_{-\theta_{jr}^+} \mathbf{g}_{jr}^+ + P_{\mathbf{h}}^T \mathcal{U}^{\mathbf{h}}_{-\theta_{jr}^+} \mathbf{h}_r = P_{\mathbf{g}}^T \mathcal{U}^{\mathbf{g}}_{-\theta_{jr}^+} \mathbf{g}_j + P_{\mathbf{h}}^T \mathcal{U}^{\mathbf{h}}_{-\theta_{jr}^+} \mathbf{h}_j, \\ P_{\mathbf{g}}^T \mathcal{U}^{\mathbf{g}}_{-\theta_{jr}^-} \mathbf{g}_{jr}^- + P_{\mathbf{h}}^T \mathcal{U}^{\mathbf{h}}_{-\theta_{jr}^-} \mathbf{h}_r = P_{\mathbf{g}}^T \mathcal{U}^{\mathbf{g}}_{-\theta_{jr}^-} \mathbf{g}_j + P_{\mathbf{h}}^T \mathcal{U}^{\mathbf{h}}_{-\theta_{jr}^-} \mathbf{h}_j, \end{cases} \tag{3.27}$$

and the conservation is given by

$$\sum_{j \in \mathcal{J}_r} l_{jr}^+ \mathcal{U}^{\mathbf{h}}_{\theta_{jr}^+} A^T \mathcal{U}^{\mathbf{g}}_{-\theta_{jr}^+} \mathbf{g}_{jr}^+ + l_{jr}^- \mathcal{U}^{\mathbf{h}}_{\theta_{jr}^-} A^T \mathcal{U}^{\mathbf{g}}_{-\theta_{jr}^-} \mathbf{g}_{jr}^- = \mathbf{0}. \tag{3.28}$$

As depicted on Figure 3.2, the outgoing normals considered at the node r of cell j are now chosen as

$$\begin{cases} \mathbf{N}_{jr}^+ := -\dfrac{1}{2}(\mathbf{x}_{r+1} - \mathbf{x}_r)^\perp, \quad l_{jr}^+ := \|\mathbf{N}_{jr}^+\|, \quad \mathbf{n}_{jr}^+ := -\dfrac{1}{l_{jr}^+}\mathbf{N}_{jr}^+, \\ \mathbf{N}_{jr}^- := -\dfrac{1}{2}(\mathbf{x}_r - \mathbf{x}_{r-1})^\perp, \quad l_{jr}^- := \|\mathbf{N}_{jr}^-\|, \quad \mathbf{n}_{jr}^- := -\dfrac{1}{l_{jr}^-}\mathbf{N}_{jr}^-. \end{cases}$$

One has $\mathbf{C}_{jr} = \mathbf{N}_{jr}^+ + \mathbf{N}_{jr}^-$. One then defines the angles $\theta_{jr}^\pm$ such that $\mathbf{n}_{jr}^\pm = (\cos\theta_{jr}^\pm, \sin\theta_{jr}^\pm)$.

Note that since $l_{jr}\mathbf{n}_{jr} = l_{jr}^+\mathbf{n}_{jr}^+ + l_{jr}^-\mathbf{n}_{jr}^-$, a direct consequence of Property 2.5 is

$$l_{jr}^+ \mathcal{U}_{\theta_{jr}^+} \mathcal{A}_1 \mathcal{U}_{-\theta_{jr}^+} + l_{jr}^- \mathcal{U}_{\theta_{jr}^-} \mathcal{A}_1 \mathcal{U}_{-\theta_{jr}^-} = l_{jr} \mathcal{U}_{\theta_{jr}} \mathcal{A}_1 \mathcal{U}_{-\theta_{jr}}.$$

By injecting (3.27) into (3.28), we find

$$\left(\sum_{j \in \mathcal{J}_r} M_{jr} \right) \mathbf{h}_r = \sum_{j \in \mathcal{J}_r} M_{jr} \mathbf{h}_j + \sum_{j \in \mathcal{J}_r} l_{jr} \mathcal{U}^{\mathbf{h}}_{\theta_{jr}} A^T \mathcal{U}^{\mathbf{g}}_{-\theta_{jr}} \mathbf{g}_j,$$

with

$$M_{jr} = l_{jr}^+ \mathcal{U}^{\mathbf{h}}_{\theta_{jr}^+} M \mathcal{U}^{\mathbf{h}}_{-\theta_{jr}^+} + l_{jr}^- \mathcal{U}^{\mathbf{h}}_{\theta_{jr}^-} M \mathcal{U}^{\mathbf{h}}_{-\theta_{jr}^-}. \tag{3.29}$$

This matrix is invertible according to the Theorem 3.7. We notice that, as for the Glace scheme, the Eucclhyd scheme is put in the form (3.25)–(3.26) with the particular choice of M_{jr} given by (3.29).

3.1.3. *Boundary conditions*

General boundary conditions for the P_N model can be quite complex. In the case of nodal solvers, one can directly impose the fluxes $\mathbf{h}_r$ or $\mathbf{g}_{jr}$ in the same fashion that it is done for Lagrangian hydrodynamics (see for instance [5]). For the sake of simplicity, we limit ourselves here to the case of symmetry boundary conditions (periodic boundary conditions treatment being straightforward).

Let us first recall the special case of particular interest where the boundary's normal vector is $\mathbf{n} = (1, 0)$.

Proposition 3.9 ([14])**.** *Let $\mathbf{n} = (1, 0)$. If $\mathbf{x} \in \partial\Omega$, then the symmetry boundary condition*

$$\forall (\omega, t) \in \mathbb{S}^2 \times [0, +\infty[\,, \quad f(\mathbf{x}, \omega, t) = f(\mathbf{x}, \omega - 2(\omega \cdot \mathbf{n})\mathbf{n}, t), \quad \textit{if} \quad \omega \cdot \mathbf{n} \leq 0, \tag{3.30}$$

implies the condition on the moments of f

$$\forall (\mathbf{x}, t) \in \partial\Omega \times [0, +\infty[\,, \quad f_k^m = 0 \quad \textit{if} \quad m > 0 \quad \textit{odd}.$$

If we now set $\mathbf{n} = (\cos\theta, \sin\theta)$, i.e. the boundary of Ω is arbitrary, then considering the rotation matrices $\mathcal{U}_\theta$, we come back to the case of the Proposition 3.9.

Proposition 3.10. *Take* $\mathbf{n} = (\cos\theta, \sin\theta)$ *with* $\theta \in [0, 2\pi[$. *If* $\mathbf{x} \in \partial\Omega$, *then the condition at the symmetry boundary condition*

$$\forall (\omega, t) \in \mathbb{S}^2 \times [0, +\infty[\,, \quad f(\mathbf{x}, \omega, t) = f(\mathbf{x}, \omega - 2(\omega \cdot \mathbf{n})\mathbf{n}, t) \quad \textit{if} \quad \omega \cdot \mathbf{n} \leq 0, \tag{3.31}$$

implies the condition on $\mathbf{u}$

$$\forall (\mathbf{x}, t) \in \partial\Omega \times [0, +\infty[\,, \quad (\mathcal{U}_{-\theta}\mathbf{u})_k^m (\mathbf{x}, t) = 0 \quad \textit{if} \quad m > 0 \quad \textit{odd}.$$

To apply the boundary conditions to the scheme (i.e. to compute the fluxes), we notice that we only need to make modifications on the computation of $\mathbf{h}_r$. Thus, if r is a node of the boundary of Ω, we take the linear system

$$M_r \mathbf{h}_r = \mathbf{B}_r,$$

with $M_r = \sum_{j \in \mathcal{J}} M_{jr}$ and $\mathbf{B}_r = \sum_{j \in \mathcal{J}_r} M_{jr}\mathbf{h}_j + \sum_{j \in \mathcal{J}_r} l_{jr}\mathcal{U}^{\mathbf{h}}_{\theta_{jr}} A^T \mathcal{U}^{\mathbf{g}}_{-\theta_{jr}} \mathbf{g}_j$. We must then change the basis with the rotation matrices to return to the case of Proposition 3.9, and delete the rows and columns that correspond to $m > 0$.

3.2. **Properties of the nodal finite volume Schemes**

We now discuss some properties of the schemes that we have just defined. For the sake of simplicity we limit ourselves to the case of periodic boundary conditions. Other boundary conditions could be considered at the price of technical adjustments.

3.2.1. *Conservativity*

In this Section, we show that the Glace and Eucclhyd schemes are conservative.

Lemma 3.11. *We have the following equalities*

$$\begin{cases} \displaystyle\sum_{r \in \mathcal{R}_j} l_{jr}\mathcal{U}^{\mathbf{g}}_{\theta_{jr}} A \mathcal{U}^{\mathbf{h}}_{-\theta_{jr}} = 0, \quad \displaystyle\sum_{j \in \mathcal{J}_r} l_{jr}\mathcal{U}^{\mathbf{g}}_{\theta_{jr}} A \mathcal{U}^{\mathbf{h}}_{-\theta_{jr}} = 0, \\ \displaystyle\sum_{r \in \mathcal{R}_j} l_{jr}\mathcal{U}^{\mathbf{h}}_{\theta_{jr}} A^T \mathcal{U}^{\mathbf{g}}_{-\theta_{jr}} = 0, \quad \displaystyle\sum_{j \in \mathcal{J}_r} l_{jr}\mathcal{U}^{\mathbf{h}}_{\theta_{jr}} A^T \mathcal{U}^{\mathbf{g}}_{-\theta_{jr}} = 0. \end{cases}$$

Proof. This follows directly from the following equalities

$$\sum_{j \in \mathcal{J}_r} \mathbf{C}_{jr} = \mathbf{0}, \qquad \sum_{r \in \mathcal{R}_j} \mathbf{C}_{jr} = \mathbf{0}, \tag{3.32}$$

with $\mathbf{C}_{jr} = l_{jr}\mathbf{n}_{jr}$. Let us write the proof only for the first equality, the others being treated in the same way.
One has

$$\begin{aligned} \sum_{r \in \mathcal{R}_j} l_{jr}\mathcal{U}^{\mathbf{g}}_{\theta_{jr}} A \mathcal{U}^{\mathbf{h}}_{-\theta_{jr}} &= \sum_{r \in \mathcal{R}_j} l_{jr}(\cos\theta_{jr} A + \sin\theta_{jr} B), \\ &= \underbrace{\left(\sum_{r \in \mathcal{R}_j} l_{jr} n^x_{jr}\right)}_{=0} A + \underbrace{\left(\sum_{r \in \mathcal{R}_j} l_{jr} n^y_{jr}\right)}_{=0} B = 0, \end{aligned}$$

where we used (3.32) to ensure that the sums are zero. ∎

Proposition 3.12. *The scheme* (3.25)-(3.26) *is conservative.*

Proof. Let us treat each (3.25) equation separately. On the one hand, for the first equation

$$\sum_{j\in\mathcal{J}} V_j \frac{d}{dt}\mathbf{g}_j = -\sum_{j\in\mathcal{J}}\sum_{r\in\mathcal{R}_j} l_{jr}\mathcal{U}^{\mathbf{g}}_{\theta_{jr}} A \mathcal{U}^{\mathbf{h}}_{-\theta_{jr}}\mathbf{h}_r,$$
$$= -\sum_{r\in\mathcal{R}} \underbrace{\left(\sum_{j\in\mathcal{J}_r} l_{jr}\mathcal{U}^{\mathbf{g}}_{\theta_{jr}} A \mathcal{U}^{\mathbf{h}}_{-\theta_{jr}}\right)}_{=0 \text{ using Lemma 3.11}} \mathbf{h}_r = \mathbf{0}.$$

On the other hand, for the second equation

$$\sum_{j\in\mathcal{J}} V_j \frac{d}{dt}\mathbf{h}_j = -\sum_{j\in\mathcal{J}}\sum_{r\in\mathcal{R}_j} \mathbf{F}_{jr},$$
$$= -\sum_{r\in\mathcal{R}} \underbrace{\left(\sum_{j\in\mathcal{J}_r} \mathbf{F}_{jr}\right)}_{=0 \text{ with (3.26)}} = \mathbf{0}.$$

■

Remark 3.13. This same result can be obtained in the same way for the discrete time scheme.

3.2.2. *L^2 stability*

We place ourselves on $\Omega = \mathbb{R}^2/\mathbb{Z}^2$, the 2D torus. We denote without distinction $\|\cdot\|_{L^2(\Omega)}$ and $\|\cdot\|_{H^s(\Omega)}$ the norm L^2 and H^s of a vector or scalar quantity for $s \in \mathbb{N}$. Let us write the P_N model in dimension 2

$$\begin{cases} \partial_t \mathbf{u} + \mathcal{A}_1 \partial_x \mathbf{u} + \mathcal{A}_2 \partial_y \mathbf{u} = \mathbf{0}, \\ \mathbf{u}(\,\cdot\,, t=0) = \mathbf{u}_0 \in [H^s(\Omega)]^{m^{2D}}, \end{cases} \tag{3.33}$$

with

$$\mathbf{u} = \begin{pmatrix} \mathbf{g} \\ \mathbf{h} \end{pmatrix}.$$

Proposition 3.14. *Let* $\mathbf{u}$ *be a solution of* (3.33)*, then* $\forall s \in \mathbb{N}$*,*

$$\forall t \geq 0, \qquad \|\mathbf{u}(t)\|_{H^s(\Omega)} = \|\mathbf{u}_0\|_{H^s(\Omega)}.$$

Proof. First we start by showing the result for the L^2 norm. Taking the scalar product with $\mathbf{u}$ and integrating over Ω we obtain

$$\frac{1}{2}\partial_t \|\mathbf{u}\|^2_{L^2(\Omega)} + \int_\Omega (\mathcal{A}_1 \partial_x \mathbf{u}, \mathbf{u}) d\mathbf{x} + \int_\Omega (\mathcal{A}_2 \partial_y \mathbf{u}, \mathbf{u}) d\mathbf{x} = 0.$$

Using the fact that we are on a torus (which is a manifold without boundary), we obtain after an integration by part

$$\int_\Omega (\mathcal{A}_1 \partial_x \mathbf{u}, \mathbf{u}) d\mathbf{x} = -\int_\Omega (\mathcal{A}_1 \mathbf{u}, \partial_x \mathbf{u}) d\mathbf{x},$$

finally, since $\mathcal{A}_1$ is symmetric, the right hand side rewrites

$$-\int_\Omega (\mathcal{A}_1 \mathbf{u}, \partial_x \mathbf{u}) d\mathbf{x} = -\int_\Omega (\mathbf{u}, \mathcal{A}_1 \partial_x \mathbf{u}) d\mathbf{x},$$

from which

$$\int_\Omega (\mathcal{A}_1 \partial_x \mathbf{u}, \mathbf{u}) d\mathbf{x} = -\int_\Omega (\mathcal{A}_1 \partial_x \mathbf{u}, \mathbf{u}) d\mathbf{x},$$

therefore

$$\int_\Omega (\mathcal{A}_1 \partial_x \mathbf{u}, \mathbf{u}) d\mathbf{x} = 0.$$

The same arguments give $\int_\Omega (\mathcal{A}_2 \partial_y \mathbf{u}, \mathbf{u}) d\mathbf{x} = 0$. We obtain finally

$$\partial_t \|\mathbf{u}\|^2_{L^2(\Omega)} = 0,$$

hence the result. Moreover the function $\partial^\alpha \mathbf{u}$ with α a multi-index, is also a solution of the equation, so the same result is true in H^s norm, with $s \in \mathbb{N}$. ∎

L^2-stability for the continous in time scheme. Let us now study the L^2-stability of the semi-discrete scheme (3.25)-(3.26), that we recall here

$$\begin{cases} \dfrac{d}{dt}\mathbf{g}_j + \dfrac{1}{V_j}\displaystyle\sum_{r\in\mathcal{R}_j} l_{jr}\mathcal{U}^{\mathbf{g}}_{\theta_{jr}} A \mathcal{U}^{\mathbf{h}}_{-\theta_{jr}} \mathbf{h}_r = \mathbf{0}, \\ \dfrac{d}{dt}\mathbf{h}_j + \dfrac{1}{V_j}\displaystyle\sum_{r\in\mathcal{R}_j} \mathbf{F}_{jr} = \mathbf{0}, \end{cases}$$

with

$$\begin{cases} \mathbf{F}_{jr} = l_{jr}\mathcal{U}^{\mathbf{h}}_{\theta_{jr}} A^T \mathcal{U}^{\mathbf{g}}_{-\theta_{jr}} \mathbf{g}_j + M_{jr}(\mathbf{h}_j - \mathbf{h}_r), \\ \displaystyle\sum_{j\in\mathcal{J}_r} \mathbf{F}_{jr} = \mathbf{0}, \end{cases}$$

where M_{jr} is defined by (3.21) for the Glace scheme, and by (3.29) in the case of Eucclhyd scheme.

In the following, we denote $\mathbf{u}_h(\mathbf{x},t) = \sum_{j\in\mathcal{J}} \mathbf{1}_j(\mathbf{x})\mathbf{u}_j(t)$ and we identify the function $\mathbf{u}_h$ and the vector $(\mathbf{u}_j)_{j\in\mathcal{J}}$. Also, we set

$$E(t) = \frac{1}{2}\int_\Omega \|\mathbf{u}_h(\mathbf{x},t)\|^2 d\mathbf{x} \geq 0. \tag{3.34}$$

Proposition 3.15. *The scheme* (3.25)-(3.26) *is L^2 stable, in the sense that*

$$\forall t \geq 0, \qquad E(t) \leq E(0).$$

More precisely, we have

$$E'(t) = -\sum_{j\in\mathcal{J}}\sum_{r\in\mathcal{R}_j} (M_{jr}(\mathbf{h}_j - \mathbf{h}_r), \mathbf{h}_j - \mathbf{h}_r) \leq 0.$$

Proof. The proof is inspired by the one done in [1] for the case $N = 1$. We have

$$\begin{aligned} E'(t) &= \frac{1}{2}\frac{d}{dt}\int_\Omega \|\mathbf{u}_h(\mathbf{x},t)\|^2 d\mathbf{x}, \\ &= \frac{1}{2}\frac{d}{dt}\sum_{j\in\mathcal{J}} V_j \|\mathbf{u}_j(t)\|^2, \\ &= \frac{1}{2}\frac{d}{dt}\sum_{j\in\mathcal{J}} V_j \left((\mathbf{g}_j(t),\mathbf{g}_j(t)) + (\mathbf{h}_j(t),\mathbf{h}_j(t))\right), \\ &= \sum_{j\in\mathcal{J}} V_j \left((\mathbf{g}_j(t),\mathbf{g}'_j(t)) + (\mathbf{h}'_j(t),\mathbf{h}_j(t))\right). \end{aligned}$$

Using the definition of the scheme, one gets

$$E' = \underbrace{-\sum_{j\in\mathcal{J}}\sum_{r\in\mathcal{R}_j} (\mathbf{g}_j, l_{jr}\mathcal{U}^{\mathbf{g}}_{\theta_{jr}} A \mathcal{U}^{\mathbf{h}}_{-\theta_{jr}} \mathbf{h}_r)}_{A_1} \underbrace{-\sum_{j\in\mathcal{J}}\sum_{r\in\mathcal{R}_j} (\mathbf{F}_{jr}, \mathbf{h}_j)}_{A_2}.$$

We develop the second term of the previous equation

$$\begin{aligned} A_2 &= \sum_{j\in\mathcal{J}}\sum_{r\in\mathcal{R}_j}(\mathbf{F}_{jr},\mathbf{h}_j), \\ &= \sum_{j\in\mathcal{J}}\sum_{r\in\mathcal{R}_j}(l_{jr}\mathcal{U}^{\mathbf{h}}_{\theta_{jr}}A^T\mathcal{U}^{\mathbf{g}}_{-\theta_{jr}}\mathbf{g}_j,\mathbf{h}_j)+\sum_{j\in\mathcal{J}}\sum_{r\in\mathcal{R}_j}(M_{jr}(\mathbf{h}_j-\mathbf{h}_r),\mathbf{h}_j). \end{aligned} \tag{3.35}$$

Since

$$\sum_{r\in\mathcal{R}_j} l_{jr}\mathcal{U}^{\mathbf{h}}_{\theta_{jr}}A^T\mathcal{U}^{\mathbf{g}}_{-\theta_{jr}}=0,$$

by the Lemma 3.11, the first term of (3.35) is zero.
By taking the scalar product with $\mathbf{h}_r$ and then summing over r in the second equation of (3.26) and permuting the sums, we find

$$\sum_{j\in\mathcal{J}}\sum_{r\in\mathcal{R}_j}(M_{jr}\mathbf{h}_r,\mathbf{h}_r)=\sum_{j\in\mathcal{J}}\sum_{r\in\mathcal{R}_j}(M_{jr}\mathbf{h}_j,\mathbf{h}_r)+\sum_{j\in\mathcal{J}}\sum_{r\in\mathcal{R}_j} l_{jr}(\mathcal{U}^{\mathbf{h}}_{\theta_{jr}}A^T\mathcal{U}^{\mathbf{g}}_{-\theta_{jr}}\mathbf{g}_j,\mathbf{h}_r).$$

Thus

$$\begin{aligned} A_1 &= \sum_{j\in\mathcal{J}}\sum_{r\in\mathcal{R}_j}(\mathbf{g}_j,l_{jr}\mathcal{U}^{\mathbf{g}}_{\theta_{jr}}A\mathcal{U}^{\mathbf{h}}_{-\theta_{jr}}\mathbf{h}_r), \\ &= \sum_{j\in\mathcal{J}}\sum_{r\in\mathcal{R}_j}(M_{jr}\mathbf{h}_r,\mathbf{h}_r)-\sum_{j\in\mathcal{J}}\sum_{r\in\mathcal{R}_j}(M_{jr}\mathbf{h}_j,\mathbf{h}_r), \\ &= -\sum_{j\in\mathcal{J}}\sum_{r\in\mathcal{R}_j}(M_{jr}(\mathbf{h}_j-\mathbf{h}_r),\mathbf{h}_r). \end{aligned}$$

Finally, we find that

$$\begin{aligned} E' &= \sum_{j\in\mathcal{J}}\sum_{r\in\mathcal{R}_j}(M_{jr}(\mathbf{h}_j-\mathbf{h}_r),\mathbf{h}_r)-\sum_{j\in\mathcal{J}}\sum_{r\in\mathcal{R}_j}(M_{jr}(\mathbf{h}_j-\mathbf{h}_r),\mathbf{h}_j), \\ &= -\sum_{j\in\mathcal{J}}\sum_{r\in\mathcal{R}_j}(M_{jr}(\mathbf{h}_j-\mathbf{h}_r),\mathbf{h}_j-\mathbf{h}_r), \end{aligned}$$

so, using Proposition 3.5, we get the desired result. ∎

Remark 3.16. The proof is independent of whether the Glace or Eucclhyd scheme is used.

L^2-stability for the explicit in time scheme. We now study the stability of the explicit in time scheme

$$\begin{cases} \mathbf{g}_j^{n+1}=\mathbf{g}_j^n-\dfrac{\Delta t}{V_j}\displaystyle\sum_{r\in\mathcal{R}_j} l_{jr}\mathcal{U}^{\mathbf{g}}_{\theta_{jr}}A\mathcal{U}^{\mathbf{h}}_{-\theta_{jr}}\mathbf{h}_r^n, \\ \mathbf{h}_j^{n+1}=\mathbf{h}_j^n-\dfrac{\Delta t}{V_j}\displaystyle\sum_{r\in\mathcal{R}_j}\mathbf{F}_{jr}^n, \end{cases} \tag{3.36}$$

with

$$\begin{cases} \mathbf{F}_{jr}^n = l_{jr}\mathcal{U}^{\mathbf{h}}_{\theta_{jr}}A^T\mathcal{U}^{\mathbf{g}}_{-\theta_{jr}}\mathbf{g}_j^n+M_{jr}(\mathbf{h}_j^n-\mathbf{h}_r^n), \\ \displaystyle\sum_{j\in\mathcal{J}_r}\mathbf{F}_{jr}^n=\mathbf{0}. \end{cases} \tag{3.37}$$

Let

$$E^n=\frac{1}{2}\sum_{j\in\mathcal{J}}V_j\|\mathbf{u}_j^n\|^2=\frac{1}{2}\sum_{j\in\mathcal{J}}V_j\left[(\mathbf{g}_j^n,\mathbf{g}_j^n)+(\mathbf{h}_j^n,\mathbf{h}_j^n)\right],$$

we note $\mathbf{G}_{jr}^n=l_{jr}\mathcal{U}^{\mathbf{g}}_{\theta_{jr}}A\mathcal{U}^{\mathbf{h}}_{-\theta_{jr}}\mathbf{h}_r^n$.

Proposition 3.17. *One has the following alternative*

(1) *if* $\mathbf{u}_h^n$ *is constant i.e.* $\exists \mathbf{v} \in \mathbb{R}^{m^{2D}}$ *s.t.* $\forall j \in \mathcal{J}, \mathbf{u}_j^n = \mathbf{v}$, *then set* $\Delta t_{\max} = +\infty$,

(2) *else, set*

$$\Delta t_{\max} = \frac{\displaystyle\sum_{j\in\mathcal{J}}\sum_{r\in\mathcal{R}_j} (M_{jr}(\mathbf{h}_j^n - \mathbf{h}_r^n), \mathbf{h}_j^n - \mathbf{h}_r^n)}{\displaystyle\sum_{j\in\mathcal{J}} \frac{1}{V_j}\left[\left(\sum_{r\in\mathcal{R}_j}\mathbf{G}_{jr}^n, \sum_{r\in\mathcal{R}_j}\mathbf{G}_{jr}^n\right) + \left(\sum_{r\in\mathcal{R}_j}\mathbf{F}_{jr}^n, \sum_{r\in\mathcal{R}_j}\mathbf{F}_{jr}^n\right)\right]}. \tag{3.38}$$

Then the explicit scheme (3.36)-(3.37) *is* L^2*-stable if* $0 < \Delta t \leq \Delta t_{\max}$.

Proof. The first case is obvious. If $\mathbf{u}_h^n$ is constant then, for all $j \in \mathcal{J}$ and $r \in \mathcal{R}$, $\mathbf{h}_r^n = \mathbf{h}_j^n$ and $\mathbf{g}_{jr}^n = \mathbf{g}_j^n$, so according to Lemma 3.11, $\forall \Delta t > 0$, $E^{n+1} = E^n$.
Let us now focus on the second case. One has

$$E^{n+1} = \frac{1}{2}\sum_{j\in\mathcal{J}} V_j \left[(\mathbf{g}_j^{n+1}, \mathbf{g}_j^{n+1}) + (\mathbf{h}_j^{n+1}, \mathbf{h}_j^{n+1})\right],$$

thus, substituting the scheme reads

$$E^{n+1} = \frac{1}{2}\sum_{j\in\mathcal{J}} V_j \left[\left(\mathbf{g}_j^n - \frac{\Delta t}{V_j}\sum_{r\in\mathcal{R}_j}\mathbf{G}_{jr}^n,\ \mathbf{g}_j^n - \frac{\Delta t}{V_j}\sum_{r\in\mathcal{R}_j}\mathbf{G}_{jr}^n\right) + \left(\mathbf{h}_j^n - \frac{\Delta t}{V_j}\sum_{r\in\mathcal{R}_j}\mathbf{F}_{jr}^n,\ \mathbf{h}_j^n - \frac{\Delta t}{V_j}\sum_{r\in\mathcal{R}_j}\mathbf{F}_{jr}^n\right)\right],$$

which develops as

$$E^{n+1} = \frac{1}{2}\sum_{j\in\mathcal{J}} V_j \left[(\mathbf{g}_j^n, \mathbf{g}_j^n) + (\mathbf{h}_j^n, \mathbf{h}_j^n) - 2\frac{\Delta t}{V_j}\sum_{r\in\mathcal{R}_j}\left(\mathbf{g}_j^n, \mathbf{G}_{jr}^n\right) - 2\frac{\Delta t}{V_j}\sum_{r\in\mathcal{R}_j}(\mathbf{F}_{jr}^n, \mathbf{h}_j^n) + \frac{\Delta t^2}{V_j^2}\left(\sum_{r\in\mathcal{R}_j}\mathbf{G}_{jr}^n, \sum_{r\in\mathcal{R}_j}\mathbf{G}_{jr}^n\right) + \frac{\Delta t^2}{V_j^2}\left(\sum_{r\in\mathcal{R}_j}\mathbf{F}_{jr}^n, \sum_{r\in\mathcal{R}_j}\mathbf{F}_{jr}^n\right)\right].$$

Using the calculation made in Proposition 3.15, we find

$$E^{n+1} = E^n - \Delta t\sum_{j\in\mathcal{J}}\sum_{r\in\mathcal{R}_j}(M_{jr}(\mathbf{h}_j^n - \mathbf{h}_r^n), \mathbf{h}_j^n - \mathbf{h}_r^n) + \sum_{j\in\mathcal{J}}\frac{\Delta t^2}{2V_j}\left[\left(\sum_{r\in\mathcal{R}_j}\mathbf{G}_{jr}^n, \sum_{r\in\mathcal{R}_j}\mathbf{G}_{jr}^n\right) + \left(\sum_{r\in\mathcal{R}_j}\mathbf{F}_{jr}^n, \sum_{r\in\mathcal{R}_j}\mathbf{F}_{jr}^n\right)\right].$$

It is a polynomial of the second degree in Δt, whose Δt^2's coefficient is nonzero since $\mathbf{u}_h^n$ is not constant in space. We choose to impose a time step that corresponds to the minimum of this polynomial (which is negative)

$$\Delta t_{\max} = \frac{\displaystyle\sum_{j\in\mathcal{J}}\sum_{r\in\mathcal{R}_j} (M_{jr}(\mathbf{h}_j^n - \mathbf{h}_r^n), \mathbf{h}_j^n - \mathbf{h}_r^n)}{\displaystyle\sum_{j\in\mathcal{J}} \frac{1}{V_j}\left[\left(\sum_{r\in\mathcal{R}_j}\mathbf{G}_{jr}^n, \sum_{r\in\mathcal{R}_j}\mathbf{G}_{jr}^n\right) + \left(\sum_{r\in\mathcal{R}_j}\mathbf{F}_{jr}^n, \sum_{r\in\mathcal{R}_j}\mathbf{F}_{jr}^n\right)\right]}.$$

Finally we obtain $E^{n+1} \leq E^n$. ∎

In view of showing that the scheme is convergent, we need to provide a positive lower bound to $\Delta t_{\max}$ in (3.38) that constrains the time step Δt to ensure L^2-stability.

Proposition 3.18. *Let $\Delta t_{\max}$ be defined by (3.38), and τ_h defined by*

$$\tau_h := \frac{\min\limits_{j\in\mathcal{J}} V_j}{2\max\limits_{j\in\mathcal{J}}(1+2\#\mathcal{R}_j)\max\limits_{\substack{j\in\mathcal{J}\\ r\in\mathcal{R}_j}} l_{jr}}. \tag{3.39}$$

Then in the case of the Glace scheme, one has

$$\Delta t_{\max} \geq \tau_h > 0. \tag{3.40}$$

Proof. The proof is quite technical and thus is provided in Appendix A. ∎

Remark 3.19. Similar result could be obtained for the Eucclhyd scheme at the cost of technical adjustments.

Example 3.20. In the case of a uniform cartesian mesh made of squares, formula (3.40) recasts to

$$\Delta t_{\max} \geq \frac{\sqrt{2}}{18} h > 0,$$

where h is the squares edge length. Indeed, in that case $\#\mathcal{R}_j = 4$, $V_j = h^2$ and $l_{jr} = \frac{\sqrt{2}}{2h}$.

3.3. **Convergence**

We shall now prove that the proposed nodal finite volume schemes converge under some regularity assumptions. We establish the convergence of the semi-discrete schemes.

Once again we assume that $\Omega = \mathbb{R}^2/\mathbb{Z}^2$. We will also assume that the admissible mesh $\mathcal{M}$ of Ω is of size h and has a bounded aspect ratio. That is, there exists a constant $C > 0$ such that

$$\max_{r,r'\in\mathcal{R}_j} |\mathbf{x}_r - \mathbf{x}_{r'}| \leq h, \qquad h^2 \leq C V_j, \forall j \in \mathcal{J}. \tag{3.41}$$

Let us recall that we denote $\mathbf{u}_h(\mathbf{x},t) = \mathbf{u}_j(t)$ if $\mathbf{x} \in j$, and that we identify the function $\mathbf{u}_h$ and the vector $(\mathbf{u}_j)_{j\in\mathcal{J}}$. The discrete initial condition $\mathbf{u}_h^0$ is chosen such that

$$\mathbf{u}_h^0(\mathbf{x}) = \frac{1}{V_j}\int_j \mathbf{u}_0(\mathbf{y})d\mathbf{y}, \qquad \text{if } \mathbf{x} \in j.$$

Theorem 3.21. *On unstructured meshes of size h (3.41), the semi-discrete Glace scheme for the P_N model converges to order $h^{1/2}$ for an initial data $\mathbf{u}_0 \in H^3(\Omega)$. More precisely, there exists a constant $C > 0$ such that*

$$\|\mathbf{u}_h(t) - \mathbf{u}(t)\|_{L^2(\Omega)} \leq C\sqrt{(1+t)\|\nabla\mathbf{u}_0\|^2_{L^2(\Omega)} + t|\mathbf{u}_0|^2_{H^3(\Omega)}}\, h^{1/2}.$$

Proof. The proof is quite long, thus it is given in Appendix B. ∎

Remark 3.22. Again, similar result could be obtained for the Eucclhyd scheme for P_N using slightly more complex algebra.

4. **Numerical results**

In this Section, we present numerical results for the Glace and Eucclhyd schemes. Our first test case is a Riemann problem, which has the advantage of admitting an exact solution. It is also easy to check that the scheme reproduces the expected wave velocities. Our second test case is an initial condition equal to a Dirac distribution, this test case is interesting because it is a classical test case of the wave equation. This test case presenting important numerical artifacts, we propose a third test case which consists in taking an initial condition equal to a "regularized" Dirac distribution, i.e. an initial condition of the form of an element of a regularizing sequence φ_n, with n sufficiently large. Finally, we propose a last test case, for which we can compare the numerical solution to a smooth exact solution and thus draw convergence curves. For all these tests, the time step is computed using formula (3.38).

4.1. **Riemann problem**

For this test case, we consider a Riemann problem. We set $\Omega =]-1,1[\times]-0.1,0.1[$. The initial condition is

$$f_0^0(x,y) = \begin{cases} 1, & \text{if } x < 0, \\ 0, & \text{if } x > 0, \end{cases}$$

and $f_k^m = 0$ for all $k > 0$, $|m| \leq k$.

To better understand the numerical results, let us look at the exact solution of this problem at least in the case $N = 3$. Since there is no variation according to y, this is a 1D problem:

$$\partial_t \mathbf{u} + \mathcal{A}_1 \partial_x \mathbf{u} = \mathbf{0}.$$

It is then classical that

$$\mathbf{u}(x,t) = \sum_{i=1}^{m^{2D}} w_i(x,t)\mathbf{r}_i = \sum_{i=1}^{m^{2D}} w_i^0(x-\lambda_i t)\mathbf{r}_i = \sum_{i=1}^{m^{2D}} \left(\mathbf{u}^0(x-\lambda_i t), \mathbf{l}_i\right)\mathbf{r}_i,$$

with $\mathbf{l}_i, \mathbf{r}_i$, the i-th eigenvectors on the left and right of $\mathcal{A}_1$ and $\mathbf{w} = (w_i)_{1 \leq i \leq m^{2D}}$ the Riemann invariants. Since $\mathcal{A}_1$ is symmetric, $\mathbf{r}_i^T = \mathbf{l}_i$ for all i. Now the eigenvector matrix P (with the eigenvalues ordered by decreasing modulus) of $\mathcal{A}_1$ is

$$P = \begin{pmatrix}
-\frac{2}{3}\sqrt{\frac{2}{35}\left(4\sqrt{30}+75\right)} & \frac{2}{3}\sqrt{\frac{2}{35}\left(4\sqrt{30}+75\right)} & 0 & 0 & 0 & 0 & \frac{2}{3}\sqrt{\frac{2}{35}\left(75-4\sqrt{30}\right)} & -\frac{2}{3}\sqrt{\frac{2}{35}\left(75-4\sqrt{30}\right)} & 0 & 0 \\
0 & 0 & \sqrt{30} & -\sqrt{30} & 0 & 0 & 0 & 0 & 0 & 0 \\
\frac{1}{3}\sqrt{4\sqrt{\frac{6}{5}}+6} & -\frac{1}{3}\sqrt{4\sqrt{\frac{6}{5}}+6} & 0 & 0 & -\sqrt{2} & \sqrt{2} & \frac{1}{3}\sqrt{6-4\sqrt{\frac{6}{5}}} & -\frac{1}{3}\sqrt{6-4\sqrt{\frac{6}{5}}} & 0 & 0 \\
-\sqrt{4\sqrt{\frac{2}{15}}+2} & \sqrt{4\sqrt{\frac{2}{15}}+2} & 0 & 0 & -\sqrt{\frac{2}{3}} & \sqrt{\frac{2}{3}} & -\sqrt{2-4\sqrt{\frac{2}{15}}} & \sqrt{2-4\sqrt{\frac{2}{15}}} & 0 & 0 \\
0 & 0 & -\sqrt{14} & -\sqrt{14} & 0 & 0 & 0 & 0 & \frac{1}{\sqrt{14}} & -\sqrt{\frac{15}{14}} \\
\frac{2\left(\sqrt{30}+10\right)}{5\sqrt{7}} & \frac{2\left(\sqrt{30}+10\right)}{5\sqrt{7}} & 0 & 0 & 0 & 0 & \frac{2\left(\sqrt{30}-10\right)}{5\sqrt{7}} & \frac{2\left(\sqrt{30}-10\right)}{5\sqrt{7}} & 0 & 0 \\
0 & 0 & -\sqrt{15} & -\sqrt{15} & 0 & 0 & 0 & 0 & 0 & 1 \\
0 & 0 & 1 & 1 & 0 & 0 & 0 & 0 & 1 & 0 \\
-\sqrt{\frac{3}{5}} & -\sqrt{\frac{3}{5}} & 0 & 0 & \sqrt{\frac{5}{3}} & \sqrt{\frac{5}{3}} & -\sqrt{\frac{3}{5}} & -\sqrt{\frac{3}{5}} & 0 & 0 \\
1 & 1 & 0 & 0 & 1 & 1 & 1 & 1 & 0 & 0
\end{pmatrix}.$$

We then notice that the only eigenvectors that correspond to positive eigenvalues that have their first component not zero are those associated to the eigenvalues $\lambda_1^{\text{theo}} = \sqrt{\frac{1}{35}\left(2\sqrt{30}+15\right)}$ and $\lambda_4^{\text{theo}} = \sqrt{\frac{1}{35}\left(15-2\sqrt{30}\right)}$. Thus, for P_3, we expect to see only two waves going to the right and two going to the left. By the same reasoning, we expect to see three waves going to the right for the P_5 model, and three going to the left.

Cartesian grid. First, we place ourselves on a cartesian meshes. In Figure 4.1, we measure wave velocities of $\lambda_1 = 0.339$ and $\lambda_4 = 0.858$ against $\lambda_1^{\text{theo}} \approx 0.339981$ and $\lambda_4^{\text{theo}} \approx 0.861136$ for the theoretical values. We observe the correct structure of the eigenvalues of $\mathcal{A}_1$, if λ is an eigenvalue: then $-\lambda$ is also an eigenvalue. We also observe an additional couple of waves for P_5 which was expected. We observe a very similar results in the case of the Eucclhyd scheme in Figure 4.3.

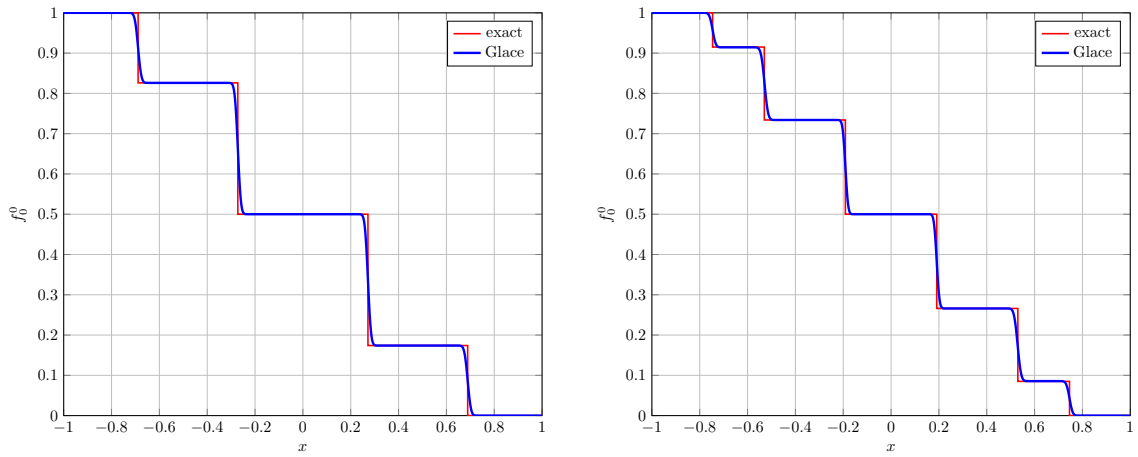

(A) P_3 (B) P_5

FIGURE 4.1. Riemann problem with the Glace scheme on a cartesian mesh 3840×4 at time $t = 0.8$.

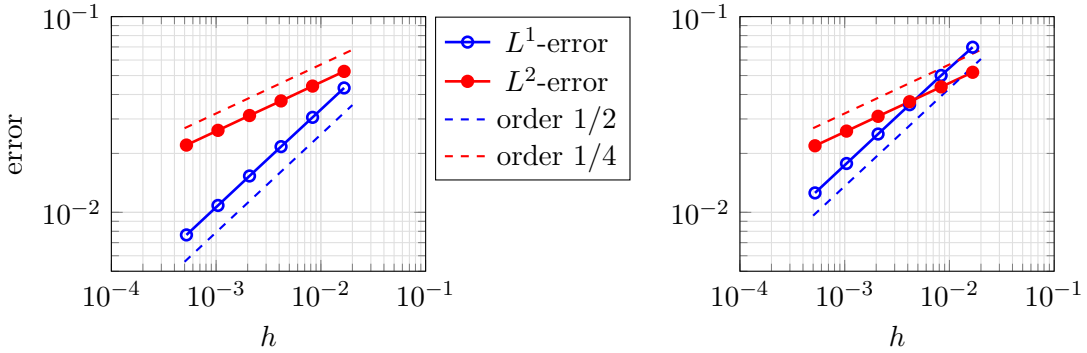

(A) P_3 (B) P_5

FIGURE 4.2. Convergence for Riemann problems for Glace scheme on cartesian grids

We perform a convergence study, see Figure 4.2 and 4.4. One obtains the expected[5] rates of convergence: $O(h^{1/2})$ in the L^1-norm and $O(h^{1/4})$ in the L^2-norm for the whole vector of unknowns $(\mathbf{g}_j, \mathbf{h}_j)_{j\in\mathcal{J}}$. This is conform to the general finite volume theory, see [10].

Random meshes. We now consider the case of random meshes. The construction of such meshes is done in the following way: we start from a cartesian mesh 320×4, we move each node according to

[5]Even for scalar problem using first-order 1D finite volume methods one cannot expect better for this kind of initial data.

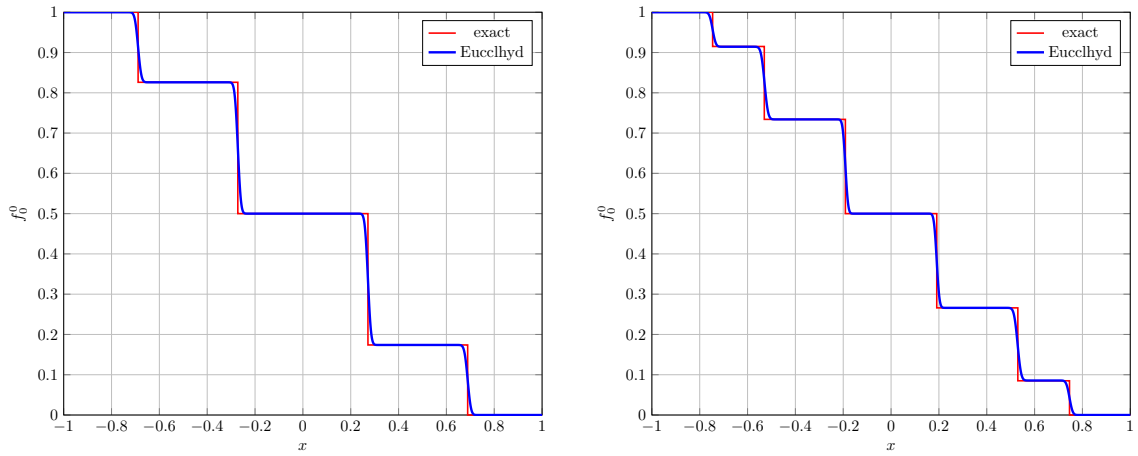

(A) P_3 (B) P_5

FIGURE 4.3. Riemann problem with the Eucclhyd scheme on a cartesian mesh 3840×4 at time $t = 0.8$.

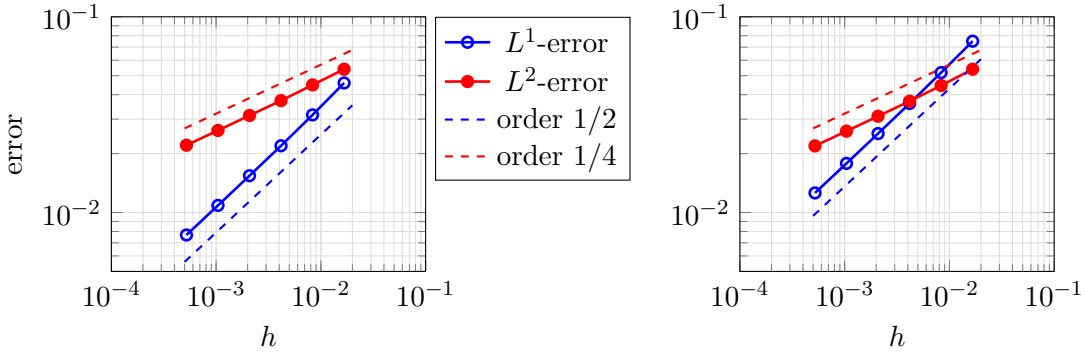

(A) P_3 (B) P_5

FIGURE 4.4. Convergence for Riemann problems for Eucclhyd scheme on cartesian grids

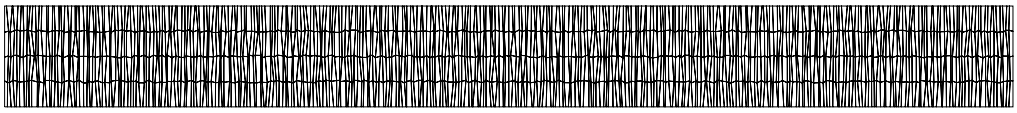

FIGURE 4.5. Random 320×4 mesh used for the Riemann problem

a uniform law in a way that cells remain untangled and preserving the initial interface, see Figure 4.5. The results are illustrated in Figure 4.6 for the Glace scheme and in Figure 4.8 for Eucclhyd.

Again the convergence study displayed in Figure 4.7 and 4.9 gives an $O(h^{1/2})$ rate in the L^1-norm and $O(h^{1/4})$ in the L^2-norm.

These two set of tests illustrate that the scheme converges well, while the initial condition is not in H^3 (it is not even in H^1). This suggests that the regularity condition of the Theorem 3.21 is suboptimal with regard to the minimal regularity of the initial condition.

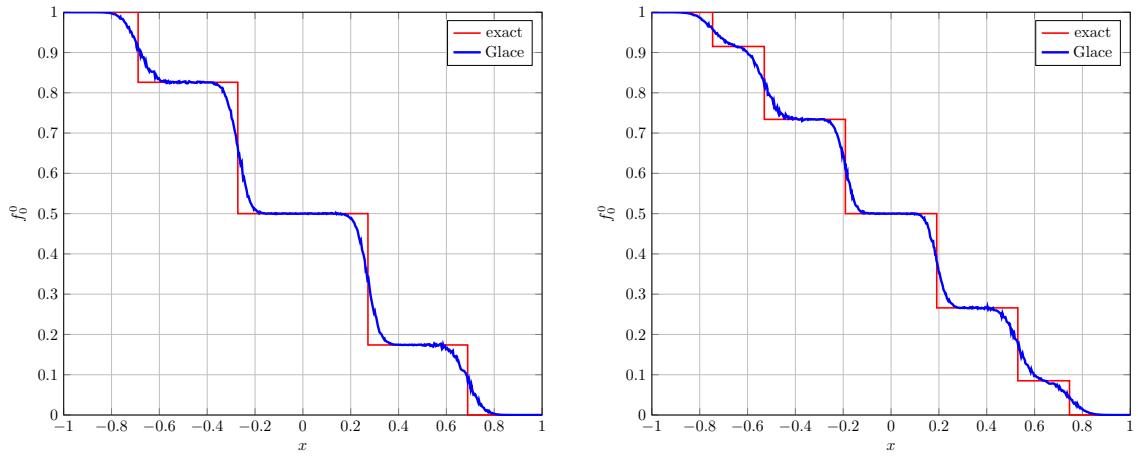

(A) P_3 (B) P_5

FIGURE 4.6. Riemann problem with the Glace scheme on a random mesh 320×4 at time $t = 0.8$.

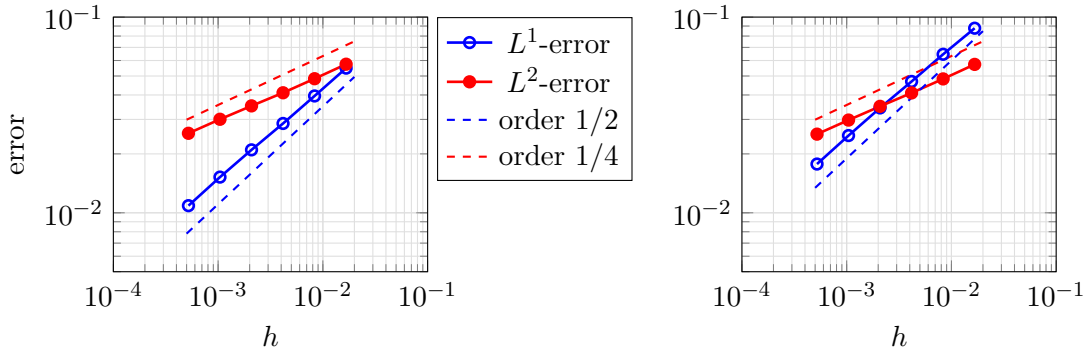

(A) P_3 (B) P_5

FIGURE 4.7. Convergence for Riemann problems for Glace scheme on random grids

4.2. **Dirac**

These tests are run on both cartesian and randomized cartesian grids. As previously, the random grids are build as displacing randomly the vertex of the corresponding uniform mesh (preserving the geometry and insuring that resulting cells are not tangled). An example of such a mesh is given in Figure 4.10.

For this test case, we set $\Omega =]-1.5, 1.5[^2$, and consider the initial condition

$$f_0^0(x, y) = \delta_{(0,0)}.$$

Numerically, this initial condition is approximated by

$$f_0^0(x, y) = \frac{1}{V_{j_0}} \mathbf{1}_{j_0}(x, y)$$

where j_0 is the cell located at the center of the mesh. We observe in Figures 4.11a and 4.11b that this test case is problematic for these schemes. For the Glace scheme, we observe that the solution looks like a 2D Dirac comb, and we observe many spurious modes along the diagonal. For the Eucclhyd

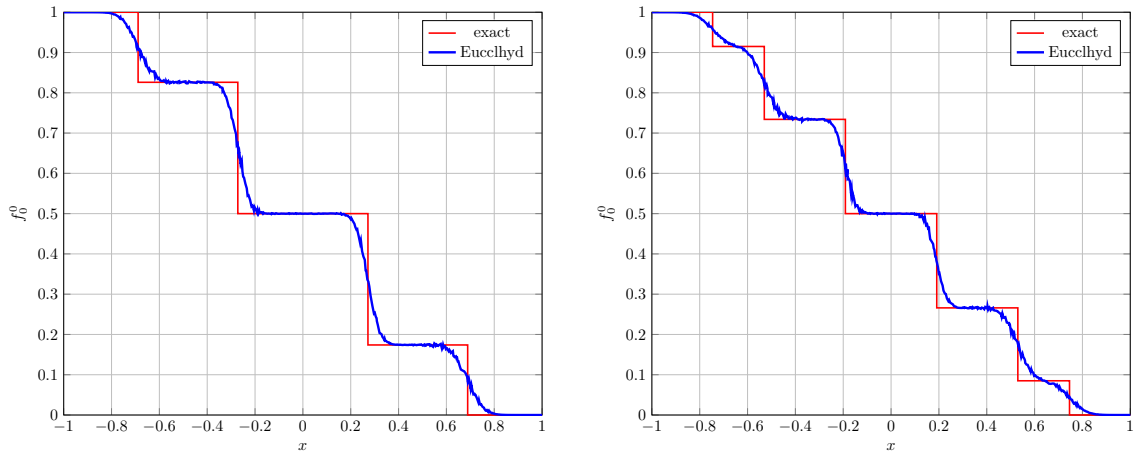

(A) P_3 (B) P_5

FIGURE 4.8. Riemann problem with the Eucclhyd scheme, random meshes 320×4, $t = 0.8$.

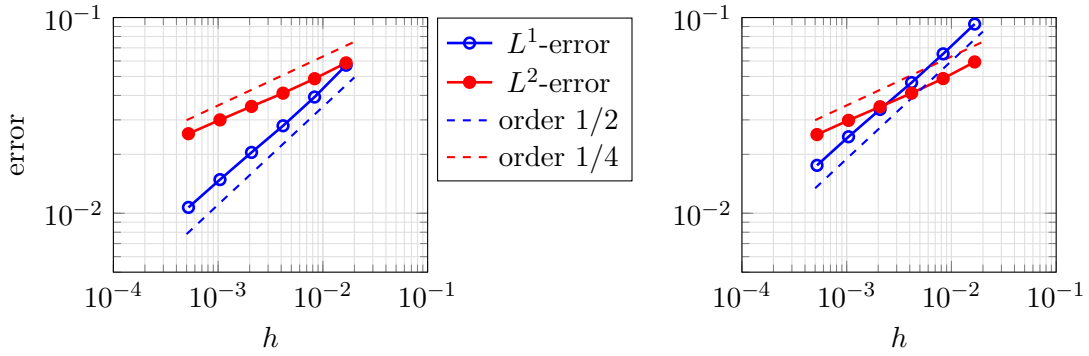

(A) P_3 (B) P_5

FIGURE 4.9. Convergence for Riemann problems for Eucclhyd scheme on random grids

scheme, the Dirac comb and the spurious modes along the diagonal disappear, however we observe that a large part of the particles remain in the center of the domain. These parasitic modes seem to disappear when the mesh is no longer cartesian for the Glace scheme (see Figure 4.11c). For the Eucclhyd scheme, this is not the case and a large part of the particles still remain in the center of the domain (see Figure 4.11d).

4.3. **Regularized Dirac**

For this test case, we set $\Omega =]-1.5, 1.5[^2$ and we consider the initial condition

$$f_0^0(x, y) = 30e^{-30^2(x^2+y^2)}.$$

We first use a random mesh (see an illustration in Figure). We observe that the Eucclhyd scheme produces more numerical diffusion than the Glace scheme (see Figure 4.12).

Finally, we present the solution on an unstructured Delaunay mesh. We observe spurious modes in the center of the domain. The fact that the Eucclhyd scheme produces more numerical dissipation

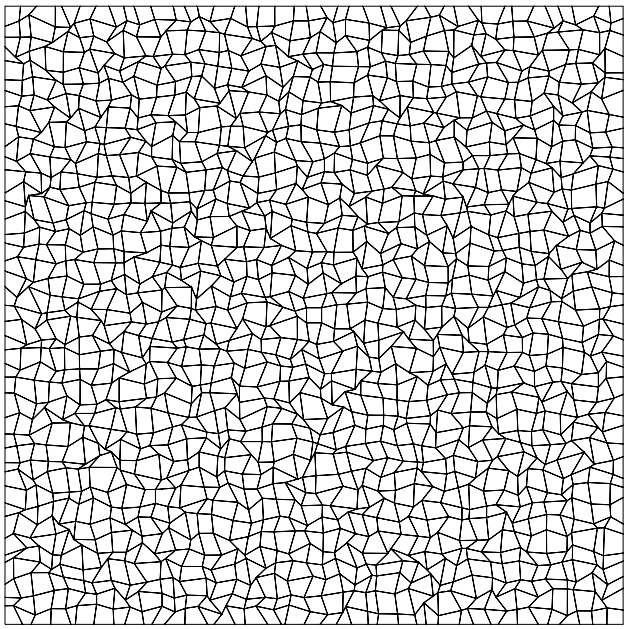

FIGURE 4.10. Example of a random mesh used for the Dirac-like tests. Here, starting a 41×41 uniform cartesian grid is randomized ensuring that cell do not tangle.

is still present (see Figure 4.13). We have no theoretical explanation with regard to these spurious modes. However, according to Theorem 3.21, these should not prevent L^2-convergence.

4.4. **Analytical solution**

We now set $\Omega =]-1,1[^2$. The P_N model is written

$$\partial_t \mathbf{u} + \mathcal{A}_1 \partial_x \mathbf{u} + \mathcal{A}_2 \partial_y \mathbf{u} = \mathbf{0}.$$

Let $(\mathbf{x}, t) \in \Omega \times [0, +\infty[$, we are looking for a solution of the form $\mathbf{u}(\mathbf{x}, t) = e^{-\alpha t}\mathbf{v}(x)$, with $\mathbf{v} : \mathbb{R} \to \mathbb{R}^{m^{2D}}$ a function of class C^1 and $\alpha > 0$. By injecting into the equation, we find

$$\mathcal{A}_1 \partial_x \mathbf{v} = \alpha \mathbf{v},$$

that is, by diagonalizing the system

$$D\partial_x \mathbf{w} = \alpha \mathbf{w}$$

with $\mathbf{w} = P^T\mathbf{v}$ and $D = \mathrm{diag}(\lambda_i)_{1 \le i \le m^{2D}}$ the eigenvalue matrix of $\mathcal{A}_1$. Let $1 \le i \le m^{2D}$, if $\lambda_i = 0$, then $w_i = 0$, otherwise we find, by imposing for example $w_i(0) = 1$

$$\forall x \in]-1,1[\,, \quad w_i(x) = e^{\frac{\alpha}{\lambda_i}x}.$$

Finally, one has

$$\forall (\mathbf{x}, t) \in \Omega \times [0, +\infty[\,, \quad \mathbf{u}(\mathbf{x}, t) = e^{-\alpha t} P \begin{pmatrix} e^{\frac{\alpha}{\lambda_1}x} \\ \vdots \\ e^{\frac{\alpha}{\lambda_{m^{2D}}}x} \end{pmatrix}.$$

We study the case $N = 3$. The exact solution $\mathbf{u}$ is written, for all $(\mathbf{x}, t)$,

$$\mathbf{u}(\mathbf{x}, t) = e^{-\alpha t}(u_i(\mathbf{x}, t))_{1 \le i \le 10},$$

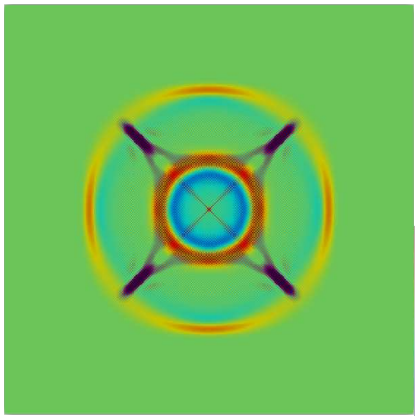

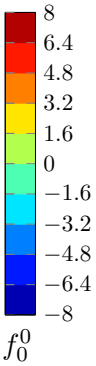

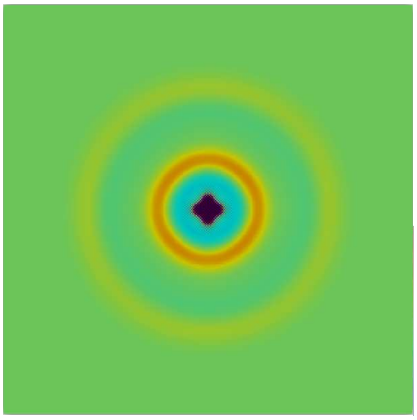

(A) Cartesian meshes 321 × 321, Glace scheme

(B) Cartesian meshes 321 × 321, Eucclhyd scheme

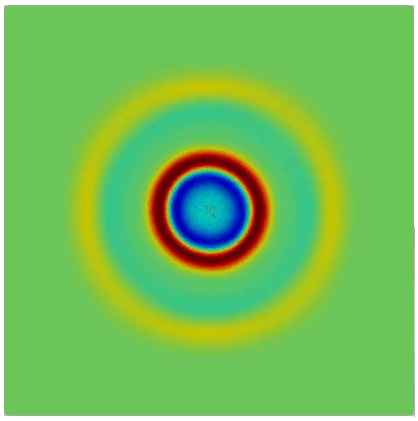

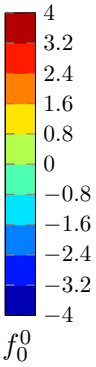

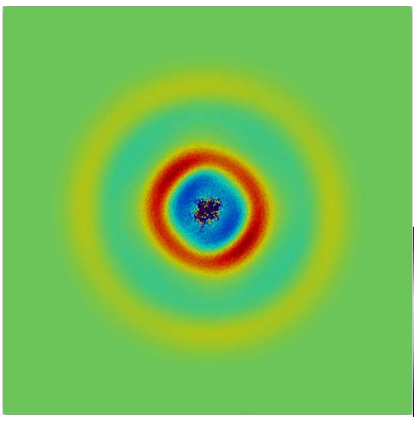

(C) Random meshes 321×321, Glace scheme

(D) Random meshes 321 × 321, Eucclhyd scheme

FIGURE 4.11. Solution for a Dirac-like initial condition for P_3 at time $t = 1$.

where the u_i are given by

$$u_1(\mathbf{x},t) = \frac{2}{3}\sqrt{\frac{2}{35}}\left(-\sqrt{4\sqrt{30}+75}e^{\frac{\alpha x}{\lambda_1}} + \sqrt{4\sqrt{30}+75}e^{\frac{\alpha x}{\lambda_2}} + \sqrt{75-4\sqrt{30}}e^{\frac{\alpha x}{\lambda_7}} - \sqrt{75-4\sqrt{30}}e^{\frac{\alpha x}{\lambda_8}}\right),$$

$$u_2(\mathbf{x},t) = \sqrt{30}\left(e^{\frac{\alpha x}{\lambda_3}} - e^{\frac{\alpha x}{\lambda_4}}\right),$$

$$u_3(\mathbf{x},t) = \frac{1}{15}\sqrt{2}\left(\sqrt{10\sqrt{30}+75}e^{\frac{\alpha x}{\lambda_1}} - \sqrt{10\sqrt{30}+75}e^{\frac{\alpha x}{\lambda_2}} - 15e^{\frac{\alpha x}{\lambda_5}} + 15e^{\frac{\alpha x}{\lambda_6}} + \sqrt{75-10\sqrt{30}}e^{\frac{\alpha x}{\lambda_7}} - \sqrt{75-10\sqrt{30}}e^{\frac{\alpha x}{\lambda_8}}\right),$$

$$u_4(\mathbf{x},t) = \frac{1}{5}\sqrt{\frac{2}{3}}\left(-\sqrt{10\sqrt{30}+75}e^{\frac{\alpha x}{\lambda_1}} + \sqrt{10\sqrt{30}+75}e^{\frac{\alpha x}{\lambda_2}} - 5e^{\frac{\alpha x}{\lambda_5}} + 5e^{\frac{\alpha x}{\lambda_6}} - \sqrt{75-10\sqrt{30}}e^{\frac{\alpha x}{\lambda_7}} + \sqrt{75-10\sqrt{30}}e^{\frac{\alpha x}{\lambda_8}}\right),$$

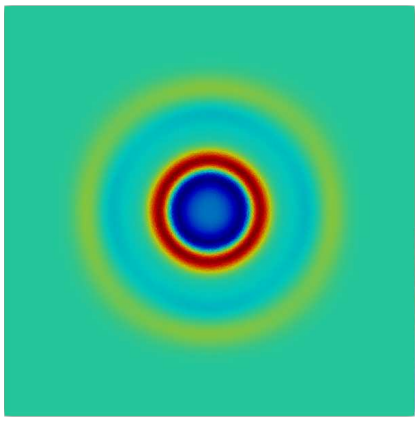

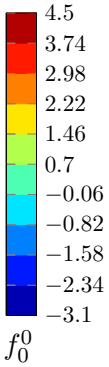

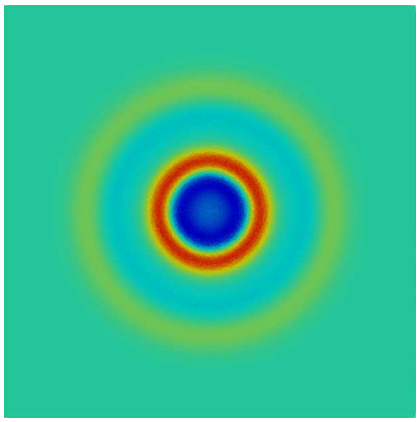

(A) P_3 on a random mesh 321×321 with the Glace scheme

(B) P_3 on a random mesh 321×321 with the Eucclhyd scheme

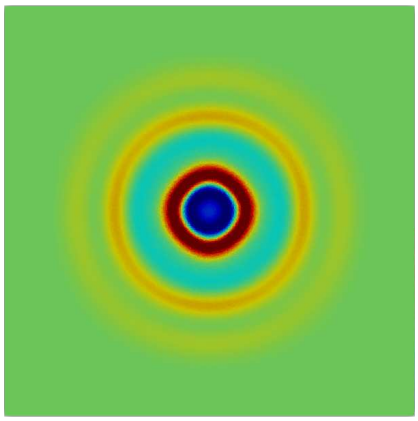

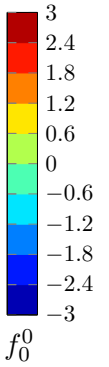

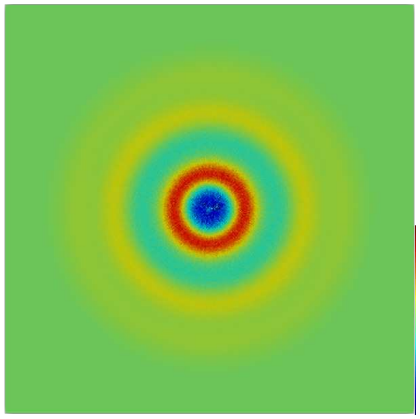

(C) P_5 on a random mesh 321×321 with the Glace scheme

(D) P_5 on a random mesh 321×321 with the Eucclhyd scheme

FIGURE 4.12. Solution on random meshes for a regularized Dirac type initial condition for P_3 andP_5 at time $t = 1$.

$$u_5(\mathbf{x},t) = -\sqrt{14}\left(e^{\frac{\alpha x}{\lambda_3}} + e^{\frac{\alpha x}{\lambda_4}}\right),$$

$$u_6(\mathbf{x},t) = \frac{2}{5\sqrt{7}}\left(\left(\sqrt{30}+10\right)e^{\frac{\alpha x}{\lambda_1}} + \left(\sqrt{30}+10\right)e^{\frac{\alpha x}{\lambda_2}} + \left(\sqrt{30}-10\right)e^{\frac{\alpha x}{\lambda_7}} + \left(\sqrt{30}-10\right)e^{\frac{\alpha x}{\lambda_8}}\right),$$

$$u_7(\mathbf{x},t) = -\sqrt{15}\left(e^{\frac{\alpha x}{\lambda_3}} + e^{\frac{\alpha x}{\lambda_4}}\right),$$

$$u_8(\mathbf{x},t) = e^{\frac{\alpha x}{\lambda_3}} + e^{\frac{\alpha x}{\lambda_4}},$$

$$u_9(\mathbf{x},t) = -\frac{3e^{\frac{\alpha x}{\lambda_1}} + 3e^{\frac{\alpha x}{\lambda_2}} - 5e^{\frac{\alpha x}{\lambda_5}} - 5e^{\frac{\alpha x}{\lambda_6}} + 3e^{\frac{\alpha x}{\lambda_7}} + 3e^{\frac{\alpha x}{\lambda_8}}}{\sqrt{15}},$$

and

$$u_{10}(\mathbf{x},t) = e^{\frac{\alpha x}{\lambda_1}} + e^{\frac{\alpha x}{\lambda_2}} + e^{\frac{\alpha x}{\lambda_5}} + e^{\frac{\alpha x}{\lambda_6}} + e^{\frac{\alpha x}{\lambda_7}} + e^{\frac{\alpha x}{\lambda_8}}.$$

On the edges $]-1,1[\times\{-1\}$ and $]-1,1[\times\{1\}$, we impose symmetries conditions in order not to break the 1D character of the solution. This imposes that the coordinates u_k^m with $m > 0$ must be null. We notice that it is enough to impose w_3 and w_4 to be null. One can see in Figures 4.14–4.15 convergence

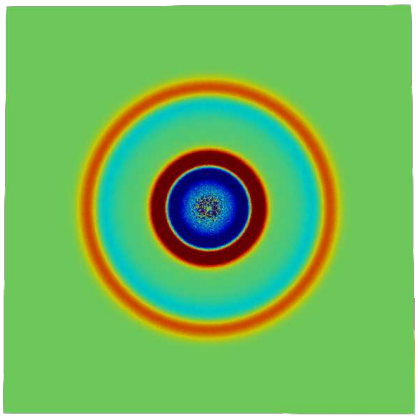

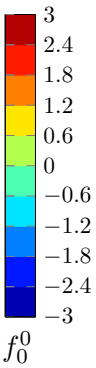

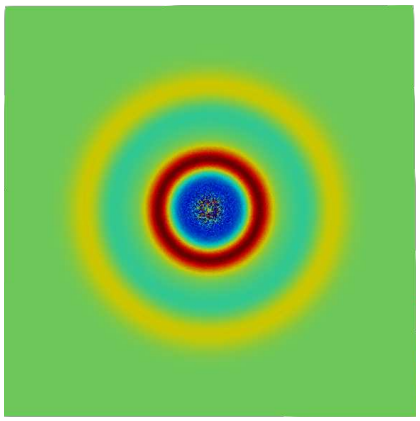

(A) P_3 with the Glace scheme

(B) P_3 with Eucclhyd scheme

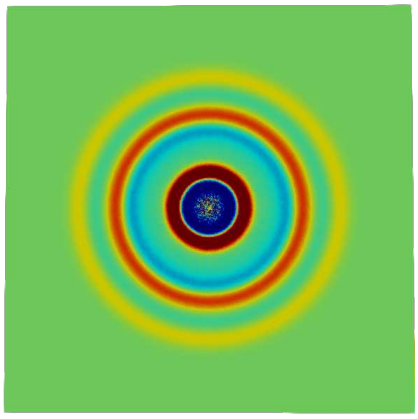

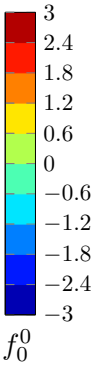

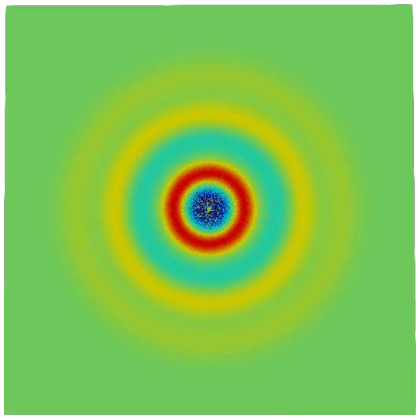

(C) P_5 with the Glace scheme

(D) P_5 with the Eucclhyd scheme

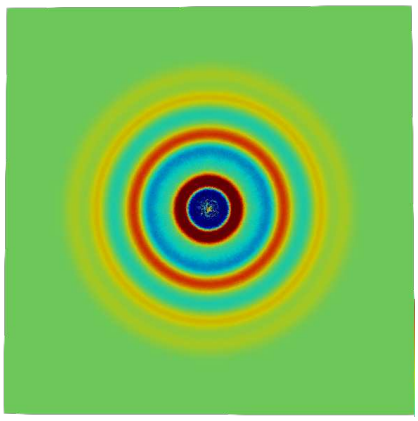

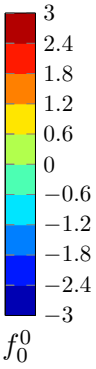

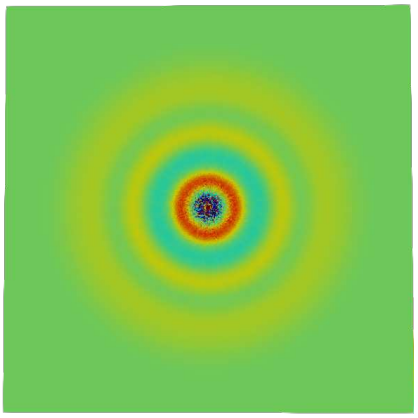

(E) P_7 with the Glace scheme

(F) P_7 with the Eucclhyd scheme

Figure 4.13. Solution for a regularized Dirac type initial condition on a Delaunay mesh ($h = 3/320$) at time $t = 1$.

curves for the L^2 norm on cartesian, random and Delaunay meshes. We observe numerically a first order convergence.

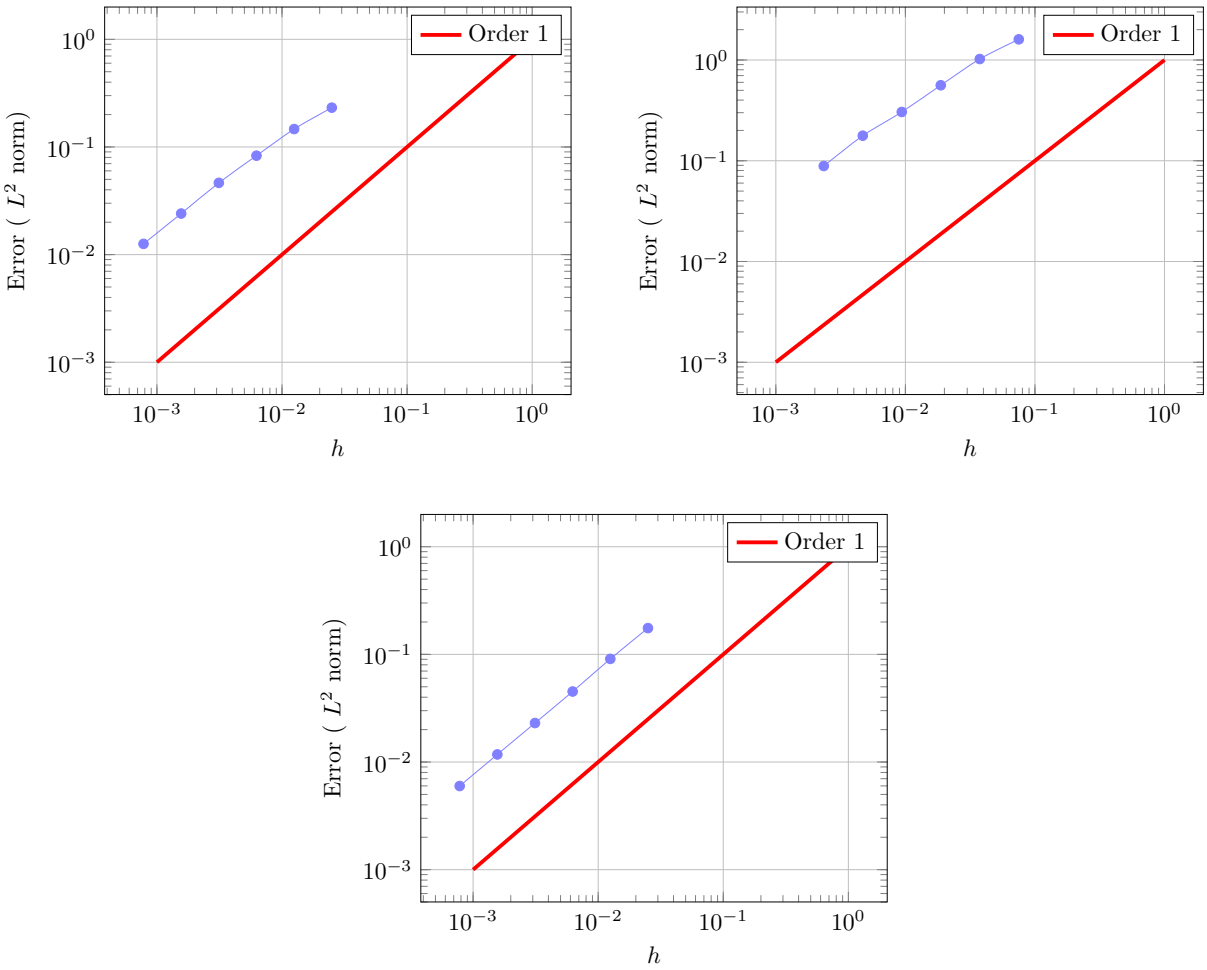

FIGURE 4.14. Convergence curve for P_3 with the Glace scheme (Log scale). Top left: random meshes, top right: Delaunay meshes, bottom: cartesian meshes.

5. Conclusion

In this paper, we have proposed two nodal finite volume schemes for the P_N model. We have proved a number of new properties for these schemes: their well-defined characters, their conservativities, their stabilities and their convergences for a sufficiently regular initial condition. We note that the time-explicit Glace and Eucclhyd schemes are much more expensive in computation time than the standard finite volume scheme. It is however important to keep in mind that a standard finite volume scheme cannot be asymptotic preserving [1], the study of nodal finite volume schemes for P_N being done in this perspective. Moreover, a way to remedy the problem of the high computational cost would be to use an implicit scheme, we could hope to find a competitive method compared to the standard finite volume scheme. It would be interesting to extend the convergence results to more general boundary conditions

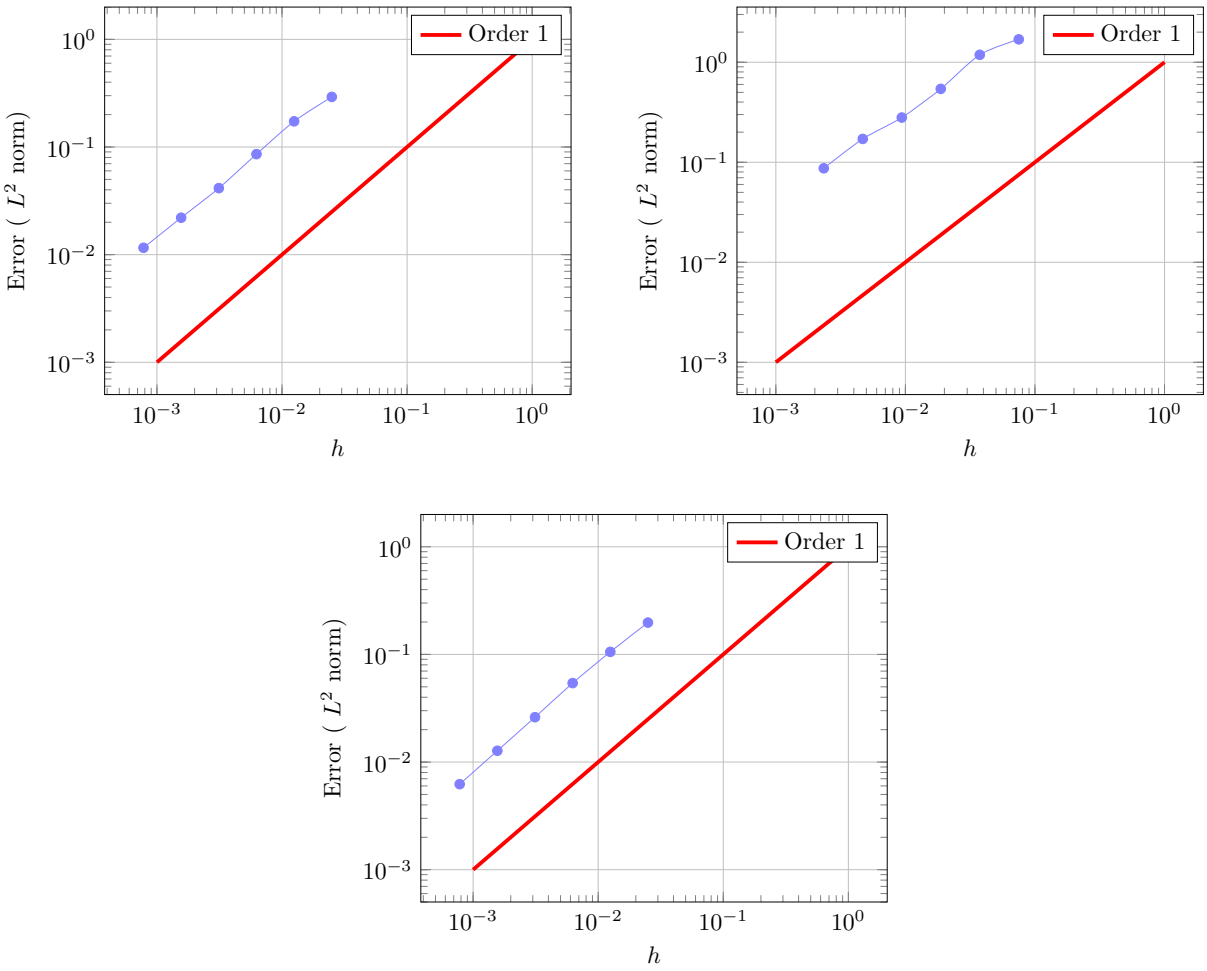

FIGURE 4.15. Convergence curve for P_3 with the Eucclhyd scheme (Log scale). Top left: random meshes, top right: Delaunay meshes, bottom: cartesian meshes.

than periodic boundary conditions, for example Dirichlet boundary conditions. The numerical results suggest that the convergence result is suboptimal with respect to the regularity of the initial solution. The natural continuation of this work would be to focus the study on the addition of the relaxation term in the flux calculation as in [1], in order to write an asymptotic preserving scheme. Moreover, it remains to study the spurious modes observed in the numerical results. One can also imagine extension to 3D. In our view, the main difficulty is practical since 3D rotation matrices are more complex to implement. From the theoretical point of view, it remains to extend Lemma 3.6 to 3D. Finally, an extension to second order of accuracy should be straightforward using classical reconstruction strategies used for finite volume schemes.

Appendix A. Proof of Proposition 3.18

Here, we give the proof of the Proposition 3.18 which gives a lower bound to $\Delta t_{\max}$

$$\Delta t_{\max} \geq \frac{\min\limits_{j\in J} V_j}{2\max\limits_{j\in\mathcal{J}}(1+2\#\mathcal{R}_j)\max\limits_{\substack{j\in\mathcal{J}\\ r\in\mathcal{R}_j}} l_{jr}} > 0.$$

Actually setting

$$N = \sum_{j\in\mathcal{J}}\sum_{r\in\mathcal{R}_j}(M_{jr}(\mathbf{h}_j^n-\mathbf{h}_r^n),\mathbf{h}_j^n-\mathbf{h}_r^n), \quad \text{and}$$

$$D = \sum_{j\in\mathcal{J}}\frac{1}{V_j}\left[\left(\sum_{r\in\mathcal{R}_j}\mathbf{G}_{jr}^n,\sum_{r\in\mathcal{R}_j}\mathbf{G}_{jr}^n\right)+\left(\sum_{r\in\mathcal{R}_j}\mathbf{F}_{jr}^n,\sum_{r\in\mathcal{R}_j}\mathbf{F}_{jr}^n\right)\right],$$

according to Property 3.17, L^2-stability is ensured if

$$\Delta t \leq \Delta t_{\max} = \frac{N}{D}.$$

Let us study the denominator D by first remarking that by (3.37)

$$\sum_{r\in\mathcal{R}_j}\mathbf{F}_{jr}^n = \sum_{r\in\mathcal{R}_j} l_{jr}\mathcal{U}_{\theta_{jr}}^{\mathbf{h}}A^T\mathcal{U}_{-\theta_{jr}}^{\mathbf{g}}\mathbf{g}_j^n + \sum_{r\in\mathcal{R}_j}M_{jr}(\mathbf{h}_j^n-\mathbf{h}_r^n),$$

which simplifies to

$$\sum_{r\in\mathcal{R}_j}\mathbf{F}_{jr}^n = \sum_{r\in\mathcal{R}_j}M_{jr}(\mathbf{h}_j^n-\mathbf{h}_r^n),$$

since, by Lemma 3.11, $\sum_{r\in\mathcal{R}_j} l_{jr}\mathcal{U}_{\theta_{jr}}^{\mathbf{h}}A^T\mathcal{U}_{-\theta_{jr}}^{\mathbf{g}} = 0$.

Thus, one has

$$\left\|\sum_{r\in\mathcal{R}_j}\mathbf{F}_{jr}^n\right\|^2 = \sum_{r\in\mathcal{R}_j}\left\|M_{jr}(\mathbf{h}_j^n-\mathbf{h}_r^n)\right\|^2 + 2\sum_{\substack{r,s\in\mathcal{R}_j\\ r<s}}\left(M_{jr}(\mathbf{h}_j^n-\mathbf{h}_r^n),M_{js}(\mathbf{h}_j^n-\mathbf{h}_s^n)\right),$$

which reads using Young's inequality

$$\left\|\sum_{r\in\mathcal{R}_j}\mathbf{F}_{jr}^n\right\|^2 \leq \sum_{r\in\mathcal{R}_j}\left\|M_{jr}(\mathbf{h}_j^n-\mathbf{h}_r^n)\right\|^2 + \sum_{\substack{r,s\in\mathcal{R}_j\\ r<s}}\left(\left\|M_{jr}(\mathbf{h}_j^n-\mathbf{h}_r^n)\right\|^2+\left\|M_{js}(\mathbf{h}_j^n-\mathbf{h}_s^n\right\|^2\right),$$

and then

$$\begin{aligned}\left\|\sum_{r\in\mathcal{R}_j}\mathbf{F}_{jr}^n\right\|^2 &\leq \sum_{r\in\mathcal{R}_j}\left\|M_{jr}(\mathbf{h}_j^n-\mathbf{h}_r^n)\right\|^2 + 2\#\mathcal{R}_j\sum_{r\in\mathcal{R}_j}\left\|M_{jr}(\mathbf{h}_j^n-\mathbf{h}_r^n)\right\|^2,\\ &\leq (1+2\#\mathcal{R}_j)\sum_{r\in\mathcal{R}_j}\left\|M_{jr}(\mathbf{h}_j^n-\mathbf{h}_r^n)\right\|^2. \qquad (A.1)\end{aligned}$$

Using again Lemma 3.11, one has

$$\sum_{r\in\mathcal{R}_j}\mathbf{G}_{jr}^n = \sum_{r\in\mathcal{R}_j} l_{jr}\mathcal{U}_{\theta_{jr}}^{\mathbf{g}}A\mathcal{U}_{-\theta_{jr}}^{\mathbf{h}}\mathbf{h}_r^n = \sum_{r\in\mathcal{R}_j} l_{jr}\mathcal{U}_{\theta_{jr}}^{\mathbf{g}}A\mathcal{U}_{-\theta_{jr}}^{\mathbf{h}}(\mathbf{h}_r^n-\mathbf{h}_j^n).$$

The same calculation as previously applies, so that

$$\left\| \sum_{r\in\mathcal{R}_j} \mathbf{G}_{jr}^n \right\|^2 \leq (1+2\#\mathcal{R}_j) \sum_{r\in\mathcal{R}_j} \left\| l_{jr}\mathcal{U}_{\theta_{jr}}^{\mathbf{g}} A\mathcal{U}_{-\theta_{jr}}^{\mathbf{h}}(\mathbf{h}_j^n - \mathbf{h}_r^n)\right\|^2. \tag{A.2}$$

In order to finish the calculation we shall now bound from above $\left\|M_{jr}(\mathbf{h}_j^n - \mathbf{h}_r^n)\right\|^2$ and $\left\|l_{jr}\mathcal{U}_{\theta_{jr}}^{\mathbf{g}} A\mathcal{U}_{-\theta_{jr}}^{\mathbf{h}}(\mathbf{h}_j^n - \mathbf{h}_r^n)\right\|^2$. On the one hand

$$\left\|M_{jr}(\mathbf{h}_j^n - \mathbf{h}_r^n)\right\|^2 = \left(M_{jr}^T M_{jr}(\mathbf{h}_j^n - \mathbf{h}_r^n), (\mathbf{h}_j^n - \mathbf{h}_r^n)\right).$$

Now, since according to (3.22), $M_{jr} = l_{jr}\mathcal{U}_{\theta_{jr}}^{\mathbf{h}} P_{\mathbf{h}} D_+ P_{\mathbf{h}}^T \mathcal{U}_{-\theta_{jr}}^{\mathbf{h}}$, one has

$$M_{jr}^T M_{jr} = l_{jr}^2 \mathcal{U}_{\theta_{jr}}^{\mathbf{h}} P_{\mathbf{h}} D_+ \underbrace{P_{\mathbf{h}}^T \mathcal{U}_{-\theta_{jr}}^{\mathbf{h}} \mathcal{U}_{\theta_{jr}}^{\mathbf{h}} P_{\mathbf{h}}}_{=I} D_+ P_{\mathbf{h}}^T \mathcal{U}_{-\theta_{jr}}^{\mathbf{h}},$$

since $P_{\mathbf{h}}$ and $\mathcal{U}_{\theta_{jr}}^{\mathbf{h}}$ are orthogonal matrices. Thus $M_{jr}^T M_{jr} = l_{jr}^2 \mathcal{U}_{\theta_{jr}}^{\mathbf{h}} P_{\mathbf{h}} D_+^2 P_{\mathbf{h}}^T \mathcal{U}_{-\theta_{jr}}^{\mathbf{h}}$, so

$$\left\|M_{jr}(\mathbf{h}_j^n - \mathbf{h}_r^n)\right\|^2 = \left(l_{jr}^2 \mathcal{U}_{\theta_{jr}}^{\mathbf{h}} P_{\mathbf{h}} D_+^2 P_{\mathbf{h}}^T \mathcal{U}_{-\theta_{jr}}^{\mathbf{h}}(\mathbf{h}_j^n - \mathbf{h}_r^n), (\mathbf{h}_j^n - \mathbf{h}_r^n)\right),$$

and

$$\left\|M_{jr}(\mathbf{h}_j^n - \mathbf{h}_r^n)\right\|^2 \leq \max_{j\in\mathcal{J}_r} l_{jr} \left(l_{jr}\mathcal{U}_{\theta_{jr}}^{\mathbf{h}} P_{\mathbf{h}} D_+ P_{\mathbf{h}}^T \mathcal{U}_{-\theta_{jr}}^{\mathbf{h}}(\mathbf{h}_j^n - \mathbf{h}_r^n), (\mathbf{h}_j^n - \mathbf{h}_r^n)\right),$$

since the eigenvalues of D_+ are positive and lower than 1 (see [11]). So one has

$$\left\|M_{jr}(\mathbf{h}_j^n - \mathbf{h}_r^n)\right\|^2 \leq \max_{j\in\mathcal{J}_r} l_{jr} \left(M_{jr}(\mathbf{h}_j^n - \mathbf{h}_r^n), (\mathbf{h}_j^n - \mathbf{h}_r^n)\right).$$

On the other hand

$$\begin{aligned}\left\|l_{jr}\mathcal{U}_{\theta_{jr}}^{\mathbf{g}} A\mathcal{U}_{-\theta_{jr}}^{\mathbf{h}}(\mathbf{h}_j^n - \mathbf{h}_r^n)\right\|^2 &= \left(l_{jr}^2 \mathcal{U}_{\theta_{jr}}^{\mathbf{h}} A^T \mathcal{U}_{-\theta_{jr}}^{\mathbf{g}} \mathcal{U}_{\theta_{jr}}^{\mathbf{g}} A\mathcal{U}_{-\theta_{jr}}^{\mathbf{h}}(\mathbf{h}_j^n - \mathbf{h}_r^n), (\mathbf{h}_j^n - \mathbf{h}_r^n)\right), \\ &= \left(l_{jr}^2 \mathcal{U}_{\theta_{jr}}^{\mathbf{h}} A^T A\mathcal{U}_{-\theta_{jr}}^{\mathbf{h}}(\mathbf{h}_j^n - \mathbf{h}_r^n), (\mathbf{h}_j^n - \mathbf{h}_r^n)\right).\end{aligned}$$

Recalling that $A^T A = P_{\mathbf{h}} D_+^2 P_{\mathbf{h}}^T$, one gets the same right hand side as previously

$$\left\|l_{jr}\mathcal{U}_{\theta_{jr}}^{\mathbf{g}} A\mathcal{U}_{-\theta_{jr}}^{\mathbf{h}}(\mathbf{h}_j^n - \mathbf{h}_r^n)\right\|^2 = \left(l_{jr}^2 \mathcal{U}_{\theta_{jr}}^{\mathbf{h}} P_{\mathbf{h}} D_+^2 P_{\mathbf{h}}^T \mathcal{U}_{-\theta_{jr}}^{\mathbf{h}}(\mathbf{h}_j^n - \mathbf{h}_r^n), (\mathbf{h}_j^n - \mathbf{h}_r^n)\right),$$

so

$$\left\|l_{jr}\mathcal{U}_{\theta_{jr}}^{\mathbf{g}} A\mathcal{U}_{-\theta_{jr}}^{\mathbf{h}}(\mathbf{h}_j^n - \mathbf{h}_r^n)\right\|^2 \leq \max_{j\in\mathcal{J}_r} l_{jr} \left(M_{jr}(\mathbf{h}_j^n - \mathbf{h}_r^n), (\mathbf{h}_j^n - \mathbf{h}_r^n)\right).$$

Injecting these upper bounds into (A.1) and (A.2), it yields

$$\left\| \sum_{r\in\mathcal{R}_j} \mathbf{F}_{jr}^n \right\|^2 + \left\| \sum_{r\in\mathcal{R}_j} \mathbf{G}_{jr}^n \right\|^2 \leq 2(1+2\#\mathcal{R}_j) \max_{j\in\mathcal{J}_r} l_{jr} \left(M_{jr}(\mathbf{h}_j^n - \mathbf{h}_r^n), (\mathbf{h}_j^n - \mathbf{h}_r^n)\right).$$

Finally, the denominator D is upper bounded by

$$\begin{aligned} D &\leq \sum_{j\in\mathcal{J}} \frac{2}{V_j}(1+2\#\mathcal{R}_j) \max_{j\in\mathcal{J}_r} l_{jr} \left(M_{jr}(\mathbf{h}_j^n - \mathbf{h}_r^n), (\mathbf{h}_j^n - \mathbf{h}_r^n)\right), \\ &\leq 2\frac{\max_{j\in\mathcal{J}}(1+2\#\mathcal{R}_j)}{\min_{j\in J} V_j} \max_{\substack{j\in\mathcal{J} \\ r\in\mathcal{R}_j}} l_{jr} \sum_{j\in\mathcal{J}} \left(M_{jr}(\mathbf{h}_j^n - \mathbf{h}_r^n), (\mathbf{h}_j^n - \mathbf{h}_r^n)\right). \end{aligned}$$

Recognizing the expression of the numerator N, one gets

$$D \leq 2\frac{\max_{j\in\mathcal{J}}(1+2\#\mathcal{R}_j)}{\min_{j\in J} V_j}\max_{\substack{j\in\mathcal{J}\\ r\in\mathcal{R}_j}} l_{jr}\ N.$$

So we established

$$\frac{N}{D} \geq \frac{\min_{j\in J} V_j}{2\max_{j\in\mathcal{J}}(1+2\#\mathcal{R}_j)\max_{\substack{j\in\mathcal{J}\\ r\in\mathcal{R}_j}} l_{jr}}.$$

Appendix B. Proof of Theorem 3.21

We give the proof of Theorem 3.21 which establishes the convergence of the semi-discrete scheme.

The scheme in the condensed form writes

$$\frac{d}{dt}\mathbf{u}_j + \frac{1}{V_j}\sum_{r\in\mathcal{R}_j}\mathbb{A}_{jr}\mathbf{u}_{jr} = 0,$$

with

$$\mathbf{u}_j = \begin{pmatrix}\mathbf{g}_j\\ \mathbf{h}_j\end{pmatrix}, \qquad \mathbb{A}_{jr} = \begin{pmatrix}0 & l_{jr}\mathcal{U}^{\mathbf{g}}_{\theta_{jr}}A\mathcal{U}^{\mathbf{h}}_{-\theta_{jr}}\\ l_{jr}\mathcal{U}^{\mathbf{h}}_{\theta_{jr}}A^T\mathcal{U}^{\mathbf{g}}_{-\theta_{jr}} & 0\end{pmatrix}, \qquad \mathbf{u}_{jr} = \begin{pmatrix}\mathbf{g}_{jr}\\ \mathbf{h}_r\end{pmatrix}.$$

In all this Section, C denotes a strictly positive constant, which can change from one line to another. The proof is given in the case of the Glace scheme, but it can be easily extended to the case of the Eucclhyd scheme. We will study the quantity

$$\mathcal{E}(t) = \frac{1}{2}\|\mathbf{u}_h(t) - \mathbf{u}(t)\|^2_{L^2(\Omega)}$$

for $t \in]0,+\infty[$. We compute

$$\mathcal{E}'(t) = \underbrace{\frac{1}{2}\int_\Omega \left(\mathbf{u}_h^2\right)' d\mathbf{x}}_{\mathcal{D}_1:=} + \underbrace{\frac{1}{2}\int_\Omega \left(\mathbf{u}^2\right)' d\mathbf{x}}_{\mathcal{D}_2:=} + \underbrace{\int_\Omega -\left(\mathbf{u}_h', \mathbf{u}\right) d\mathbf{x}}_{\mathcal{D}_3:=} + \underbrace{\int_\Omega -\left(\mathbf{u}_h, \mathbf{u}'\right) d\mathbf{x}}_{\mathcal{D}_4:=},$$

and we estimate each term of the sum.

B.1. Estimation of $\mathcal{D}_1$

Using Proposition 3.15, one has

$$\mathcal{D}_1 = -\sum_{j\in\mathcal{J}}\sum_{r\in\mathcal{R}_j}(M_{jr}(\mathbf{h}_j - \mathbf{h}_r), \mathbf{h}_j - \mathbf{h}_r).$$

B.2. Estimation of $\mathcal{D}_2$

From Proposition 3.14,

$$\mathcal{D}_2 = 0.$$

B.3. **Estimation of $\mathcal{D}_3$**

A direct calculation gives

$$\mathcal{D}_3 = -\sum_{j\in\mathcal{J}}\left(\mathbf{u}_j', \int_j \mathbf{u}d\mathbf{x}\right) = \sum_{j\in\mathcal{J}}\sum_{r\in\mathcal{R}_j}\left(\mathbb{A}_{jr}\mathbf{u}_{jr}, \frac{1}{V_j}\int_j \mathbf{u}d\mathbf{x}\right),$$

and since $\sum_{r\in\mathcal{R}_j}\mathbb{A}_{jr} = 0$,

$$\mathcal{D}_3 = \sum_{j\in\mathcal{J}}\sum_{r\in\mathcal{R}_j}\left(\mathbb{A}_{jr}(\mathbf{u}_{jr}-\mathbf{u}_j), \frac{1}{V_j}\int_j \mathbf{u}d\mathbf{x}\right).$$

Moreover,

$$\mathcal{D}_3 = \sum_{j\in\mathcal{J}}\sum_{r\in\mathcal{R}_j}\left(\mathbb{A}_{jr}(\mathbf{u}_{jr}-\mathbf{u}_j), \frac{1}{V_j}\int_j \mathbf{u}d\mathbf{x}-\mathbf{u}(\mathbf{x}_r)\right) + \sum_{j\in\mathcal{J}}\sum_{r\in\mathcal{R}_j}\left(\mathbb{A}_{jr}(\mathbf{u}_{jr}-\mathbf{u}_j), \mathbf{u}(\mathbf{x}_r)\right),$$

and since $\sum_{j\in\mathcal{J}}\sum_{r\in\mathcal{R}_j}\left(\mathbb{A}_{jr}\mathbf{u}_{jr}, \mathbf{u}(\mathbf{x}_r)\right) = 0$,

$$\mathcal{D}_3 = \sum_{j\in\mathcal{J}}\sum_{r\in\mathcal{R}_j}\left(\mathbb{A}_{jr}(\mathbf{u}_{jr}-\mathbf{u}_j), \frac{1}{V_j}\int_j \mathbf{u}d\mathbf{x}-\mathbf{u}(\mathbf{x}_r)\right) - \sum_{j\in\mathcal{J}}\sum_{r\in\mathcal{R}_j}\left(\mathbb{A}_{jr}\mathbf{u}_j, \mathbf{u}(\mathbf{x}_r)\right).$$

To simplify the notations, we denote

$$\begin{pmatrix}\delta\mathbf{g}_{jr}\\ \delta\mathbf{h}_{jr}\end{pmatrix} = \frac{1}{V_j}\int_j \mathbf{u}d\mathbf{x}-\mathbf{u}(\mathbf{x}_r).$$

With these notations, we have

$$\left(\mathbb{A}_{jr}(\mathbf{u}_{jr}-\mathbf{u}_j), \frac{1}{V_j}\int_j \mathbf{u}d\mathbf{x}-\mathbf{u}(\mathbf{x}_r)\right) = l_{jr}\left[\mathcal{U}^{\mathbf{g}}_{\theta_{jr}}A\mathcal{U}^{\mathbf{h}}_{-\theta_{jr}}(\mathbf{h}_r-\mathbf{h}_j)\right]\cdot\delta\mathbf{g}_{jr} + l_{jr}\left[\mathcal{U}^{\mathbf{h}}_{\theta_{jr}}A^T\mathcal{U}^{\mathbf{g}}_{-\theta_{jr}}(\mathbf{g}_{jr}-\mathbf{g}_j)\right]\cdot\delta\mathbf{h}_{jr}.$$

By the Young's inequality, one gets

$$\left(\mathbb{A}_{jr}(\mathbf{u}_{jr}-\mathbf{u}_j), \frac{1}{V_j}\int_j \mathbf{u}d\mathbf{x}-\mathbf{u}(\mathbf{x}_r)\right) \le \frac{1}{2}\underbrace{\|\sqrt{l_{jr}}\mathcal{U}^{\mathbf{g}}_{\theta_{jr}}A\mathcal{U}^{\mathbf{h}}_{-\theta_{jr}}(\mathbf{h}_r-\mathbf{h}_j)\|^2}_{a:=} + \frac{l_{jr}}{2}\|\delta\mathbf{g}_{jr}\|^2 + \frac{1}{2}\underbrace{\|\sqrt{l_{jr}}\mathcal{U}^{\mathbf{h}}_{\theta_{jr}}A^T\mathcal{U}^{\mathbf{g}}_{-\theta_{jr}}(\mathbf{g}_{jr}-\mathbf{g}_j)\|^2}_{b:=} + \frac{l_{jr}}{2}\|\delta\mathbf{h}_{jr}\|^2.$$

Let use first estimate the term a. One has

$$\begin{aligned} a &= \left(\sqrt{l_{jr}}\mathcal{U}^{\mathbf{g}}_{\theta_{jr}}A\mathcal{U}^{\mathbf{h}}_{-\theta_{jr}}(\mathbf{h}_r-\mathbf{h}_j), \sqrt{l_{jr}}\mathcal{U}^{\mathbf{g}}_{\theta_{jr}}A\mathcal{U}^{\mathbf{h}}_{-\theta_{jr}}(\mathbf{h}_r-\mathbf{h}_j)\right),\\ &= \left(l_{jr}\mathcal{U}^{\mathbf{h}}_{\theta_{jr}}A^TA\mathcal{U}^{\mathbf{h}}_{-\theta_{jr}}(\mathbf{h}_r-\mathbf{h}_j), \mathbf{h}_r-\mathbf{h}_j\right).\end{aligned}$$

Recalling that $A^TA = P_{\mathbf{h}}D_+^2P_{\mathbf{h}}^T$, one gets

$$a = \left(l_{jr}\mathcal{U}^{\mathbf{h}}_{\theta_{jr}}P_{\mathbf{h}}D_+^2P_{\mathbf{h}}^T\mathcal{U}^{\mathbf{h}}_{-\theta_{jr}}(\mathbf{h}_r-\mathbf{h}_j), \mathbf{h}_r-\mathbf{h}_j\right).$$

Since the eigenvalues of $\mathcal{A}_1$ are less than 1

$$a \le \left(l_{jr}\mathcal{U}^{\mathbf{h}}_{\theta_{jr}}P_{\mathbf{h}}D_+P_{\mathbf{h}}^T\mathcal{U}^{\mathbf{h}}_{-\theta_{jr}}(\mathbf{h}_r-\mathbf{h}_j), \mathbf{h}_r-\mathbf{h}_j\right),$$

which rewrites

$$a \le \left(M_{jr}(\mathbf{h}_r-\mathbf{h}_j), \mathbf{h}_r-\mathbf{h}_j\right).$$

We now estimate b. Using the equality (3.18), one has

$$\begin{aligned} b &= \|\sqrt{l_{jr}}\mathcal{U}^{\mathbf{h}}_{\theta_{jr}} P_{\mathbf{h}} D_+ P^T_{\mathbf{h}} \mathcal{U}^{\mathbf{h}}_{-\theta_{jr}}(\mathbf{h}_r - \mathbf{h}_j)\|^2, \\ &= \left(l_{jr}\mathcal{U}^{\mathbf{h}}_{\theta_{jr}} P_{\mathbf{h}} D^2_+ P^T_{\mathbf{h}} \mathcal{U}^{\mathbf{g}}_{-\theta_{jr}}(\mathbf{h}_r - \mathbf{h}_j), \mathbf{h}_r - \mathbf{h}_j\right), \end{aligned}$$

and using the same arguments as previously

$$b \leq \left(M_{jr}(\mathbf{h}_r - \mathbf{h}_j), \mathbf{h}_r - \mathbf{h}_j\right).$$

Finally, one gets the following estimate

$$\begin{aligned} \mathcal{D}_3 \leq \sum_{j\in\mathcal{J}}\sum_{r\in\mathcal{R}_j}\left(\frac{l_{jr}}{2}\|\delta\mathbf{g}_{jr}\|^2 + \frac{l_{jr}}{2}\|\delta\mathbf{h}_{jr}\|^2\right) \\ + \sum_{j\in\mathcal{J}}\sum_{r\in\mathcal{R}_j}(M_{jr}(\mathbf{h}_j - \mathbf{h}_r), \mathbf{h}_j - \mathbf{h}_r) - \sum_{j\in\mathcal{J}}\sum_{r\in\mathcal{R}_j}(\mathbb{A}_{jr}\mathbf{u}_j, \mathbf{u}(\mathbf{x}_r)). \end{aligned}$$

B.4. **Estimation of $\mathcal{D}_4$**

This last term does not depend on the scheme, we have

$$\mathcal{D}_4 = \int_\Omega -(\mathbf{u}_h, \mathbf{u}')d\mathbf{x} = -\sum_{j\in\mathcal{J}}(\mathbf{u}_j, \int_j \mathbf{u}' d\mathbf{x}).$$

By denoting Γ_{jk} the k-th edge of the cell j, and $\mathbf{n}_{jk} = (\cos\theta_{jk}, \sin\theta_{jk})$ the associated normal, which we choose so that

$$l_{jr}\mathbf{n}_{jr} = \frac{1}{2}(l^+_{jk}\mathbf{n}^+_{jk} + l^-_{jk}\mathbf{n}^-_{jk}).$$

We have

$$\begin{aligned} -\int_j \mathbf{u}' d\mathbf{x} &= \int_j \mathcal{A}_1\partial_x\mathbf{u} + \int_j \mathcal{A}_2\partial_y\mathbf{u}d\mathbf{x}, \\ &= \int_{\partial j} n^x_j\mathcal{A}_1\mathbf{u}d\sigma + \int_{\partial j} n^y_j\mathcal{A}_2\mathbf{u}d\sigma, \\ &= \sum_{k\in\mathcal{K}_j}\int_{\Gamma_{jk}}(n^x_{jk}\mathcal{A}_1 + n^y_{jk}\mathcal{A}_2)\mathbf{u}d\sigma, \end{aligned}$$

thus according to Proposition 2.5,

$$-\int_j \mathbf{u}' d\mathbf{x} = \sum_{k\in\mathcal{K}_j}\int_{\Gamma_{jk}} \mathcal{U}_{\theta_{jk}}\mathcal{A}_1\mathcal{U}_{-\theta_{jk}}\mathbf{u}d\sigma,$$

therefore

$$\mathcal{D}_4 = \sum_{j\in\mathcal{J}}\sum_{k\in\mathcal{K}_j}\left(\mathbf{u}_j, \mathcal{U}_{\theta_{jk}}\mathcal{A}_1\mathcal{U}_{-\theta_{jk}}\int_{\Gamma_{jk}}\mathbf{u}d\sigma\right).$$

The idea is to rewrite this estimate at nodes in order to balance $\mathcal{D}_3$. We write $\mathcal{D}_4$ in the form

$$\begin{aligned} \mathcal{D}_4 = \sum_{j\in\mathcal{J}}\sum_{k\in\mathcal{K}_j}\left(\mathbf{u}_j, l_{jk}\mathcal{U}_{\theta_{jk}}\mathcal{A}_1\mathcal{U}_{-\theta_{jk}}\frac{\mathbf{u}(\mathbf{x}_{r^+}) + \mathbf{u}(\mathbf{x}_r)}{2}\right) \\ + \sum_{j\in\mathcal{J}}\sum_{k\in\mathcal{K}_j}\left(\mathcal{U}_{\theta_{jk}}\mathcal{A}_1\mathcal{U}_{-\theta_{jk}}\mathbf{u}_j, \int_{\Gamma_{jk}}\mathbf{u}d\sigma - l_{jk}\frac{\mathbf{u}(\mathbf{x}_{r^+}) + \mathbf{u}(\mathbf{x}_r)}{2}\right), \end{aligned}$$

where $\mathbf{x}_r$ and $\mathbf{x}_{r^+}$ are the nodes on the edge Γ_{jk}, oriented in the trigonometric direction, and $\mathcal{K}_j$ is the set of edges of the cell j. By grouping the sums on the edges into sums on the nodes, we obtain

$$\sum_{j\in\mathcal{J}}\sum_{k\in\mathcal{K}_j}\left(\mathbf{u}_j, l_{jk}\mathcal{U}_{\theta_{jk}}\mathcal{A}_1\mathcal{U}_{-\theta_{jk}}\frac{\mathbf{u}(\mathbf{x}_{r^+})+\mathbf{u}(\mathbf{x}_r)}{2}\right)=\sum_{j\in\mathcal{J}}\sum_{r\in\mathcal{R}_j}\left(\mathbb{A}_{jr}\mathbf{u}_j,\mathbf{u}(\mathbf{x}_r)\right).$$

It remains to study the second term of the sum. We will use the following Lemma.

Lemma B.1 ([18])**.** *If $f\in H^2(]0,h[)$ with $h>0$, then*

$$\left|\int_0^h f(s)ds - h\frac{f(0)+f(h)}{2}\right|\leq\frac{h^{5/2}}{2\sqrt{30}}\|f''\|_{L^2(]0,h[)}.$$

Proof. Indeed, we can characterize $H^1_{]0,1[}$ as the set of absolutely continuous functions with a derivative almost every where in $L^2]0,1[$ and we can reiterate on $H^2_{]0,2[}$. Using a Taylor expansion with integral remainder we have:

$$f(s)=f(0)+sf'(0)+\int_0^s(s-t)f''(t)dt,$$

and

$$f(h)=f(0)+hf'(0)+\int_0^h(s-t)f''(t)dt,$$

which gives

$$f(s)-\frac{f(0)+f(h)}{2}=(s-\frac{h}{2})f'(0)+\int_0^s(s-t)f''(t)dt-\frac{h}{2}\int_0^h(h-t)f''(t)dt.$$

Integrating with respect to s on $[0,1]$ and since the integral of an affine function is null on the considered interval, we have

$$\begin{aligned}f(s)-\frac{f(0)+f(h)}{2}&=\int_{s=0}^{s=h}\int_{t=0}^{t=s}(s-t)f''(t)dtds-\frac{h}{2}\int_{t=0}^{t=h}(h-t)f'(t)dt\\&=\int_{t=0}^{t=h}\int_{s=t}^{s=h}(s-t)f''(t)dsdt-\frac{h}{2}\int_{t=0}^{t=h}(h-t)f''(t)dt\\&=\int_{t=0}^{t=h}\frac{t}{2}(t-h)f''(t)dt.\end{aligned}$$

Thus using the Hölder inequality

$$\left|\int_0^h f(s)ds-h\frac{f(0)+f(h)}{2}\right|\leq\sqrt{\int_0^h\left(\frac{t(t-h)}{2}\right)^2}\|f''\|_{L^2(]0,h[)},$$

which, after calculation, corresponds to the desired estimate. ∎

Applying this Lemma on each edge Γ_{jk}, we obtain the estimate

$$\mathcal{D}_4\leq\sum_{j\in\mathcal{J}}\sum_{k\in\mathcal{K}_j}\left(\mathbb{A}_{jr}\mathbf{u}_j,\mathbf{u}(\mathbf{x}_r)\right)+C\sum_{j\in\mathcal{J}}\sum_{k\in\mathcal{K}_j}l_{jk}^{5/2}\|\mathbf{u}_j\|\|\nabla^2\mathbf{u}\|_{L^2(\Gamma_{jk})}.$$

B.5. **Estimation of $\mathcal{E}$**

Adding the four estimates, since M_{jr} is nonnegative, we obtain

$$\mathcal{E}'(t)\leq\sum_{j\in\mathcal{J}}\sum_{r\in\mathcal{R}_j}\left(\frac{l_{jr}}{2}\|\delta\mathbf{g}_{jr}\|^2+\frac{l_{jr}}{2}\|\delta\mathbf{h}_{jr}\|^2\right)+C\sum_{j\in\mathcal{J}}\sum_{k\in\mathcal{K}_j}l_{jk}^{5/2}\|\mathbf{u}_j\|\|\nabla^2\mathbf{u}\|_{L^2(\Gamma_{jk})}.$$

Let us estimate the first term. We decompose the nodal term $\delta\mathbf{g}_{jr}$ by introducing the edge term $\delta\mathbf{g}_{jk}$ as

$$\delta\mathbf{g}_{jk} = \frac{1}{V_j}\int_j \mathbf{u}d\mathbf{x} - \frac{1}{l_{jk}}\int_{\Gamma_{jk}} \mathbf{u}d\sigma,$$

and therefore

$$\delta\mathbf{g}_{jr} = \delta\mathbf{g}_{jk} + \frac{1}{l_{jk}}\int_{\Gamma_{jk}} \mathbf{g}d\sigma - \mathbf{g}(\mathbf{x}_r).$$

It is classical that

$$\|\delta\mathbf{g}_{jk}\| \leq C\|\nabla\mathbf{g}\|_{L^2(j)}.$$

On the other hand, a calculation shows that

$$\begin{aligned}
\left\|\frac{1}{l_{jk}}\int_{\Gamma_{jk}} \mathbf{g}d\sigma - \mathbf{g}(r)\right\| &= \left\|\frac{1}{l_{jk}}\int_{\Gamma_{jk}} \mathbf{g}d\sigma - \frac{1}{l_{jk}}\int_{\Gamma_{jk}} \mathbf{g}(r)d\sigma\right\|, \\
&\leq \int_{\Gamma_{jk}} \frac{1}{l_{jk}}\|\mathbf{g} - \mathbf{g}(r)\|d\sigma, \\
&\leq \left(\int_{\Gamma_{jk}} \frac{1}{l_{jk}^2}d\sigma\right)^{1/2}\left(\int_{\Gamma_{jk}} l_{jk}^2\|\nabla\mathbf{g}\|^2 d\sigma\right)^{1/2}, \\
&= l_{jk}^{1/2}\|\nabla\mathbf{g}\|_{L^2(\Gamma_{jk})}, \\
&\leq Ch^{1/2}\|\nabla\mathbf{g}\|_{H^1(j)}.
\end{aligned}$$

Therefore, for h bounded, one has

$$\|\delta\mathbf{g}_{jr}\| \leq C\|\nabla\mathbf{g}\|_{H^1(j)}.$$

The same calculation for $\delta\mathbf{h}_{jr}$ gives

$$\sum_{j\in\mathcal{J}}\sum_{r\in\mathcal{R}_j}\left(\frac{l_{jr}}{2}\|\delta\mathbf{g}_{jr}\|^2 + \frac{l_{jr}}{2}\|\delta\mathbf{h}_{jr}\|^2\right) \leq Ch\|\nabla\mathbf{u}\|^2_{H^1(\Omega)}.$$

Let us now estimate the second term. Since $\mathbf{u}\in H^3(\Omega)$ one has

$$\|\nabla^2\mathbf{u}\|_{L^2(\Gamma_{jk})} \leq C\|\mathbf{u}\|_{H^3(\Omega)}.$$

We have

$$\begin{aligned}
\sum_{j\in\mathcal{J}}\sum_{k\in\mathcal{K}_j} l_{jk}^{5/2}\|\mathbf{u}_j\|\|\nabla^2\mathbf{u}\|_{L^2(\Gamma_{jk})} &\leq \frac{1}{2}\sum_{j\in\mathcal{J}}\sum_{k\in\mathcal{K}_j}\left(l_{jk}^3\|\mathbf{u}\|^2 + l_{jk}C\|\mathbf{u}\|^2_{H^3(j)}\right), \\
&\leq C_1 h\sum_{j\in\mathcal{J}} V_j\|\mathbf{u}_j\|^2 + C_2 h\|\mathbf{u}\|^2_{H^3(\Omega)}, \\
&\leq C_1 h\|\mathbf{u}_h\|^2_{L^2(\Omega)} + C_2 h\|\mathbf{u}\|^2_{H^3(\Omega)}.
\end{aligned}$$

By Proposition 3.15, the scheme is dissipative, so

$$\|\mathbf{u}_h\|^2_{L^2(\Omega)} \leq \|\mathbf{u}_h^0\|^2_{L^2(\Omega)} \leq \|\mathbf{u}_0\|^2_{L^2(\Omega)}.$$

Moreover, according to Proposition 3.14

$$\|\mathbf{u}\|_{H^3(\Omega)} = \|\mathbf{u}_0\|_{H^3(\Omega)},$$

and therefore

$$\sum_{j\in\mathcal{J}}\sum_{k\in\mathcal{K}_j} l_{jk}^{5/2}\|\mathbf{u}_j\|\|\nabla^2\mathbf{u}\|_{L^2(\Gamma_{jk})} \leq Ch\|\mathbf{u}_0\|^2_{H^3(\Omega)}.$$

Finally we obtain the estimate on $\mathcal{E}'(t)$

$$\mathcal{E}'(t) \leq Ch\|\nabla\mathbf{u}\|^2_{H^1(\Omega)} + C'h\|\mathbf{u}_0\|^2_{H^3(\Omega)}.$$

By the Steklov–Poincaré inequality (see for instance [9, Lemma 3.24, p. 27]), we have

$$\mathcal{E}(0) \leq Ch\|\nabla \mathbf{u}_0\|^2_{L^2(\Omega)},$$

and finally we obtain for $h < 1$, by integrating in time

$$\|\mathbf{u}_h(t) - \mathbf{u}(t)\|_{L^2(\Omega)} \leq C\sqrt{(1+t)\|\nabla \mathbf{u}_0\|^2_{L^2(\Omega)} + t\|\mathbf{u}_0\|^2_{H^3(\Omega)}}h^{1/2}.$$

Appendix C. Examples of A, $\mathcal{U}_\theta^{\mathbf{g}}$ and $\mathcal{U}_\theta^{\mathbf{h}}$

For $N = 3$, we have

$$A = \begin{pmatrix} 0 & \frac{1}{\sqrt{3}} & 0 & 0 & 0 & 0 \\ \frac{1}{\sqrt{5}} & 0 & \sqrt{\frac{3}{14}} & -\frac{1}{\sqrt{70}} & 0 & 0 \\ 0 & -\frac{1}{\sqrt{15}} & 0 & 0 & \sqrt{\frac{6}{35}} & 0 \\ 0 & -\frac{1}{\sqrt{5}} & 0 & 0 & -\frac{1}{\sqrt{70}} & \sqrt{\frac{3}{14}} \end{pmatrix},$$

$$\mathcal{U}_\theta^{\mathbf{g}} = \begin{pmatrix} 1 & 0 & 0 & 0 \\ 0 & \cos 2\theta & 0 & \sin 2\theta \\ 0 & 0 & 1 & 0 \\ 0 & -\sin 2\theta & 0 & \cos 2\theta \end{pmatrix}, \qquad \mathcal{U}_\theta^{\mathbf{h}} = \begin{pmatrix} \cos\theta & \sin\theta & 0 & 0 & 0 & 0 \\ -\sin\theta & \cos\theta & 0 & 0 & 0 & 0 \\ 0 & 0 & \cos 3\theta & 0 & 0 & \sin 3\theta \\ 0 & 0 & 0 & \cos\theta & \sin\theta & 0 \\ 0 & 0 & 0 & -\sin\theta & \cos\theta & 0 \\ 0 & 0 & -\sin 3\theta & 0 & 0 & \cos 3\theta \end{pmatrix}.$$

For $N = 5$, we have

$$A = \begin{pmatrix} 0 & \frac{1}{\sqrt{3}} & 0 & 0 & 0 & 0 & 0 & 0 & 0 & 0 & 0 & 0 \\ \frac{1}{\sqrt{5}} & 0 & \sqrt{\frac{3}{14}} & -\frac{1}{\sqrt{70}} & 0 & 0 & 0 & 0 & 0 & 0 & 0 & 0 \\ 0 & -\frac{1}{\sqrt{15}} & 0 & 0 & \sqrt{\frac{6}{35}} & 0 & 0 & 0 & 0 & 0 & 0 & 0 \\ 0 & \frac{1}{\sqrt{5}} & 0 & 0 & -\frac{1}{\sqrt{70}} & \sqrt{\frac{3}{14}} & 0 & 0 & 0 & 0 & 0 & 0 \\ 0 & 0 & \frac{\sqrt{2}}{3} & 0 & 0 & 0 & \sqrt{\frac{5}{22}} & -\frac{1}{3\sqrt{22}} & 0 & 0 & 0 & 0 \\ 0 & 0 & -\frac{1}{3\sqrt{14}} & \sqrt{\frac{5}{42}} & 0 & 0 & 0 & \frac{\sqrt{\frac{14}{11}}}{3} & -\frac{1}{\sqrt{33}} & 0 & 0 & 0 \\ 0 & 0 & 0 & 0 & -\sqrt{\frac{2}{21}} & 0 & 0 & 0 & 0 & \sqrt{\frac{5}{33}} & 0 & 0 \\ 0 & 0 & 0 & 0 & \sqrt{\frac{5}{42}} & -\frac{1}{3\sqrt{14}} & 0 & 0 & 0 & -\frac{1}{\sqrt{33}} & \frac{\sqrt{\frac{14}{11}}}{3} & 0 \\ 0 & 0 & 0 & 0 & 0 & \frac{\sqrt{2}}{3} & 0 & 0 & 0 & 0 & -\frac{1}{3\sqrt{22}} & \sqrt{\frac{5}{22}} \end{pmatrix},$$

$$\mathcal{U}_\theta^{\mathbf{g}} = \begin{pmatrix} 1 & 0 & 0 & 0 & 0 & 0 & 0 & 0 & 0 \\ 0 & \cos(2\theta) & 0 & \sin(2\theta) & 0 & 0 & 0 & 0 & 0 \\ 0 & 0 & 1 & 0 & 0 & 0 & 0 & 0 & 0 \\ 0 & -\sin(2\theta) & 0 & \cos(2\theta) & 0 & 0 & 0 & 0 & 0 \\ 0 & 0 & 0 & 0 & \cos(4\theta) & 0 & 0 & 0 & \sin(4\theta) \\ 0 & 0 & 0 & 0 & 0 & \cos(2\theta) & 0 & \sin(2\theta) & 0 \\ 0 & 0 & 0 & 0 & 0 & 0 & 1 & 0 & 0 \\ 0 & 0 & 0 & 0 & 0 & -\sin(2\theta) & 0 & \cos(2\theta) & 0 \\ 0 & 0 & 0 & 0 & -\sin(4\theta) & 0 & 0 & 0 & \cos(4\theta) \end{pmatrix},$$

$$\mathcal{U}_\theta^{\mathbf{h}} = \begin{pmatrix}
\cos(\theta) & \sin(\theta) & 0 & 0 & 0 & 0 & 0 & 0 & 0 & 0 & 0 & 0 \\
-\sin(\theta) & \cos(\theta) & 0 & 0 & 0 & 0 & 0 & 0 & 0 & 0 & 0 & 0 \\
0 & 0 & \cos(3\theta) & 0 & 0 & \sin(3\theta) & 0 & 0 & 0 & 0 & 0 & 0 \\
0 & 0 & 0 & \cos(\theta) & \sin(\theta) & 0 & 0 & 0 & 0 & 0 & 0 & 0 \\
0 & 0 & 0 & -\sin(\theta) & \cos(\theta) & 0 & 0 & 0 & 0 & 0 & 0 & 0 \\
0 & 0 & -\sin(3\theta) & 0 & 0 & \cos(3\theta) & 0 & 0 & 0 & 0 & 0 & 0 \\
0 & 0 & 0 & 0 & 0 & 0 & \cos(5\theta) & 0 & 0 & 0 & 0 & \sin(5\theta) \\
0 & 0 & 0 & 0 & 0 & 0 & 0 & \cos(3\theta) & 0 & 0 & \sin(3\theta) & 0 \\
0 & 0 & 0 & 0 & 0 & 0 & 0 & 0 & \cos(\theta) & \sin(\theta) & 0 & 0 \\
0 & 0 & 0 & 0 & 0 & 0 & 0 & 0 & -\sin(\theta) & \cos(\theta) & 0 & 0 \\
0 & 0 & 0 & 0 & 0 & 0 & 0 & -\sin(3\theta) & 0 & 0 & \cos(3\theta) & 0 \\
0 & 0 & 0 & 0 & 0 & 0 & -\sin(5\theta) & 0 & 0 & 0 & 0 & \cos(5\theta)
\end{pmatrix}.$$

References

[1] C. Buet, B. Després, and E. Franck. Design of asymptotic preserving finite volume schemes for the hyperbolic heat equation on unstructured meshes. *Numer. Math.*, 122:227–278, 2012.

[2] C. Buet, B. Després, and G. Morel. Approximation Properties of Vectorial Exponential Functions. *Commun. Appl. Math. Comput.*, 6:1801–1831, 2023.

[3] J. Bünger, N. Sarna, and M. Torrilhon. Stable Boundary Conditions and Discretization for P_N Equations. *J. Comput. Math.*, 40(6):977–1003, 2022.

[4] B. G. Carlson and K. D. Lathrop. *Computing Methods in Reactor Physics*. Gordon and Breach, 1968.

[5] G. Carré, S. Del Pino, B. Després, and E. Labourasse. A cell-centered Lagrangian hydrodynamics scheme on general unstructured meshes in arbitrary dimension. *J. Comput. Phys.*, 228(14):5160–5183, 2009.

[6] B. Després and C. Mazeran. Lagrangian Gas Dynamics in Two Dimensions and Lagrangian systems. *Arch. Ration. Mech. Anal.*, 178(3):327–372, 2005.

[7] H. Egger and M. Schlottbom. A mixed variational framework for the radiative transfer equation. *Math. Models Methods Appl. Sci.*, 22(3): article no. 1150014 (30 pages), 2012.

[8] H. Egger and M. Schlottbom. A class of Galerkin schemes for time-dependent radiative transfer. *SIAM J. Numer. Anal.*, 54(6):3577–3599, 2016.

[9] A. Ern and J.-L. Guermond. *Finite elements I: Approximation and interpolation*, volume 72 of *Texts in Applied Mathematics*. Springer, 2021.

[10] R. Eymard, T. Gallouët, and R. Herbin. Finite volume methods. In *Solution of equations in* $\mathbb{R}^n$ *(Part 3)*, volume 7 of *Handbook of Numerical Analysis*, pages 713–1018. Elsevier, 2000.

[11] C. Kristopher Garrett and Cory D. Hauck. On the eigenstructure of spherical harmonic equations for radiative transport. *Comput. Math. Appl.*, 72(2):264–270, 2016. The Proceedings of ICMMES 2014.

[12] E. Godlewski and P-A. Raviart. *Numerical Approximation of Hyperbolic Systems of Conservation Laws*. Springer, 1996.

[13] F. Hermeline. Une méthode de volumes finis pour les équations elliptiques du second ordre. *C. R. Math.*, 326(12):1433–1436, 1998.

[14] F. Hermeline. A discretization of the multigroup P_N radiative transfer equation on general meshes. *J. Comput. Phys.*, 313:549–582, 2016.

[15] E. S. Kuznetsov. Radiative equilibrium of a gaseous sphere surrounding an absolutely black sphere. *Izv. An. SSSR Ser. Geophys.*, 2:69–93, 1951.

[16] P-H. Maire, R. Abgrall, J. Breil, and J. Ovadia. A cell-centered Lagrangian scheme for two dimensional compressible flow problems. *SIAM J. Sci. Comput.*, 29(4):1781–1824, 2007.

[17] J. Mallet, S. Brull, and B. Dubroca. General moment system for plasma physics based on minimum entropy principle. *Kinet. Relat. Models*, 8(3):533–558, 2015.

[18] C. Mazeran. *Sur la structure mathématique et l'approximation numérique de l'hydrodynamique lagrangienne bidimensionnelle*. PhD thesis, Université de Bordeaux I, 2007. Thèse de doctorat dirigée par C.-H. Bruneau et B. Després. `https://oskar-bordeaux.fr/handle/20.500.12278/25073`, 1 vol. (164 p.).

[19] D. Mihalas and B. W. Mihalas. *Foundations of Radiation Hydrodynamics*. Oxford University Press, 1984.

[20] G. Morel. *Asymptotic-preserving and well-balanced schemes for transport models using Trefftz discontinuous Galerkin method*. PhD thesis, Mathématiques Appliquées, Sorbonne Université, 2018. Thèse de doctorat dirigée par B. Després et C. Buet. `http://www.theses.fr/2018SORUS556`.

[21] E. Olbrant, E. W. Larsen, M. Frank, and B. Seibold. Asymptotic derivation and numerical investigation of time-dependent simplified Pn equations. *J. Comput. Phys.*, 238:315–336, 2013.

[22] D. Pinchon and P. E. Hoggan. Rotation matrices for real spherical harmonics: general rotations of atomic orbitals in space-fixed axes. *J. Phys. A. Math. Theor.*, 40(7):1597–1610, 2007.

[23] G. C. Pomraning. *The equations of radiation hydrodynamics*. International Series of Monographs in Natural Philosophy. Pergamon Press, 1973.

[24] B. Seibold and M. Frank. Starmap. A second order staggered grid method for spherical harmonics moment equations of radiative transfer. *ACM Trans. Math. Softw.*, 41(1): article no. 4 (28 pages), 2015.

[25] E. F. Toro. *Riemann Solvers and Numerical Methods for Fluid Dynamics*. Springer, 1999.

[26] S. Van Criekingen, R. Beauwens, J. W. Jerome, and E. E. Lewis. Mixed-hybrid discretization methods for the linear Boltzmann transport equation. *Comput. Methods Appl. Mech. Eng.*, 195(19-22):2719–2741, 2006.

[27] S. Van Criekingen, E. E. Lewis, and R. Beauwens. Mixed-hybrid transport discretization using even and odd P_N expansions. *Nuclear Science and Engineering*, 152(2):149–163, 2006.

[28] V. S. Vladimirov. Mathematical problems in the one-velocity theory of particle transport. Technical report, Atomic Energy of Canada Limited, 1963.

[29] E. P. Wigner. *Symmetries and Reflections*. Indiana University Press, 1967.